A Role for Toll-like Receptor-4 in Pulmonary Angiogenesis Following Multiple Exposures to Swine Barn Air

A Thesis submitted to the
College of Graduate Studies and Research
in partial fulfillment of the requirements
for the Degree of Master of Science in the
Toxicology Graduate Program
University of Saskatchewan
Saskatoon

By

Vanessa Jade Juneau

Permission for Use of Thesis

In presenting this Thesis in partial fulfillment of the requirements for a Postgraduate Degree from the University of Saskatchewan, I agree that the Libraries of this University may make it freely available for inspection. I further agree that permission for copying this Thesis in any manner, in whole or in part, for scholarly purposes may be granted by the professor or professors who supervised my thesis work, or in their absence, by the Head of the Department or Dean of the College in which my thesis work was done. It is understood that any copying of publication or use of this Thesis or parts thereof for financial gain shall not be allowed without my written consent. It is also understood that due recognition shall be given to me and to the University of Saskatchewan in any scholarly use which may be made of any material contained within this Thesis.

Requests for permission to copy or to make use of material in this thesis in whole or in part should be addressed to:

Chair, Toxicology Centre
University of Saskatchewan
Saskatoon, SK
S7N 5B3
Canada

Abstract

Swine barn air is a heterogeneous mixture of dust, bacteria and irritant chemicals including ammonia and hydrogen sulphide. Gram-negative bacteria are commonly found in swine barn air and significantly contribute to pulmonary disease in unprotected swine barn workers, through the endotoxin moiety, lipopolysaccharide (LPS). Toll-like Receptor-4 is the ligand for LPS. It is found on many cell types including monocytes, macrophages, neutrophils, endothelial cells, and to a lesser extent, epithelial cells. The severity and outcome of acute lung injury following barn air exposures depends upon the balance between epithelial and vascular endothelial repair mechanisms, including angiogenesis. Vascular Endothelial Growth Factor (VEGF) is an endothelial mitogen produced by mesenchymal and alveolar Type II epithelial cells and by activated bronchial airway epithelial cells. Research investigating the role of cytokines in angiogenesis has shown that close proximity of immune cells and endothelial cells modulates the production of various compounds that regulate vascular function. Given that LPS is the ligand for TLR4 there appeared to be a role for TLR4 in angiogenesis, particularly following endotoxin exposure. To determine whether this was occurring, we examined whether exposure to swine barn air alters vascular density in the lungs and the role of TLR4 using a murine model. Toll-like Receptor-4 wild-type (C3HeB/FeJ) and TLR4 mutant (C3H/HeJ) mice were obtained and exposed to swine barn air for 1-, 5-, or 20-days for 8 hours/day. Wild-type animals showed a 127% increase in vascular density after 20-days barn air exposure. Vascular Endothelial Growth Factor-A protein levels were decreased by 0.62-fold after one-day swine barn air exposure in wild-type animals, indicating that VEGF-A is being used as a pro-angiogenic mitogen. Transcription of VEGF-A mRNA was increased in wild-type animals after all swine barn air exposure periods. The receptor VEGFR-1 showed increased mRNA transcription over all time points. These effects were only observed in TLR4 wild-type animals, indicating that these effects are mediated by TLR4. Further, VEGF-A and VEGFR-1 appear to be involved in the manifestation of TLR4-induced angiogenesis in the lung

Acknowledgements

I would like to extend great appreciation to Dr. Baljit Singh for his support and guidance during this Master of Sciences project. I would also like to thank the other members of my committee Dr. Barry Blakley and Dr. James Dosman as well as my external examiner Dr. Andrew van Kessel for their time, insight, and support.

The PHARE Graduate Training Program, the Saskatchewan Lung Association and the Toxicology Graduate Program financially supported this research project, and their generosity is greatly appreciated. I also wish to thank the following people: Mr. Max Woodcock for the generous use of his swine facilities, my colleagues at the Pulmonary Pathology Laboratory for their advice and collaboration, Dr. S.S. Suni, Prairie Diagnostic Services for the use of equipment, Dr. Aarti Nayyar for her assistance with whole-body plethysmography, Ms. Jennifer Town for her assistance with ELISA spectrophotometry, and all my friends and colleagues at the Toxicology Centre and within the Veterinary Biomedical Sciences Department.

This Thesis is dedicated to my family.

Most especially, I dedicate this to my parents, Bernard and Leslie-Ann,

for their love, support, understanding, and wisdom.

Table of Contents

List of Tables and Figures

Tables **Page**

Figures

List of Abbreviations

ANOVA	Analysis of Variance
AR	Airway Responsiveness
BAL	broncho-alveolar lavage
BALF	broncho-alveolar lavage fluid
C3H/HeJ	TLR4-mutant mouse strain
C3HeB/FeJ	wild-type mouse strain
CD34	a cell marker
dRn	a measure of relative fluorescence used in qPCR
ELISA	Enzyme-Linked Immunosorbent Assay
Endotoxin	Unrefined lipopolysaccharide
EU	Endotoxin Units (mg/m^3)
Flt-1	Vascular Endothelial Growth Factor Receptor 1
Flk-1	Vascular Endothelial Growth Factor Receptor 2
ft^3	cubic foot
H&E	Hematoxylin and Eosin stain
HBSS	Hank's Balanced Salt Solution
HCl	Hydrochloric acid
IHC	Immunohistochemistry
kg	kilogram
L	litre
LBP	Lipopolysaccharide Binding Protein
LPS	Lipopolysaccharide

qPCR	Real-Time Reverse Transcriptase - Polymerase Chain Reaction
ppm	parts per million (10^{-6})
M	mutant mouse strain; C3H/HeJ
m^3	cubic metre (1 m^3 = 1000 L)
min	minute
mg	milligram
mL	millilitre
PBS	phosphate-buffered saline
rcf	X centrifugal force
rpm	revoluteions per minute
TLR2	Toll-like receptor-2
TLR4	Toll-like receptor-4
μg	microgram
μL	microlitre
VDA	Vascular Density Analysis
VEGF-A	Vascular Endothelial Growth Factor – A isoform
VEGFR-1	Vascular Endothelial Growth Factor Receptor 1
VEGFR-2	Vascular Endothelial Growth Factor Receptor 2
WT	wild-type mouse strain; C3HeB/FeJ

1.0 INTRODUCTION

1.1 Swine Barn Air, Inflammation and Pulmonary Disease

Swine barn air is a heterogeneous mixture of dust, bacteria and irritant chemicals including ammonia and hydrogen sulphide (Zhang, 1998). These bioaerosols in the barn air are a risk factor for the development of chronic respiratory symptoms and lung dysfunction (Zejda *et al.*, 1993; Zejda *et al.*, 1994). Gram-negative bacteria are commonly found in swine barn air and significantly contribute to pulmonary disease in unprotected swine barn workers. Single, 3-5 hour exposure of naïve, healthy, non-smoking subjects to swine barn air increases interleukin (IL)-6 in serum and IL-6 and IL-8 in nasal lavage and inflammatory cells in bronchoalveolar lavage fluid (BALF) (Larsson *et al.*, 1994; Dosman *et al.*, 2000). These changes are characteristic of an inflammatory/immune response. Following exposure to an antigen, antigen presenting cells (eg. macrophages) will present the antigens to B-cells. Antigen presentation combined with cytokine expression secreted by helper T-cells (Th1 and Th2 cells) enables B-cell maturation and activation, with many feedback cycles to other lymphocytes, and initiation of the inflammatory process. Thus, biologically speaking, the changes to inflammatory cytokines after barn air exposures mean that a single exposure to the barn air initiates acute pulmonary inflammation and compromised functional capacity of the lung (Cochran *et al.*, 2002; Singh and Schwartz, 2005).

Research into pulmonary inflammation following barn air exposures has focused upon endotoxin, the lipopolysaccharide (LPS)-containing component of the Gram-negative bacteria cell wall. Lipopolysaccharide is the principal pro-inflammatory component of

the Gram-negative bacterial cell wall. Unrefined LPS is called endotoxin but for the purposes of this report endotoxin and LPS are considered synonymous. Bacterial LPS can be volatilized if sloughed from the cell wall. If inhaled, bacterial LPS can induce inflammation through the Toll-like receptor subfamily in many organs, including the lungs (Faure *et al.*, 2000; Koay *et al.*, 2002; Fan *et al.*, 2003; Heumann *et al.*, 2003; Finberg *et al.*, 2004; Gon *et al.*, 2004; Kobayashi and Flavell, 2004; Lin *et al.*, 2004; Moreno *et al.*, 2004; Muir *et al.*, 2004; Ushio *et al.*, 2004).

1.2 Toll-Like Receptor-4 (TLR4)

Toll-like receptors (TLRs) are mammalian homologues of the Toll receptors identified in *Drosophila*. To date 11 mammalian TLRs have been identified. All have a highly conserved genetic sequence [18-21], and recognize pathogen-associated molecular patterns (PAMPs) to initiate the immune response. Toll-like Receptor-4 and TLR2 recognize conserved molecular patterns associated with a wide range of microbial pathogens. When activated, they initiate transcription of proinflammatory cytokines such as interleukin (IL)-1β, TNF-α, IL-6 and IL-8 (Charavaryamath *et al.*, 2005). Mammalian TLR4 regulates the innate immune response and is the most critical sensor for the recognition of and signaling events associated with LPS. Toll-like Receptor-2 recognizes lipoteichoic acid from Gram-positive bacteria to generate inflammatory responses. Lipopolysaccharide can also influence expression of TLR2 in human leukocytes and mouse lungs (Dziarski *et al.*, 2001). Therefore it is essential to understand the expression of these proteins for a better comprehension of the host response to pathogens.

Toll-like Receptor-4 is the ligand for the endotoxin moiety (Faure *et al.*, 2000; Koay *et al.*, 2002; Fan *et al.*, 2003; Heumann *et al.*, 2003; Finberg *et al.*, 2004; Gon *et al.*, 2004; Kobayashi and Flavell, 2004; Lin *et al.*, 2004; Moreno *et al.*, 2004; Muir *et al.*, 2004; Ushio *et al.*, 2004). It is found on many cell types including monocytes, macrophages, neutrophils, mast cells, B-cells, endothelial cells, and to a lesser extent, epithelial cells (Faure *et al.*, 2000; Koay *et al.*, 2002; Gon *et al.*, 2004; Muir *et al.*, 2004; Ushio *et al.*, 2004). The molecular mechanism by which TLR4 initiates the inflammatory response is well characterized, and is represented in Figure 1-1 and Figure 1-2. The initial step of these mechanisms differ between cell-types because of the presence or lack of membrane-bound CD14, a glycoprotein required for binding of LPS to TLR4 (Heumann *et al.*, 2003; Finberg *et al.*, 2004; Lin *et al.*, 2004; Moreno *et al.*, 2004).

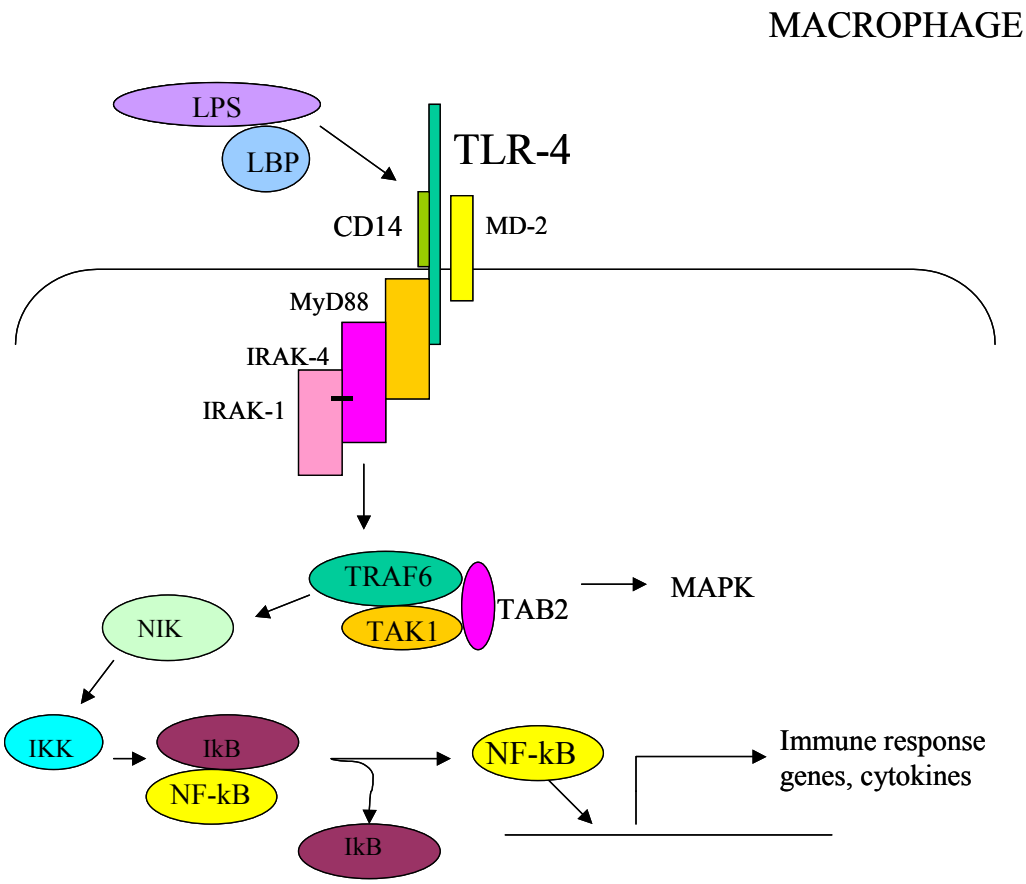

Figure 1-1: Cellular cascade initiated by ligation of LPS to TLR4 in macrophages.

List of abbreviations:
Lipopolysaccharide (LPS), lipopolysaccharide binding protein (LBP), soluble CD14 (sCD14), adaptor molecule MyD88 (MyD88), IL-1 receptor–associated kinase (IRAK), tumor necrosis factor-associated factor 6 (TRAF6), transforming growth factor-b-activated kinase (TAK), TAK1-binding protein (TAB), NIK, IκB kinase (IKK), Nuclear Factor- kappa B (NF-κB).

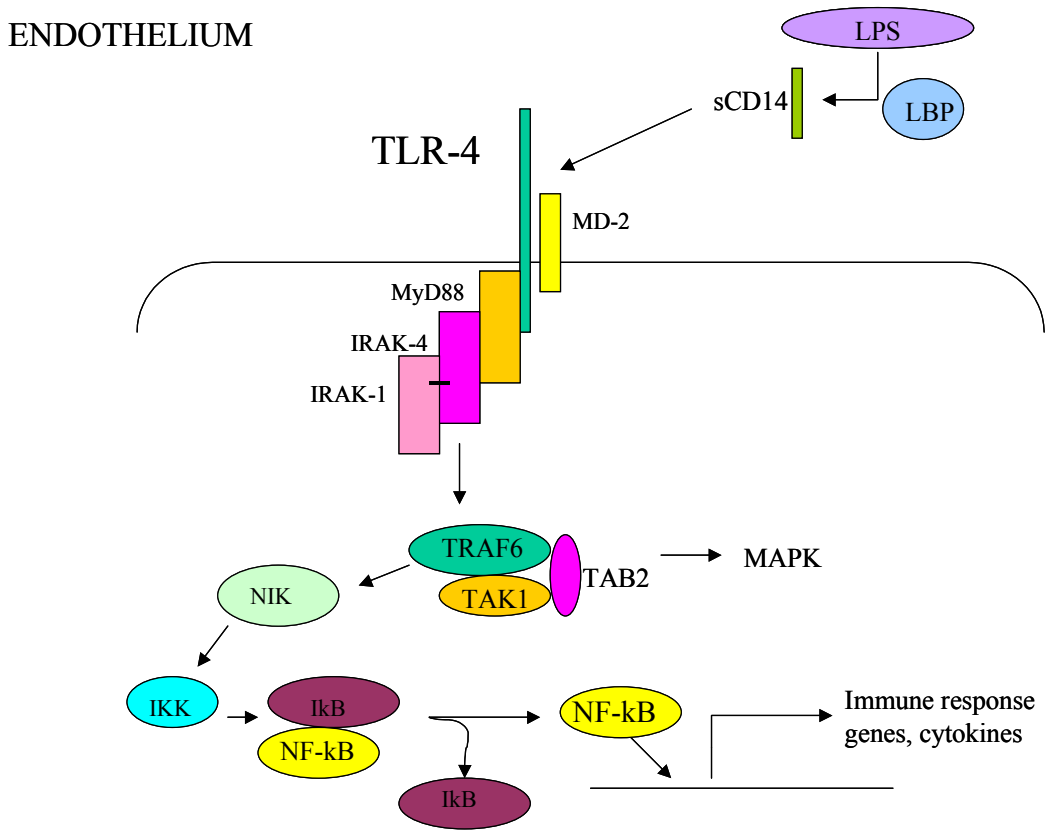

Figure 1-2: Cellular cascade initiated by ligation of LPS to TLR4 in endothelial cells.

List of abbreviations:
Lipopolysaccharide (LPS), lipopolysaccharide binding protein (LBP), soluble CD14 (sCD14), adaptor molecule MyD88 (MyD88), IL-1 receptor–associated kinase (IRAK), tumor necrosis factor-associated factor 6 (TRAF6), transforming growth factor-b-activated kinase (TAK), TAK1-binding protein (TAB), NIK, IκB kinase (IKK), Nuclear Factor- kappa B (NF-κB).

Toll-like Receptor-4 activation by LPS induces multimerization of TLR4/CD14/MD-2 and recruitment of MyD88 or IRAK proteins. The proximity of IL-1 receptor–associated kinases (IRAKs) causes a conformational change via auto- or cross-phosphorylation resulting in reduced affinity for the TLR signalling complex. The IRAKs released by activation of the TLR4 complex activate downstream molecules such as tumor necrosis factor (TNF) receptor-associated factor (TRAF)-6, ultimately causing NF-κB transcription. The presence of NF-κB initiates transcription of pro-inflammatory molecules including tumor necrosis factor-alpha (TNF-α), IFN-β, granulocyte-macrophage colony stimulating factor (GM-CSF), granulocyte colony stimulating factor (G-CSF), induced nitric oxide synthase (iNOS), and IL-6 (Suzuki, 1999; Miggin and O'Neill, 2006).

Negative feedback of the TLR4 signalling cascade is mediated, in part, by IRAK-M, which is recruited to the signalling complex together with IRAK-1 and IRAK-4 (not shown). This association inhibits the release of IRAK-1/IRAK-4 from the TLR signalling complex by inhibiting the phosphorylation of IRAK-1/IRAK-4 or stabilizing the TLR-MyD88-IRAK-1/IRAK-4 complex. Both these mechanisms result in the interruption of downstream signalling (Kobayashi and Flavell, 2004; Tsan and Gao, 2004). Other suppressor molecules include SHIP, Suppressor of cytokine signalling (SOCS)-1 and Toll-interacting protein (Tollip) which directly inhibit TLR4 signalling through interactions with IRAK-1 (Kobayashi and Flavell, 2004; Yoshimura *et al.*, 2004), and A20 which has inhibitory effects on NF-kB (Gon *et al.*, 2004).

1.3 Lipopolysaccharide Binding Protein (LBP)

Lipopolysaccharide binding protein (LBP) is critical to the LPS response (Brass *et al.*, 2004). It is a 60 kDa serum glycoprotein present at low levels in the lung (Martin, 2000). Lipopolysaccharide binding protein binds the lipid A component of LPS to form a high-affinity LBP/LPS complex that potentiates the cellular response to LPS by transferring LPS to CD14 (Brass *et al.*, 2004).

Following LPS exposures, LBP protein and LBP mRNA are increased in the lung. Animals expressing LBP were demonstrated to have enhanced LPS inflammatory response in the lower respiratory tract, and a more severe fibrotic response in subepithelial mucosa following endotoxin exposures (Brass *et al.*, 2004).

1.4 CD14

CD14 is part of a multimeric receptor complex for LPS. CD14 can be membrane-bound or found within the serum as a soluble protein [16]. Monocytes, macrophages and neutrophils express membrane-bound CD14 (Gangloff and Gay, 2004; Lin *et al.*, 2004; Moreno *et al.*, 2004). Stimulation of endothelial and epithelial cells by LPS appears to be soluble CD14-dependent (Pugin *et al.*, 1993; Backhed *et al.*, 2002; Lin *et al.*, 2004). CD14 has no intracellular domain, thus a physical association between CD14 and TLR4/MD-2 is required (Finberg *et al.*, 2004; Fitzgerald *et al.*, 2004; Gangloff and Gay, 2004; Lin *et al.*, 2004; Moreno *et al.*, 2004) to induce the inflammatory response.

1.5 Endotoxin Tolerance

The phenomenon of endotoxin tolerance has been widely observed in the literature (Nomura *et al.*, 2000; Qu *et al.*, 2003; Fan and Cook, 2004; Lin *et al.*, 2004; Moreno *et al.*, 2004; Sly *et al.*, 2004; Charavaryamath *et al.*, 2005). As the name implies, prolonged exposure to LPS has been demonstrated to result in a reduced cellular response, or the development of tolerance. There are several theories surrounding this process, including:

1) Reduced expression of membrane TLR4 (Nomura *et al.*, 2000);
2) Altered TLR4 signaling cascade (Fan and Cook, 2004);
3) Depletion of soluble CD14 (endothelial and epithelial response) (Lin *et al.*, 2004; Moreno *et al.*, 2004);
4) Depletion of LBP (Brass *et al.*, 2004);
5) Increased SHIP expression. SHIP-mediated LPS tolerance is associated with inhibition of both NF-kB and STAT-1 activation: two of the principal endpoints of LPS signal transduction (Qu *et al.*, 2003; Sly *et al.*, 2004);
6) Potential cytokine interactions (Qu *et al.*, 2003; Moreno *et al.*, 2004; Peck *et al.*, 2004).

Observation of endotoxin tolerance is anticipated for this model. Determination of the mechanism by which tolerance occurs is, however, outside the scope of this research.

1.6 Angiogenesis

Angiogenesis is the process whereby new blood vessels are differentiated from existing vascular endothelial cells. Several factors have contributed to our interest in angiogenesis with respect to pulmonary inflammation. First, the severity and outcome of

acute lung injury depends upon the balance between epithelial and vascular endothelial repair mechanisms (Mura *et al.*, 2004). Since endothelial repair can include angiogenesis, this process will be of interest with respect to the inflammatory process following LPS exposure. Second, an increase in vascular density within the lung will allow for increased leukocyte infiltration following pulmonary insult, thus, potentially exacerbating pulmonary inflammation following LPS exposure.

There are many factors known to promote angiogenesis, as reviewed by (Papetti and Herman, 2002) (Table 1-1 and Table 1-2). Of these, this project will focus on the Vascular Endothelial Growth Factor (VEGF) family and its receptors.

Table 1-1: Important Pro-Angiogenic Growth Factors

Factor	Function
VEGF family	• Increases endothelial cell permeability • Stimulates endothelial cell proliferation • Inhibits endothelial cell apoptosis • Enhances endothelial cell migration • Stimulates in vivo angiogenesis
TGF-β	• Supports anchorage-independent growth of fibroblasts • Stimulates/inhibits formation of endothelial cell tubes in vitro • Inhibits production of other proteases/stimulates production of protease inhibitors • Stimulates VSMA production by pericytes • Chemotactic for monocytes and fibroblasts • Stimulates in vivo angiogenesis in presence of inflammatory response • Increases vessel wall stability
Angiogenin	• Stimulates angiogenesis *in vivo* • Supports endothelial cell binding and spreading
Angiotropin	• Stimulates random capillary endothelial cell migration • Stimulates endothelial cell tube formation • Stimulates in vivo angiogenesis
$\alpha_v\beta_3$ integrin	• Highly expressed on activated endothelial cells • Mediates endothelial cell attachment, spreading and migration • Present on angiogenic capillary sprouts • Required for bFGF-stimulated angiogenesis in vivo • Suppresses endothelial cell apoptosis

Table 1-2: Other Pro-Angiogenic Growth Factors*

Factor	
Ang1	Nicotinamide
Ang2	Monobutyrin
aFGF, bFGF	$\alpha_v\beta_5$ integrin
PDGF	$\alpha_v\beta_1$ integrin
TNF-α	VE-cadherin
EGF, TGF-α	Eph-4B/Ephrin-B2
G-CSF, GM-CSF	Ephrin-A1
Prostaglandin	Eph-2A

*from (Papetti and Herman, 2002)

1.7 Vascular Endothelial Growth Factor (VEGF)

The human VEGF gene family includes five isoforms: VEGF-A, VEGF-B, VEGF-C, VEGF-D and VEGF-E. These isoforms arise from alternate exon splicing (Mura *et al.*, 2004). Vascular Endothelial Growth Factor mRNA is most abundant in the lung, kidney and spleen, where transcription is localized primarily in epithelial cells and vascular smooth muscle cells (Shifren *et al.*, 1994; Corne *et al.*, 2000; Voelkel *et al.*, 2006). The major source of VEGF in both animal and human lungs are mesenchymal and alveolar Type II epithelial cells (Kaner and Crystal, 2001), though activated bronchial airway epithelial cells also release VEGF (Lee *et al.*, 2000). Further evaluations using RT-PCR have demonstrated that VEGF is produced from various sources (Wellmann *et al.*, 2001) including human peripheral blood leukocytes, which contain lymphocytes, monocytes, and other cells (Gunsilius *et al.*, 2000; Harter *et al.*, 2004; Mor *et al.*, 2004; Conejo-Garcia *et al.*, 2005). Vascular Endothelial Growth Factor released by alveolar epithelial cells may modulate the adjacent vascular endothelium in a paracrine fashion (Shifren *et al.*, 1994), thus playing a role in localized angiogenesis following epithelial damage.

1.7.1 Vascular Endothelial Growth Factor Isoforms

The most studied VEGF isoform is VEGF-A (often denoted VEGF in the literature). Vascular Endothelial Growth Factor-A is a relatively specific mitogen for vascular endothelial cells. It elicits a pronounced angiogenic response in many *in vivo* and *in vitro* models. Studies have demonstrated that VEGF-A stimulates endothelial cells to degrade the extracellular matrix (ie. via matrix metalloproteinases), to migrate, and to form capillary tubes (Veikkola and Alitalo, 1999; Voelkel *et al.*, 2006). Degradation of the extracellular matrix, and hence regulation of vascular permeability, is important to the initiation of angiogenesis (Dvorak *et al.*, 1995; Cebe-Suarez *et al.*, 2006; Voelkel *et al.*, 2006). Following matrix degradation endothelial cells may migrate, thus allowing the formation of new capillary tubes

Studies have also demonstrated that endothelial cell survival in the newly formed blood vessels is VEGF-A dependent. This is likely due to VEGF-A induced expression of anti-apoptotic proteins in endothelial cells (Alon *et al.*, 1995; Benjamin and Keshet, 1997; Gerber *et al.*, 1998).

The other isoforms of VEGF have similar roles to VEGF-A. Vascular Endothelial Growth Factor-B is involved in the regulation of extracellular matrix degradation, cell adhesion and migration (Veikkola and Alitalo, 1999); Vascular Endothelial Growth Factor-C stimulates migration and mitogenesis of cultured endothelial cells (Joukov *et al.*, 1997); and Vascular Endothelial Growth Factor-D acts as a mitogen for microvascular endothelial cells (Achen *et al.*, 1998).

1.7.2 Vascular Endothelial Growth Factor Receptors (VEGFRs)

There are three VEGF receptors (VEGFRs) (Veikkola and Alitalo, 1999). Vascular Endothelial Growth Factor Receptors are expressed on many cell types, and VEGF affinity differs depending on the isoform. The mechanism(s) by which VEGF-receptor interactions evoke endothelial cell function is not well understood; though it is known that initiation by receptor dimerization and subsequent autophosphorylation (Davis-Smyth *et al.*, 1996; Barleon *et al.*, 1997) results in a functional signaling unit (Mura *et al.*, 2004). Each consists of four regions: the extracellular ligand-binding domain, transmembrane domain, tyrosine kinase domain and a downstream carboxy terminal (Shibuya, 2006). The extracellular domains of the VEGFRs contain seven immunoglobulin-like domains (Shibuya, 2006; Shibuya and Claesson-Welsh, 2006).

Both VEGFR-1 (Flt-1) and VEGFR-2 (KDR/Flk-1) are expressed on vascular endothelial cells and act by tyrosine kinase-dependent pathways (Olsson *et al.*, 2006; Shibuya, 2006; Shibuya and Claesson-Welsh, 2006). Vascular Endothelial Growth Factor Receptor-1 is also expressed on activated macrophages and monocytes, and promotes tumour growth, metastasis and inflammation (Mura *et al.*, 2004; Shibuya, 2006; Shibuya and Claesson-Welsh, 2006). The specific roles of VEGFR-1 are still being elucidated, however, it has been suggested that VEGFR-1 is involved in vascular organization and the migration of macrophages toward VEGF-A (Fong *et al.*, 1999; Olsson *et al.*, 2006; Shibuya, 2006; Shibuya and Claesson-Welsh, 2006). Conversely, VEGFR-2 plays no role in vascular organization, but has been suggested to mediate endothelial differentiation and proliferation (Fong *et al.*, 1995; Mura *et al.*, 2004; Olsson *et al.*, 2006; Shibuya, 2006;

Shibuya and Claesson-Welsh, 2006). Unlike other tyrosine kinase-dependent receptors that use the Ras pathway, VEGFR-2 mostly relies upon the Phospholipase-Cγ-Protein kinase-C pathway to activate MAP kinases (Olsson *et al.*, 2006; Shibuya, 2006).

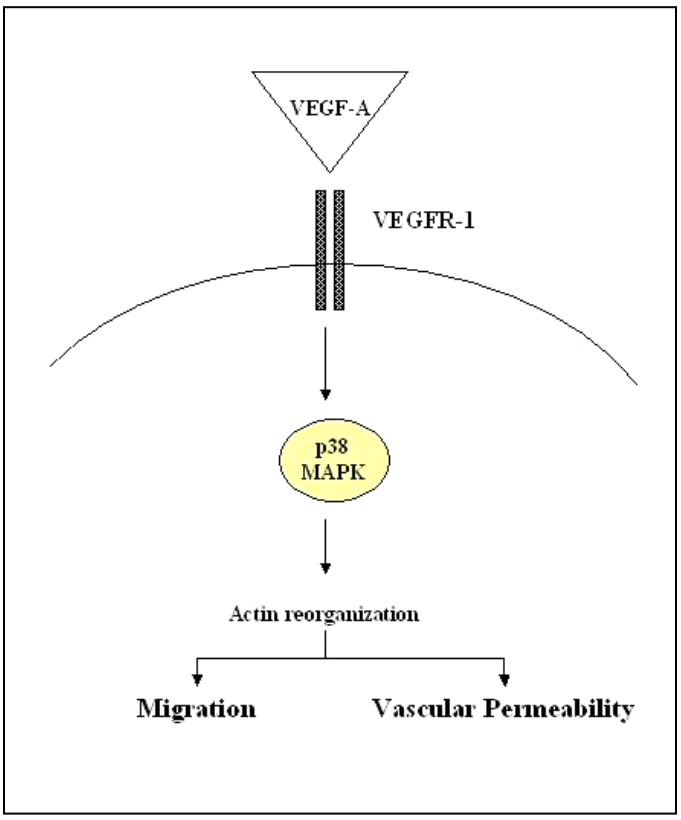

Figure 1-3: Vascular Endothelial Growth Factor Receptor-1 signalling pathway.

List of abbreviations:
Vascular Endothelial Growth Factor-A (VEGF-A), Vascular Endothelial Growth Factor Receptor-–2 (VEGFR-2), p38 mitogen-activated protein kinase (p38 MAPK).

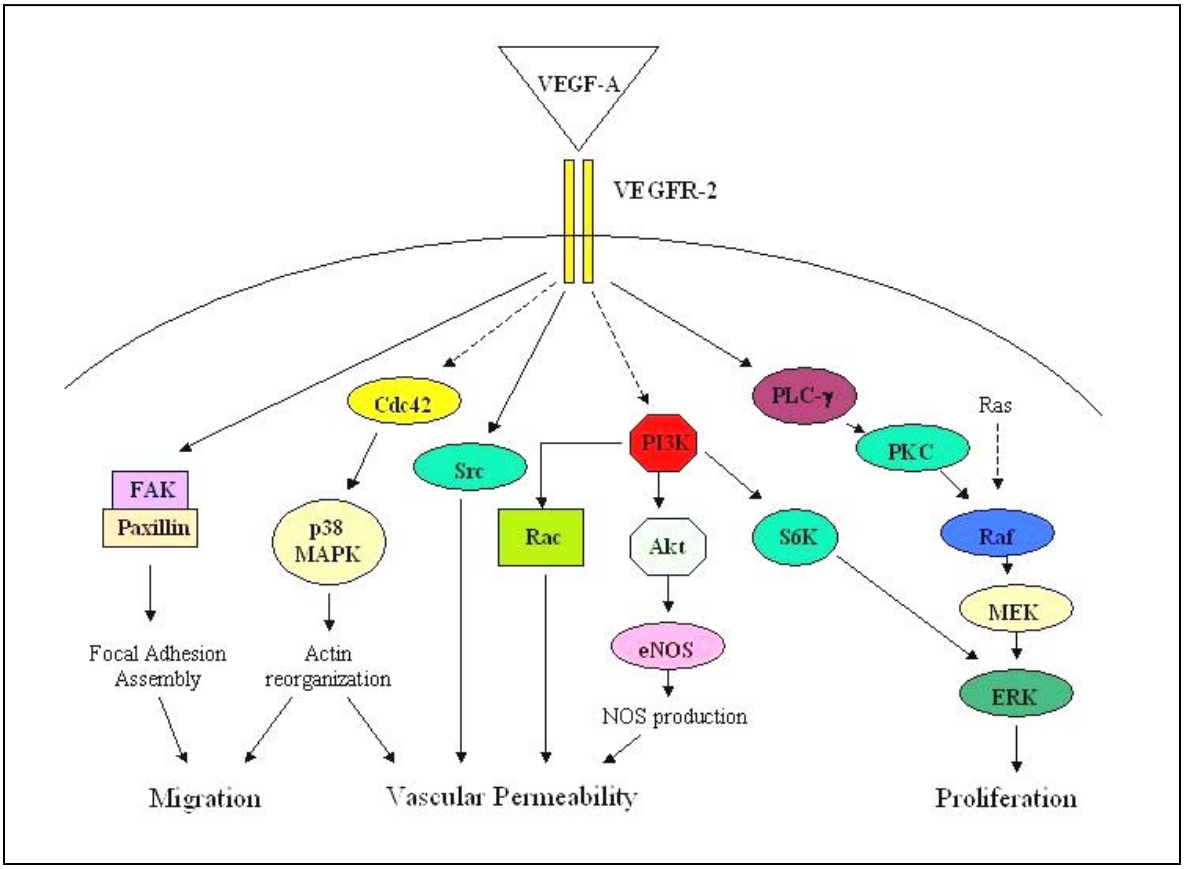

Figure 1-4: Vascular Endothelial Growth Factor Receptor-2 signalling pathway

List of abbreviations:
Vascular Endothelial Growth Factor-A (VEGF-A), Vascular Endothelial Growth Factor Receptor-–2 (VEGFR-2), Focal adhesion kinase (FAK), p38 mitogen-activated protein kinase (p38 MAPK), Endothelial NOS (eNOS), S6 kinase (S6K), Phospholipase C (PLC), Protein kinase C (PKC), Extracellular signal-regulated kinase (ERK).

1.8 Induction of Vascular Endothelial Growth Factor by Cytokines

Induction of VEGF mRNA and VEGF protein has been described *in vivo* and *in vitro* in response to several stimuli, including reactive oxygen species, glucose deprivation, growth factors (eg. TGF-β) (Lee *et al.*, 2004; Zittermann and Issekutz, 2006), several pro-inflammatory cytokines including TNF-α, IL-6 and IFN-γ, and inhibition of nitric

oxide (reviewed in (Mura *et al.*, 2004; Voelkel *et al.*, 2006; Zittermann and Issekutz, 2006)).

Macrophages in the lungs can be pro- or anti-inflammatory (Pakala *et al.*, 2002; Lamagna *et al.*, 2006; Sica *et al.*, 2006). Type I (activated) macrophages are pro-inflammatory (Lamagna *et al.*, 2006) and express pro-inflammatory cytokines. By contrast, Type II (unactivated) macrophages are anti-inflammatory and moderate the inflammatory response, phagocytose cell waste, and promote angiogenesis (Lamagna *et al.*, 2006). Research investigating the role of cytokines in angiogenesis has shown that close proximity of monocytes/macrophages and endothelial cells modulates the production of various compounds that regulate vascular function (Dahlqvist *et al.*, 1999). Several studies have demonstrated that macrophages produce endothelial cell growth factors including VEGFs, bFGF, and IL-8 (Hojo *et al.*, 2000; Pakala *et al.*, 2002), perhaps in conjunction with vascular smooth muscle cells. The same data demonstrated that TLRs, including TLR4, play a significant role in the pro-angiogenic switch in macrophages (Pinhal-Enfield *et al.*, 2003). Given that LPS is the ligand for TLR4, these factors indicate a role for TLR4 in angiogenesis, particularly following endotoxin exposure.

Thus, in situations of LPS-induced cell injury, endothelial cells may be stimulated to release VEGF-A. With respect to immune cells, macrophages become activated to the Type I phenotype and are recruited to the site of injury along with other leukocytes (e.g., T-cells, natural killer (NK) T-cells, and neutrophils) (Sica *et al.*, 2006). The products generated during vascular remodeling induce macrophages to produce IL-12, which

stimulates NK T-cells to produce IFN-γ that in turn activates additional macrophages in a positive feedback manner (Pakala *et al.*, 2002; Sica *et al.*, 2006). As indicated above, induction of VEGF mRNA and VEGF protein is also stimulated by IFN-γ, perhaps through macrophage-mediated pathways. To further complicate these reactions, neutrophils also mediate T-cell responses, thus furthering the progression of inflammation by T-cell interaction with immune and non-immune cells by the secretion of T-cell specific cytokines and chemokines (Anderton and Wraith, 2002; Ludwig *et al.*, 2006) depending on what T-helper (Th) phenotype is differentiated. Th1 cells regulate cellular immunity by secreting cytokines such as IFN- γ and TNF- α (Corthay, 2006). Th2 cells mediate B-cell immunity by producing IL-4, IL-5 and IL-13 (Corthay, 2006). A recent study demonstrated that T-cell homing to inflammatory sites (hence being in intimate contact with endothelial cells) stimulates VEGF secretion (Mor *et al.*, 2004). The same study noted that VEGF augmented IFN-γ secretion by T-cells responding to mitogenic or antigenic stimulus but and inhibited IL-10 secretion; thus, VEGF enhanced the Th1 phenotype, which may in turn activate macrophages and stimulate additional VEGF secretion through positive feedback. Other studies demonstrated a link between VEGF and Th2 cells, whereby VEGF enhanced antigen sensitization and played a role in Th2-mediated lung inflammation (Lee *et al.*, 2004).

1.9 Summary

Toll-like Receptor-4 plays a significant role in the pro-angiogenic switch in macrophages (Pinhal-Enfield *et al.*, 2003), and potentially other cells expressing TLR4 such as epithelial cells (Kaner and Crystal, 2001). Given that LPS is the ligand for TLR4, this

indicates a role for TLR4 in angiogenesis, particularly following endotoxin exposure. Research has demonstrated that in situations of LPS-induced cell injury, macrophages become activated to the Type I phenotype and are recruited to the site of injury along with other inflammatory cells (e.g., T-cells, natural killer (NK) T-cells, and neutrophils) (Sica *et al.*, 2006) where they produce endothelial cell growth factors including VEGFs (Hojo *et al.*, 2000; Pakala *et al.*, 2002). Induction of VEGF mRNA and VEGF protein has been described *in vivo* and *in vitro* in response to growth factor and pro-inflammatory stimuli (Lee *et al.*, 2004; Zittermann and Issekutz, 2006). Further research is required to determine specific interactions. To further this research, we are proposing to examine whether exposure to swine barn air alters vascular density in the lungs and, if so, to determine the role of TLR4 using a murine model.

2.0 OBJECTIVES AND HYPOTHESES

2.1 Objectives

1) To determine whether lungs exposed to swine barn air have increased vascular density.

2) To determine if expression of Vascular Endothelial Growth Factor-A and Vascular Endothelial Growth Factor Receptor-1 or Vascular Endothelial Growth Factor Receptor-2 are altered following exposure to swine barn air.

3) To determine the role of TLR4 in swine barn air-induced angiogenesis.

2.2 Hypothesis

Exposure to swine barn air will increase vascular density in the lungs associated with up-regulation of the Vascular Endothelial Growth Factor pathways and mediated by Toll-like Receptor-4.

3.0 METHODS

3.1 Animal Subjects

To assess the role of TLR4 in endotoxin-induced angiogenesis, wild-type and TLR4 mutant mice were obtained from Jackson Labs (Bar Harbor, Maine, USA) (Appendix A & Appendix B). A summary of the genotypic and phenotypic characteristics of these mice is provided in Table 3-1.

Table 3-1: Summary of genotypic and phenotypic characteristics of mice used.

Strain	**C3HeB/FeJ**	**C3H/HeJ**
Phenotype	Wild-type	Mutant
TLR4 Mutation Status	Wild-type; no mutation.	Mutation to chromosome 4. Results in proline to histidine mutation in the cytoplasmic domain of TLR4; selectively impedes signal transduction.
TLR4	Functional	Non-functional
Lipopolysaccharide response allele	*Tlr4*$^{Lps\text{-}n}$	*Tlr4*$^{Lps\text{-}d}$
Sensitivity to LPS	Sensitive	Resistant

Both strains were inbred via sibling mating, and were agouti in appearance. The mice were guaranteed virus free, and contained the retinal degeneration mutation *Pde6b*^{rdl}, causing blindness by weaning age. Wild type and mutant mice had a similar lifespan, and no specialized care was required.

Mutant (C3H/HeJ) mice contain a defective lipopolysaccharide (LPS) response allele *Tlr4*$^{Lps\text{-}d}$, making them endotoxin-resistant. The TLR4 defect is derived from a spontaneous mutation at the lipopolysaccharide response locus, which renders the mice unresponsive to the toxic effects of the lipid A component of LPS. C3H/HeJ mice are

highly susceptible to infection by Gram-negative bacteria such as *Salmonella enterica*. Mice infected with *Salmonella* exhibit delayed chemokine production, impaired nitric oxide generation, and attenuated cellular immune responses. Mortality in infected mice appears to be the result of enhanced bacterial growth within the liver Kupffer cell network (Appendix B).

3.2 Study Design

The inhalation model is unique to endotoxin research because it mimics the route of exposure for most barn workers and does not result in bacterial sepsis. Furthermore, by using an inhalation model we can realistically account for epithelial-endothelial-leukocyte interactions. In this model, the epithelium is the first line of defense following exposure to barn air. Recent data from our laboratory have shown striking parallels in lung dysfunction between swine barn workers and rodents exposed to swine barn air (Charavaryamath *et al.*, 2005).

Mice were housed in cages enriched with an exercise wheel and mouse houses, with *ad libitum* access to food and water (Figure 3-1). In the barn, mice were suspended in cages approximately six feet above ground level to approximate an adult height (Figure 3-2). Mice were exposed to swine barn air for 1-, 5- or 20-days (eight hours/day) to mimic both acute and sub-chronic occupational exposures (Table 3-2). Control animals were housed at the University of Saskatchewan animal care facilities for the duration of the project, and kept at approximately five feet above ground level. To control for traveling stress, the control animals were transported to and from the barn once daily. All

protocols were performed in accordance with the guidelines of the Canadian Council for Animal Care and were approved by the University of Saskatchewan Animal Care Committee.

Table 3-2: Experimental Design

Duration	C3HeB/FeJ (wild-type)		C3H/HeJ (mutant)	
	Exposure	Control	Exposure	Control
1 day	9	8	9	8
5 day	9		9	
20 day	7	5	7	5

Please note that the 20-day control groups were not included in data evaluation process because the assessed endpoints were consistent with the one- and five-day control groups.

Figure 3-1: Housing of test subjects.

Figure 3-2: Overhead suspension of exposure cages in swine barn.

3.3 Swine Barn Information & Dimensions

The dry sow barn used for this experiment was located in Aberdeen, Saskatchewan. The facilities were family operated, and housed approximately 70 dry sows in standing and group stalls (Figure 3-3). Ventilation consisted of a series of exhaust fans, which appeared to be activated at all times.

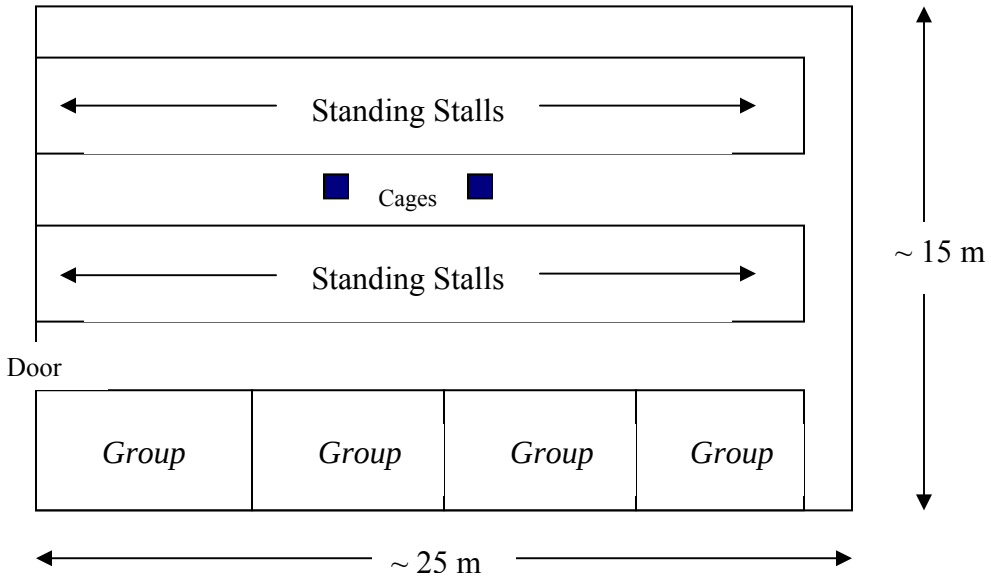

Figure 3-3: Swine barn layout and dimensions.

3.4 Air Quality Assessment

Swine barn air was analysed twice per week for both endotoxin and bacteria levels. The SKC air sampler (SKC Edmonton, Canada) with binder-free glass fibre inline filter cassettes was used to assess entodoxin levels over the eight-hour barn exposure period. Flow rate was determined to be approximately 2 L/minute using the SKC Ultraflo

Primary Gas Flow Calibrator (See "Endotoxin Analysis", below). Total bacterial counts were obtained using the Flow Sensor Microbial Sampler (Flow Sensor, USA) with a six-stage impinger and blood agar growth media. Samples were taken for 20 seconds at a flow rate of 40 ft^3/hour. Use of the six-stage impinger allowed for determination of the percent of particles in each size range (Figure 3-4). These samplers have been calibrated with monodisperse, unit density (1 g/cm^3), spherical aerosols so that all particles collected, regardless of physical size, shape or density are sized aerodynamically and can be equated to the reference particle (Manual, 1980). Particles with a diameter of less than seven micrometers were considered respirable. Knowing the air sample flow rate and the sampling time allows for the mean number of microbial particles per unit volume air to be determined.

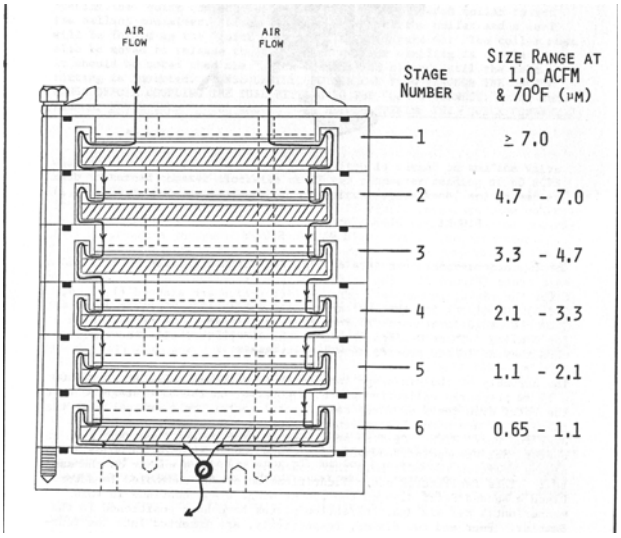

Figure 3-4: Schematic representation of the Flow Sensor Microbial Sampler six-stage impinger and the approximate particle sizes expected to impact each stage.

Control samples (n=4) for both endotoxin and total bacterial counts were taken in the animal housing facility (Animal Control Unit A, Western College of Veterinary

Medicine), using the protocol outlined above. Four (4) control SKC sample cassettes were taken en-route to the barn to control for contamination during animal transport.

3.4.1 Endotoxin Analysis

Cassettes were held in a dessicator at room temperature prior to use. After exposure the cassettes were stored in a dessicator at 4°C. Endotoxin concentration, given as endotoxin units per milligram (EU/mg) and airborne endotoxin (endotoxin units per cubic meter; EU/m^3) were measured using the dust samples collected by the SKC air-flow sample cassette filters. Total dust was determined by triplicate weighing of the filters before and after each sampling event. Cassette analyses were done at the Vaccine and Infectious Diseases Organization (VIDO, Saskatoon) using standard protocol (Appendix C).

The SKC sampler flow-rate was determined prior to and following sampling using the SKC Ultraflo Primary Gas Flow Calibrator. These data were used to calculate an average of three readings (in mL/minute). The readings were averaged and used in the calculation of actual endotoxin level (as EU/m^3). Endotoxin concentrations in the dust were converted to airborne endotoxin concentrations per cubic metre of air (EU/m^3) using the following calculation:

$$\textit{Endotoxin Level } (EU/m^3) = \frac{\textit{(Endotoxin units/mL)}}{\textit{(Average flow in cc/min)(exposure in min)}(10^6\ mL/m^3)}$$

3.4.2 Total Bacterial Count Analysis

Blood agar plates were kept at 4°C prior to use. Plates were inserted into the six-stage impinger within the barn area and the Flow Sensor microbial sampler exposed the plates by circulating air through the impinger. Exposures lasted 20 seconds, at a flow rate of 40 ft^3/hour. Following exposure, plates were inverted and incubated at 37°C for approximately 16 hours. Visual inspection allowed for numeration of bacterial colonies. Final bacterial enumeration for the barn air was based upon actual colony counts. Probable colony levels were predicted by the positive-hole method which corrected for microbial coincidence, a situation whereby multiple bacteria impact the same spot on the blood agar plate (Andersen, 1958). Conversion to colony forming units per cubic meter (CFU/m^3) was done using the following calculation:

$$\textit{Bacterial Count } (CFU/m^3) = \frac{\textit{plate count or corrected count}}{(\textit{flow rate in } ft^3/h)(1\ h/60\ min)(0.0283\ m^3/1\ ft^3)(\textit{time in min})}$$

3.5 Airway Responsiveness

After exposures were completed animals were subjected to whole-body plethysmography via methacholine challenge to assess changes to airway responsiveness. Airway responsiveness measures the change in airflow rate after inhalation of a broncho-constrictor agent, such as methacholine (Kamachi *et al.*, 2002). Mice were placed into a Plexiglas tube and exposed to increasing concentrations of methacholine (0, 0.75, 1.5, 3, 6, 12, and 24 mg methacholine/mL saline) at flow rate of 0.5 mL/minute (Figure 3-5). Analysis comprised evaluation of the recorded pattern of breathing before and after

methacholine challenge. This technique informs the investigator about airway sensitization and is widely used to assess bronchial sensitivity (Lorenz *et al.*, 2001; Cochran *et al.*, 2002; Kamachi *et al.*, 2002; Savov *et al.*, 2002). Changes to breathing after methacholine exposures were compared to control animals to determine the role of endotoxin in airway responsiveness.

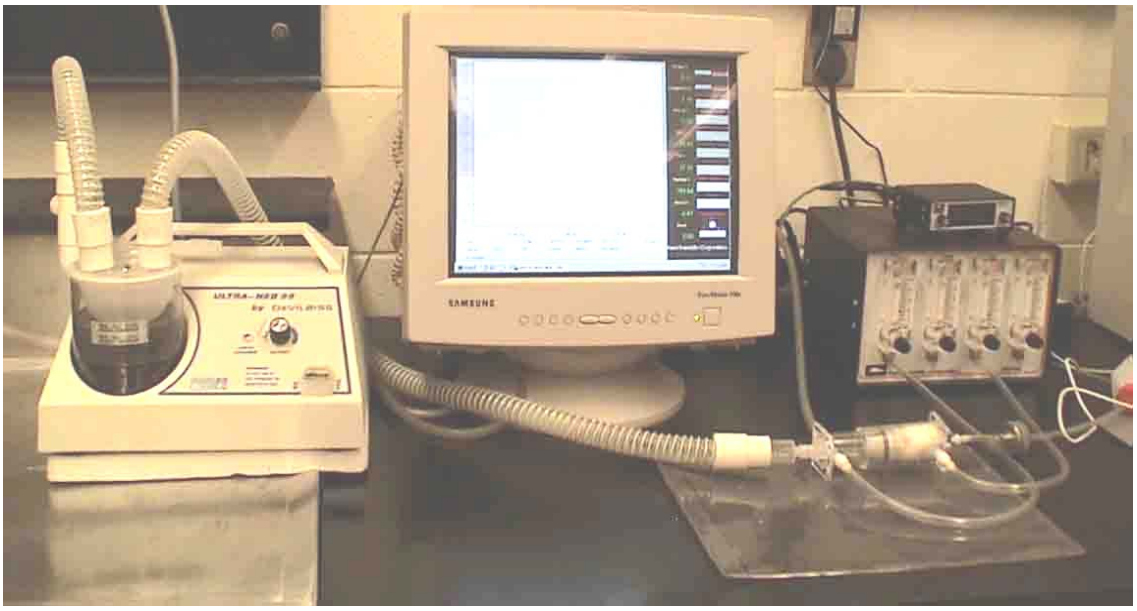

Figure 3-5: Whole-body plethysmography apparatus for mice.

3.6 Tissue Collection

Following airway responsiveness testing, animals were injected intraperitonally with 10 mg ketamine/kg body weight and 5 mg xylazine/kg body weight to induce anaesthesia. Mice were killed via cardiac puncture to allow for blood sample collection. Immediately thereafter mice lungs were flushed with 3 mL Hank's Balanced Salt Solution (HBSS; Sigma, H-4385). The bronchio-alveolar lavage fluid (BALF) was collected by three

infusions of 1 mL HBSS, with lungs being flushed twice per infusion. Following BALF collection, the right lobe of the lung was tied off and the left lobe was infused with immuno-electron microscopy (IEM) solution (2% paraformaldehyde, 1% gluteraldehyde). Fractions of liver and lung were processed for histological analysis (4% paraformaldehyde solution for 24 hours, washed with PBS and blocked in paraffin wax), or were flash-frozen in liquid nitrogen for enzyme-linked immunosorbant assay (ELISA) and quantitative real-time reverse-transcriptase polymerase chain reaction (qPCR) analysis.

3.7 Blood Total Leukocyte Count

Blood total leukocyte counts (TLC) were obtained by hemocytometer analysis following red blood cell lysis using a WBC determination kit (Unopette; #365856). Leukocytes were counted in four primary quadrants (each with 16 sub-quadrants), and the numbers were adjusted to reflect the theoretical total blood leukocyte level using the following equation:

$$TOTAL\ LEUKOCYTES/mL = (Sum\ of\ cells\ from\ 4\ quadrants)\ X\ 50\ X\ 10^3$$

3.8 Broncho-Alveolar Lavage Fluid (BALF) Total Leukocyte Count

Broncho-alveolar lavage fluid (BALF) total leukocyte counts (TLC) were obtained by hemocytometer analysis. Leukocytes were easily distinguished from the smaller red blood cells. Cells were counted in four primary quadrants (each with 16 sub-quadrants), and the numbers were adjusted to reflect the theoretical total BALF leukocyte level using

the following equation:

TOTAL LEUKOCYTES/mL = ((Total cells from 4 quadrants)/4) X 10^4

3.9 Broncho-alevolar Lavage Fluid (BALF) Cytospin Analysis

To characterize the composition of the broncho-alveolar lavage fluid (BALF) samples, cytospin slides were prepared. Broncho-alveolar lavage fluid samples (approximate volume: 3 mL) were centrifuged at 4000 rpm for 15 minutes (Beckman-Coulter; TJ-25 Centrifuge) at room temperature. Supernatent was removed leaving behind a cellular pellet, which was suspended in 100 μL of HBSS. The cellular solution was loaded into a chamber attached to a poly-L-lysine coated slide and cytocentrifuged at 1750 rpm for five minutes (Shandon; Cytospin3). Slides were fixed in 100% methanol for three minutes. Wright's staining allowed for leukocyte characterization via light microscopy. Neutrophil, macrophage and leukocyte numbers were expressed as a percentage and extrapolated to total BALF values per millilitre lavage fluid.

3.10 Tissue Analysis

Tissues, after processing (see Section 3.6), were prepared in the following manner:

3.10.1 Hematoxylin and Eosin (H&E) Staining

Sections (5-7 μm) were dewaxed in xylene and rehydrated in decreasing concentrations of ethanol followed by staining with hematoxylin (Vector; H3401) for 15 minutes. After washing, the slides were dipped in acid alcohol and run under tap water for three minutes.

Staining with eosin for two minutes was followed by a rinse in distilled water, and dehydration with an ethanol series and xylene. Cover slips were mounted.

3.10.2 Immunohistochemistry (IHC)

Sections (5-7 μm) were de-waxed in xylene and re-hydrated in decreasing concentrations of ethanol followed by incubation with 5% hydrogen peroxide (Sigma; H-1009) in methanol for 20 minutes to block endogenous peroxidase. After rinsing in water, the antigenic sites were exposed by incubation to 2 mg/mL pepsin in 0.01 N HCl for 60 minutes. The digestive action of pepsin was terminated by washing in phosphate-buffered saline (1 x PBS, pH 7.2). To prevent non-specific binding, the sections were blocked with 1% bovine serum albumin (BSA) (Sigma; A7906) in phosphate-buffered saline.

The consecutive sections were incubated with an appropriate antibody for 60 minutes followed by a secondary antibody for 30 minutes. All antibodies and the dilutions at which they were used are given in Appendix D. Horseradish peroxidase (HRP) conjugated streptavidin was added for 30 minutes, as necessary. Colour was developed for 10 minutes with a commercial kit (Vector Laboratories, Canada) and then rinsed under running water for five minutes. The IHC control sections were incubated with only secondary antibody or with primary anti-von Willebrand Factor (vWf) antibody.

3.11 Vascular Density Analysis

Mouse lungs were stained with CD34 to visualize the capillaries of the septum. Images were randomly taken of the alveolar septum proximal to bronchioles or large blood vessels. Images were taken in triplicate, digitised, and evaluated in PowerPoint. Superimposition of a 5x5 grid (area = 310 μm^2) allowed for consistent enumeration of microvessels per unit surface area. The replicates were averaged and statistical analyses were performed. Results were expressed as mean ± standard deviation.

3.12 Enzyme-Linked Immunosorbant Assay (ELISA)

Appendix E contains a detailed explanation of the ELISA protocol used for both Vascular Endothelial Growth Factor-A (VEGF-A), and Vascular Endothelial Growth Factor Receptor-1 (VEGFR-1). Briefly, the following procedure was used:

3.12.1 Tissue preparation

Tissue samples were homogenized in 1X HBSS at a dilution of 100 mg tissue per 1 mL HBSS. Homogenates were centrifuged for 15 minutes (25000 rcf at 4°C, Beckman-Coulter; TJ-25 Centrifuge) to precipitate debris. Samples were stored at –80°C. Tissue samples were thawed and further diluted in 1X HBSS (1 μL tissue sample in 3 μL HBSS) before being assayed.

3.12.2 Broncho-alveolar Lavage Fluid (BALF) preparation

Untreated BALF samples were frozen at –80°C. Samples were thawed and were assayed undiluted.

3.12.3 Enzyme-Linked Immunosorbant Assay (ELISA) procedure

Quantikine ELISA kits for mouse VEGF (R&D, Catalogue Number MMV00) and mouse sVEGFR-1 (R&D, Catalogue Number MVR100) were purchased. Both assays employ the quantitative sandwich enzyme immunoassay technique. Microplates came pre-coated with a polyclonal antibody specific for mouse VEGF or sVEGFR-1. All samples were brought to room temperature before use. Samples were assayed in triplicate.

Fifty microlitres of assay diluent were added to each well, and 50 µl of standard, control or samples were pipetted into the wells. The solutions were incubated for two hours at room temperature on a horizontal orbital microplate shaker. Each well was aspirated and washed five times with the wash buffer. One hundred microlitres of VEGF or VEGFR-1 conjugate was added to each well and incubated at room temperature for two hours on a shaker. Each well was aspirated and washed five times with wash buffer. One hundred microlitres of substrate solution were added to each well and incubated for 30 minutes at room temperature. One hundred microlitres of stop solution were added to each well and tapped gently to ensure thorough mixing. Bound proteins yielded a blue product that turned yellow when the stop solution was added. Optical density was determined using a BioRad 3550 microplate reader set to 450 nm.

3.13 Quantitative Real-time Reverse-Transcripatse Polymerase Chain Reaction (qPCR)

3.13.1 Tissue Preparation

RNA was extracted from tissues using a modified TRIzol/chloroform extraction protocol used in our laboratory (Appendix F). Five microlitres of the extracted RNA was redistributed in 450 μL RNAse-free water and optically quantified using the Pharmacia Biotech Gene Quant II Spectrophotometer with absorbance set at 260 and 280 nm. Measurement endpoints included optical density at 260 nm (OD260), the ratio of OD260 to OD280, the concentration of RNA, and the concentration of protein in the sample. The purity of extracted RNA was confirmed by running a 1.0% agarose gel. Gels were run at 100-115 V with ethidium bromide ultraviolet fluorescence detection. All extracts were used for qPCR analysis.

3.13.2 Complementary DNA synthesis

Extracted RNA was used to create complementary DNA (cDNA) using the StrataScript® QPCR cDNA Synthsis Kit (Stratagene, Catalogue #600554). Poly(A)+ mRNA was amplified by the PTC 200 Peltier Thermal Cycler (MJ Research, Massachusetts)using standard PCR and oligo dT primers. The cycles were 5 minutes at 25°C, 20 minutes at 42°C, 5 minutes at 95°C, and terminating at 4°C until samples were collected. The cDNA Master Mix allowed for production of high-quality qPCR-ready cDNA templates of the poly(A)+ RNA (mRNA). Amplified cDNA was used for qPCR analysis.

3.13.3 Quantitative Polymerase Chain Reaction (qPCR)

Quantitative PCR is an important method of gene expression analysis. Synthesized cDNA was amplified using the StrataScript® QPCR cDNA Synthesis kit and the Stratagene Mx3005P real-time reverse-transcriptase PCR machine. Primers bound to DNA sequences of interest allowed for gene quantification using the Brilliant® SYBR® Green QPCR Master Mix kit (Stratagene, Catalogue #600548). SYBR® Green 1 dye binds to the minor groove of double-stranded DNA (dsDNA), and fluoresces at 520 nm as per manufacturer's instructions. Primers used for this procedure are given in Appendix G.

3.14 Statistical Analysis

GraphPad Prism®4 statistical software was used to evaluate all data. Students' t-test were performed to compare two paired groups. One-way repeated measures ANOVA with Bonferonni post-hoc analysis were used to comapare three or more unmatched groups. Shapiro-Wilk normalcy test was used when necessary. Values were expressed as mean ± standard error of the mean (SEM). Significance was set at $p<0.05$.

4.0 RESULTS

4.1 Barn Air Quality Variables

Barn air quality variables evaluated include the total dust, in milligrams per cubic metre, actual and probable total bacteria, respirable bacteria, and non-respirable bacteria, all as colony forming units per cubic metre. Endotoxin levels were evaluated using the SKC Air Sampler, and the results were given as endotoxin units per cubic metre. Samples were taken twice per week for six weeks, and the results were averaged to give the mean (Table 4-1). Respirable bacteria comprised the majority of the bacteria sampled, with means of 8.76×10^4 and 1.11×10^5 CFU/m^3 for actual and probable counts, respectively. Total dust had a mean level of 1.87 mg/m^3, containing endotoxin at a level of 3.11×10^3 EU/m^3. Levels of bacteria and endotoxin in the Animal Care facilities and in the transport vehicle were below the levels of detection.

Table 4-1: Swine barn air quality variables including Total Dust (mg/m^3), Total Bacteria (CFU/m^3), Probably Total Bacteria (CFU/m^3), and Endotoxin Level (EU/m^3) expressed as the median, mean, and standard error of the mean (SEM).

Parameter	Median	Mean	SEM
Total Dust (mg/m^3)	1.77	1.87	0.17
Actual Total Bacteria (CFU/m^3)	1.06×10^5	1.05×10^5	9.99×10^3
Actual Respirable Bacteria (CFU/m^3)	8.98×10^4	8.76×10^4	8.15×10^3
Actual Non-respirable Bacteria (CFU/m^3)	1.57×10^4	1.78×10^4	2.12×10^3
Probable Total Bacteria (CFU/m^3)	1.36×10^5	1.61×10^5	2.29×10^4
Probable Respirable Bacteria (CFU/m^3)	1.14×10^5	1.11×10^5	1.19×10^4
Probable Non-respirable Bacteria (CFU/m^3)	2.15×10^4	5.03×10^4	1.39×10^4
Endotoxin Level (EU/m^3)	2.44×10^3	3.11×10^3	7.25×10^2

CFU = Colony forming units; EU = Endotoxin units; n = 11

4.2 Airway Responsiveness

After barn exposures were completed animals were subjected to whole-body plethysmography to assess methacholine-induced airway responsiveness. Mice were exposed to increasing concentrations of methacholine at flow rate of 0.5 mL/minute. Since some animals experienced significant distress during this procedure, not all animals were subjected to the high levels of methacholine. As such, results are given only for the doses of methacholine used for all animals (0, 0.75 and 1.5 mg methacholine/mL saline).

Wild-type and TLR4-mutant strains showed the same patterns of airway responsiveness after comparative barn exposures (Figure 4-1). Control animals showed a dose-dependent decrease in airway responsiveness, with air-flow decreasing to 50% of T_{ev1} after exposure to 1.5 mg mechacholine. Changes to airway responsiveness in one-day exposure groups were not significantly different from the control groups. After 5-days of barn air exposure both wild-type and mutant groups showed increased methacholine sensitivity ($p<0.05$) with airflow being 40% lower than control groups at 1.5 mg methacholine exposure. After 20-days barn air exposure wild-type and mutant groups showed a maximum decrease in air-flow to 20% of T_{ev1} after exposure to 1.5 mg mechacholine. Thus, after 20-days exposure, animals were less sensitive to methacholine than control groups ($p<0.05$).

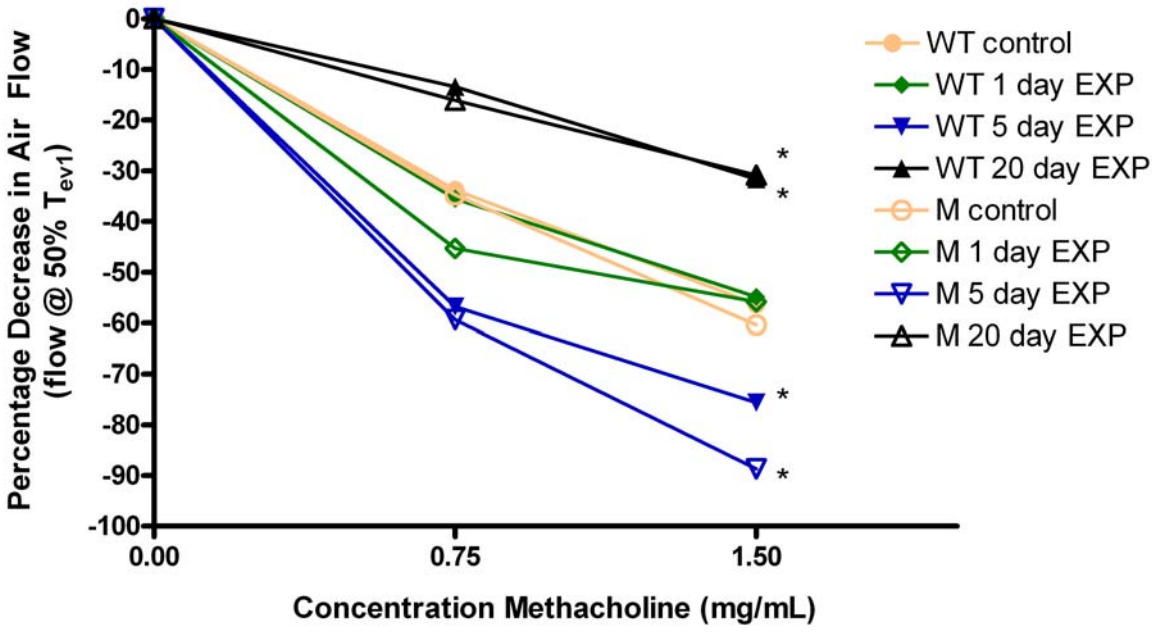

Figure 4-1: Airway responsiveness for wild-type (WT) and mutant (M) animals after 0-, 1-, 5-, or 20-day swine barn air exposures via methacholine challenge (n=76). Both strains exhibited similar patterns of methacholine response at all time periods. One-day exposure groups did not differ from control groups however, significant decreases were observed after five days exposure ($p < 0.05$). Twenty-day exposed groups showed lower airway responsiveness when compared to all other groups ($p < 0.05$). Statistics were run using one-way ANOVA and Bonferroni post-hoc analysis (* = $p<0.05$ vs. control group).

4.3 Broncho-alveolar Lavage Fluid (BALF) Total Leukocyte Count

Broncho-alveolar lavage fluid (BALF) total leukocyte counts (TLC) were obtained in a blinded fashion by hemocytometer analysis. Leukocytes were distinguished from the smaller red blood cells. After one-day barn air exposures, wild-type mice showed a 750% increase ($p<0.05$) in BALF total leukocytes compared to control groups (Figure 4-2). Five-day exposure groups were not significantly different from the control group, however, the trend toward higher leukocyte counts was preserved. After 20-days, the exposed mice showed no significant difference in leukocyte count when compared to

controls. Toll-like Receptor-4 mutant mice exhibited no significant difference in BALF total leukocyte count after one-, five- or 20-day barn air exposures when compared to control groups (Figure 4-3). Unlike with wild-type mice, there was a trend toward increased leukocyte count after five-day swine barn air exposures, but this trend was not maintained over time. Comparison of wild-type BALF total leukocytes against TLR4-mutant strain responses clearly indicated a TLR4-dependent increase in leukocyte counts after one-day swine barn air exposure (Figure 4-4). The mean leukocyte value in wild-type mice after one-day barn air exposure was 2.1 times that of their mutant counterpart ($p<0.05$).

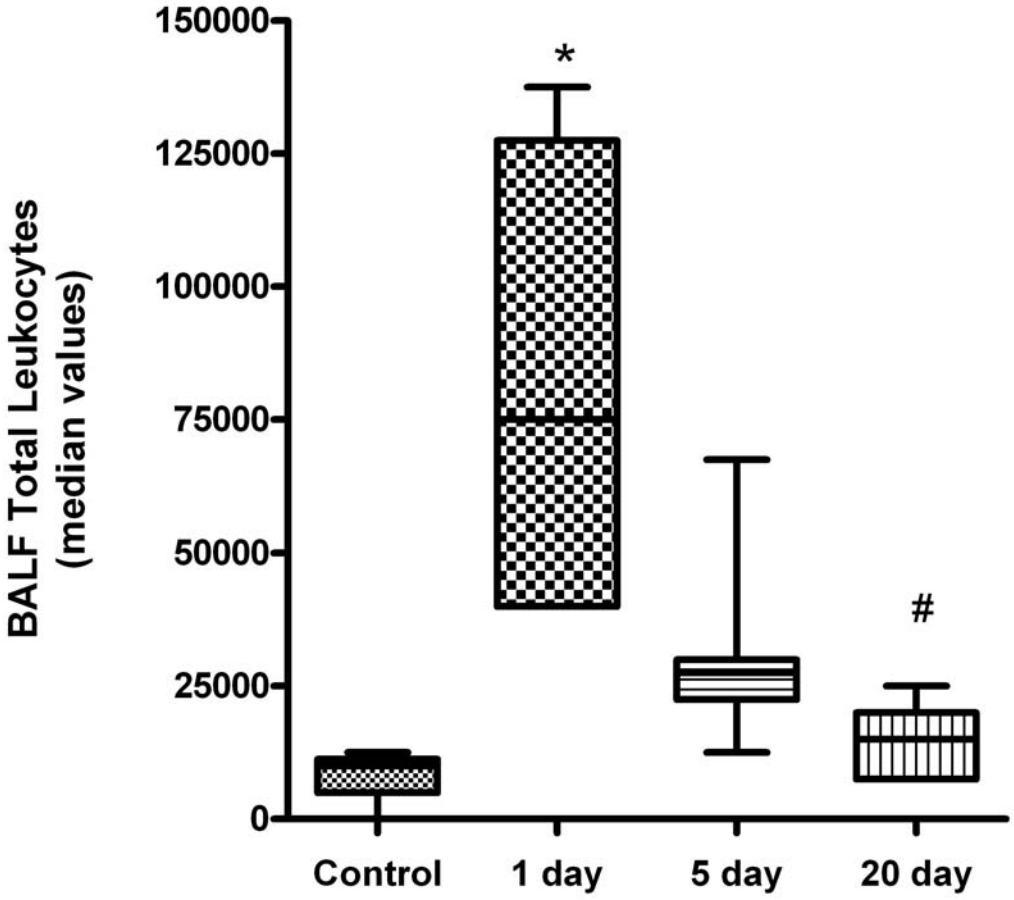

Figure 4-2: Broncho-alveolar lavage fluid (BALF) total leukocytes per millilitre BALF following 0-, 1-, 5-, or 20-day swine barn air exposures in wild-type (WT) animals. A significant increase in leukocyte numbers was observed after one-day exposure compared to the control group (n=38). Twenty-day exposure group was 20% lower than observed with the one-day exposure group (n=38). Expressed as mean ± standard deviation using one-way ANOVA and Bonferroni post-hoc analysis (* $p<0.05$ vs. control group; # $p<0.05$ vs. WT 1-day exposure group).

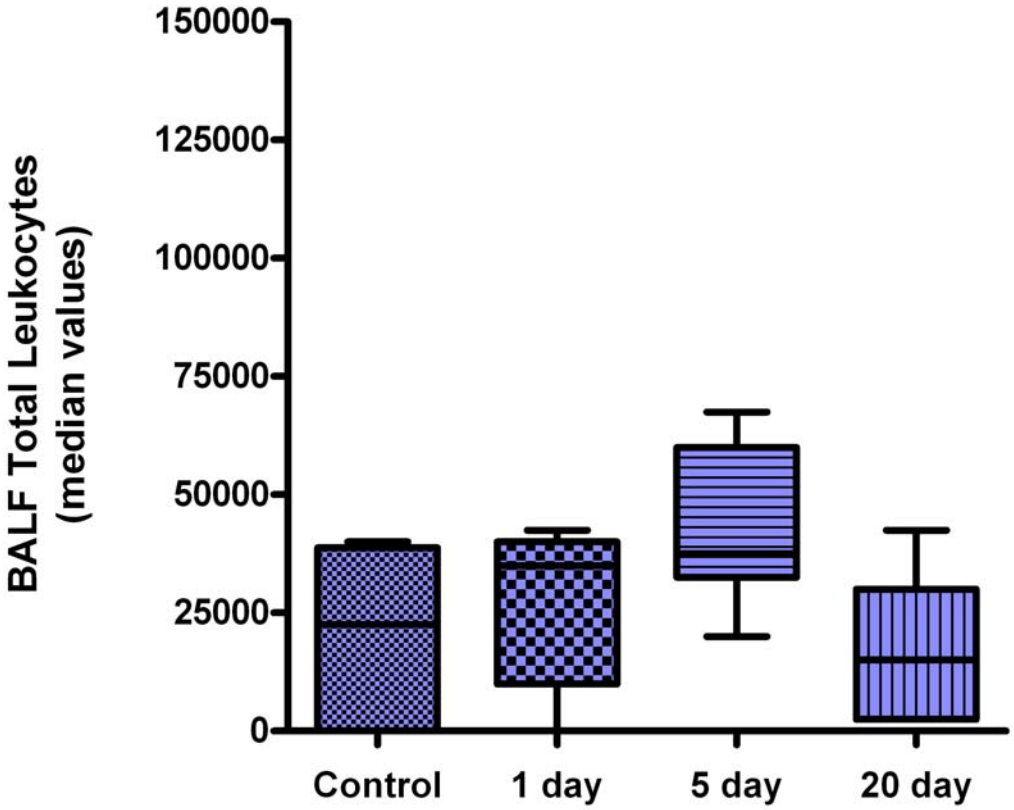

Figure 4-3: Broncho-alveolar lavage fluid (BALF) total leukocytes per millilitre BALF following 0-, 1-, 5-, or 20-day swine barn air exposures mutant (M) animals showed no significant differences between groups (n=38). Expressed as mean ± standard deviation using one-way ANOVA and Bonferroni post-hoc analysis ($p<0.05$ vs. control group).

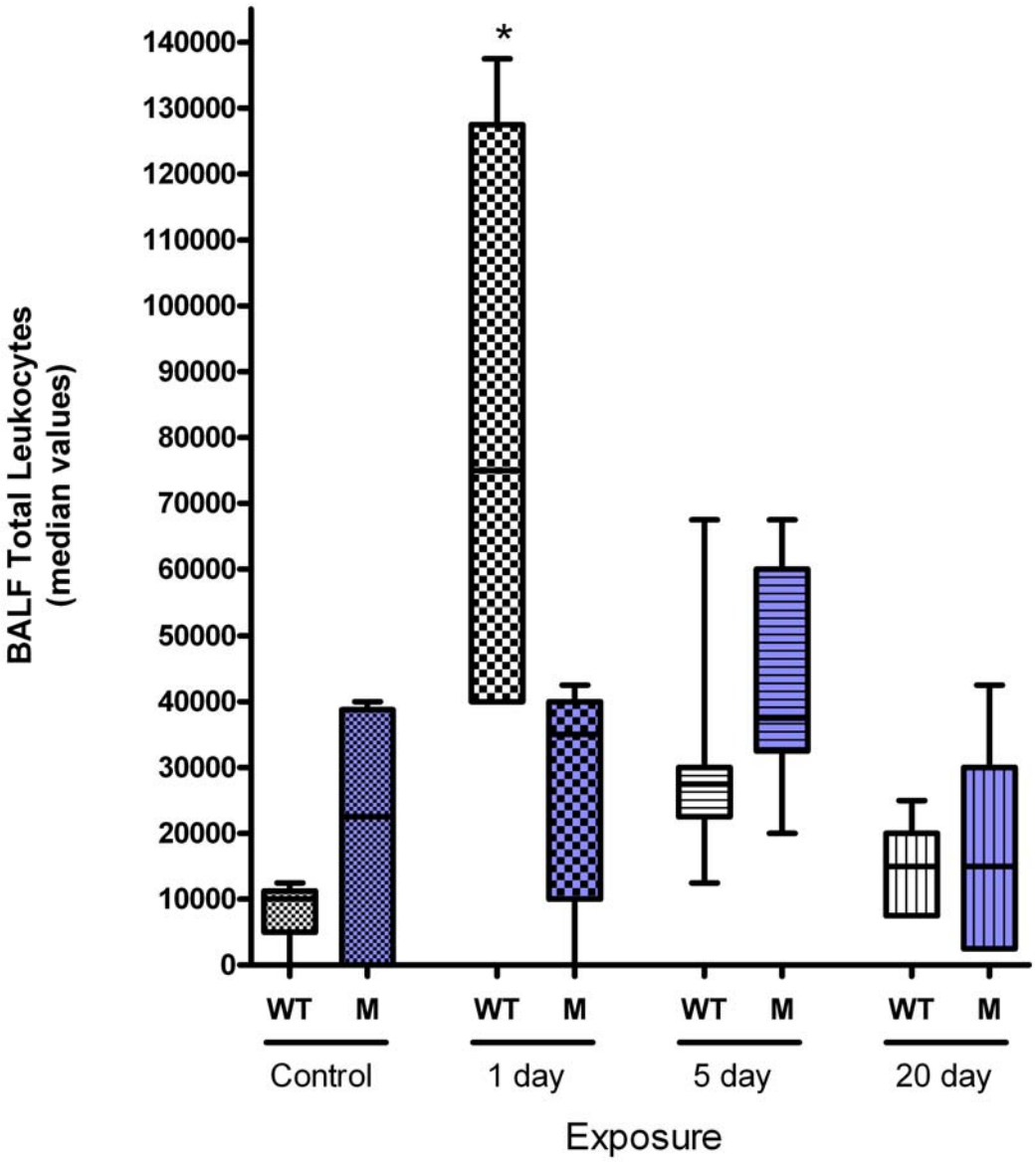

Figure 4-4: Comparative broncho-alveolar lavage fluid (BALF) total leukocyte counts in wild-type (WT) and mutant (M) animals per millilitre BALF following 0-, 1-, 5-, or 20-day swine barn air exposures (n=76). Leukocyte infiltration decreased over the 20-day exposure in wild-type and mutant strains. Expressed as mean ± standard deviation using one-way ANOVA and Bonferroni post-hoc analysis (* $p<0.05$ vs. matched M animal).

4.4 Broncho-alveolar Lavage Fluid (BALF) Cytospin Analysis

To characterize the composition of the broncho-alveolar lavage fluid (BALF) samples, cytospin slides were prepared. Wright's staining allowed for leukocyte characterization via light microscopy in a blinded fashion. Neutrophil, macrophage and leukocyte numbers were expressed as a percentage and extrapolated to total BALF values. The following figures address the changes observed in the BALF for macrophages, neutrophils, and leukocytes following Wright's staining.

4.4.1 Broncho-alveolar Lavage Fluid (BALF) Absolute Macrophage Count

A TLR4 dependent increase in BALF absolute macrophage count was observed in wild-type mice after one-day barn air exposure (Figure 4-5), with one-day exposure groups having 6.5 times the number of macrophages than the control group ($p<0.05$). Five-day and 20-day exposure groups were not significantly different from the control group. The trend toward higher leukocyte counts was preserved with median leukocyte levels being 2.6 and 0.9 that of the control group, respectively. Toll-like Receptor-4 mutant mice exhibited no difference in absolute macrophage count after one-, five- or 20-day barn air exposures when compared to control groups (Figure 4-6). Unlike with wild-type mice, there was a trend toward increased leukocyte count after five-day swine barn air exposures. Comparison of wild-type responses against TLR4-mutant strain responses clearly indicated a TLR4-dependent increase in leukocyte counts after one-day swine barn air exposure (Figure 4-7). The mean absolute macrophage count in wild-type mice after one-day barn air exposure was 2.4 times that of their mutant counterpart ($p<0.05$).

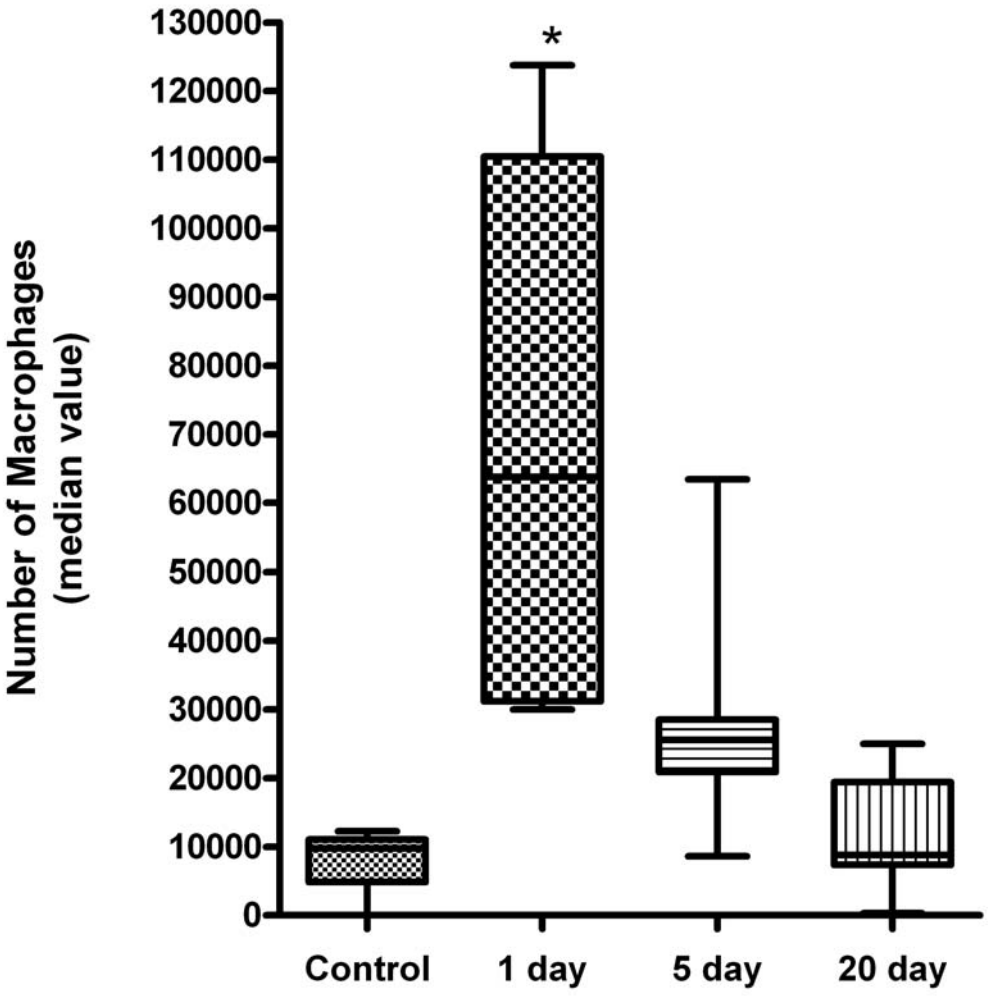

Figure 4-5: Broncho-alveolar lavage fluid (BALF) absolute macrophages per millilitre BALF following 0-, 1-, 5-, or 20-day swine barn air exposures in wild-type (WT) animals showed a significant increase in macrophage numbers after one-day exposure (n=38). Expressed as mean ± standard deviation using one-way ANOVA and Bonferroni post-hoc analysis (* $p<0.05$ vs. control group).

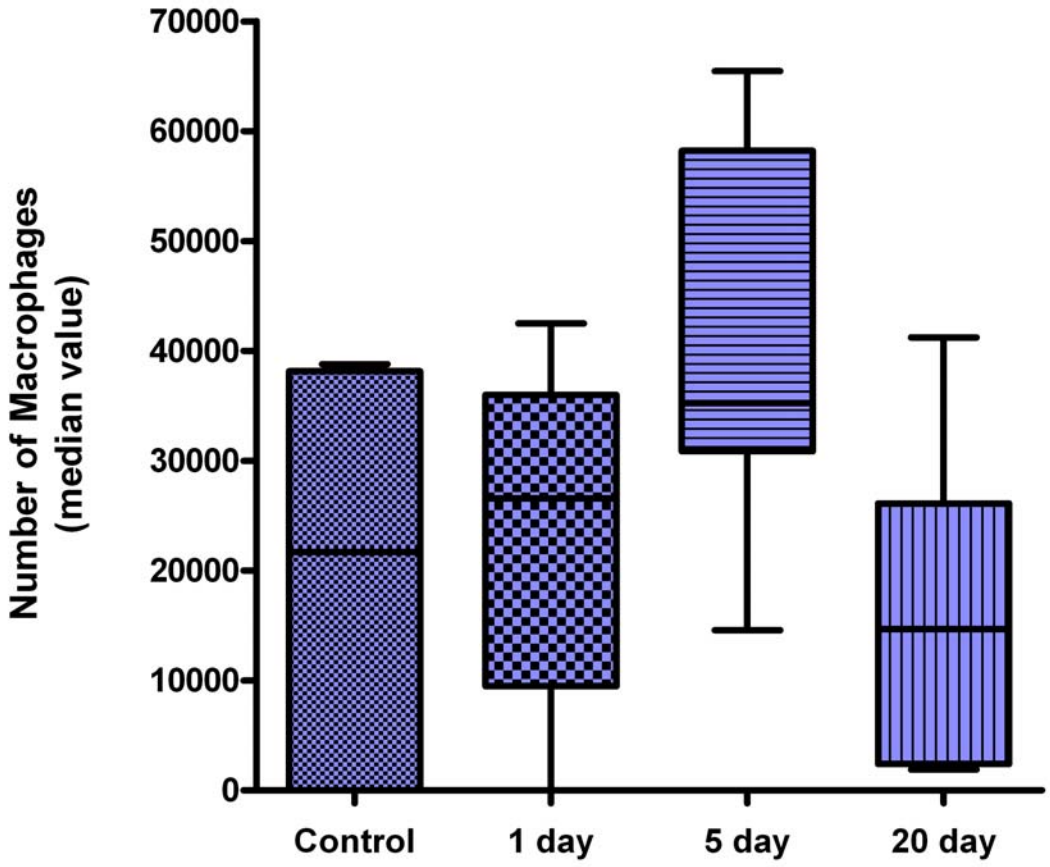

Figure 4-6: Broncho-alveolar lavage fluid (BALF) absolute macrophages per millilitre BALF following 0-, 1-, 5-, or 20-day swine barn air exposures mutant (M) animals showed no significant differences between groups (n=38). Expressed as mean ± standard deviation using one-way ANOVA and Bonferroni post-hoc analysis ($p<0.05$ vs. control group).

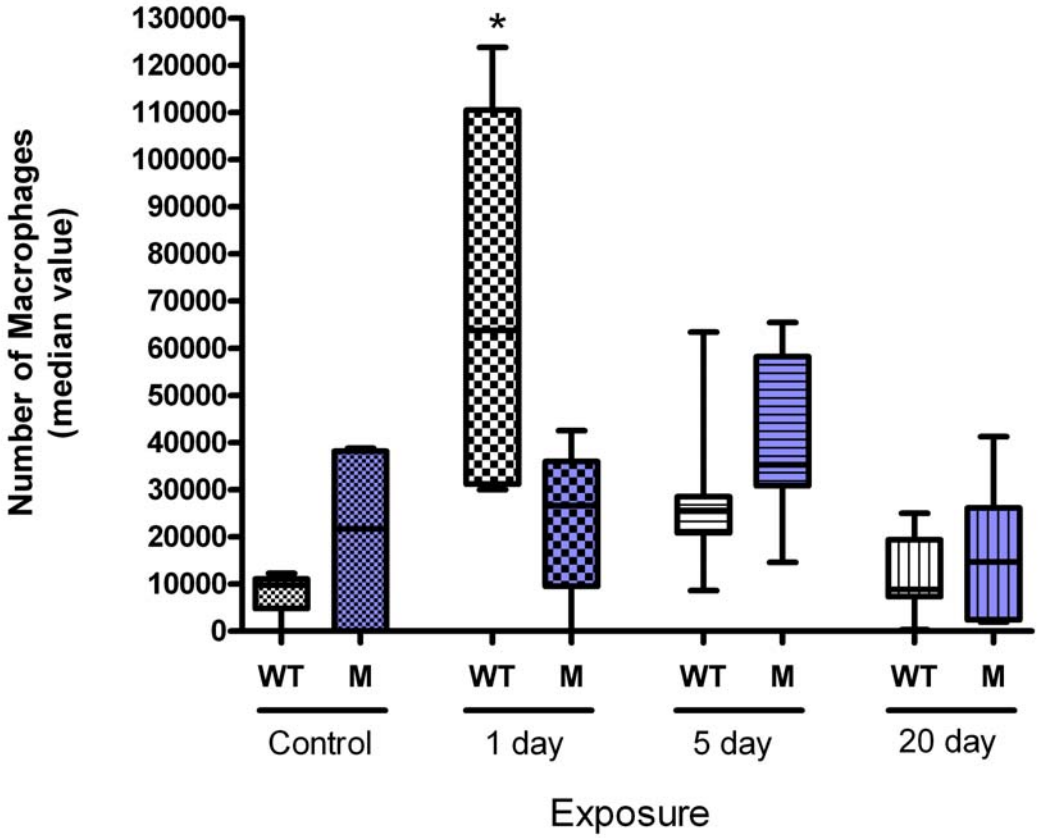

Figure 4-7: Comparative broncho-alveolar lavage fluid (BALF) absolute macrophage counts in wild-type (WT) and mutant (M) animals per millilitre BALF following 0-, 1-, 5-, or 20-day swine barn air exposures. A Toll-like receptor-4 (TR4)-dependent increase in macrophages count after one-day barn air exposure was observed in WT animals (n=76). Macrophage infiltration decreased over the 20-day exposure in wild-type and mutant strains. Expressed as mean ± standard deviation using one-way ANOVA and Bonferroni post-hoc analysis (* $p<0.05$ vs. matched M animal).

4.4.2 Broncho-alveolar Lavage Fluid (BALF) Absolute Neutrophil Count

Similar to the macrophage results, a TLR4 dependent increase in BALF absolute neutrophil count was observed in wild-type mice after one-day barn air exposure (Figure 4-8), with one-day exposure groups being 56.6-fold greater than control groups ($p<0.05$). Five-day and 20-day exposure groups were not significantly different from the control group. Toll-like Receptor-4 mutant mice exhibited no difference in absolute neutrophil count after one-, five- or 20-day barn air exposures when compared to control groups (Figure 4-9). There was a trend toward elevated neutrophil levels after one-day barn air exposure, however, this trend was not significant, and was not maintained over time. Comparison of wild-type responses against TLR4-mutant strain responses showed a TLR4-dependent increase in neutrophil counts after one-day swine barn air exposure (Figure 4-10). The mean absolute neutrophil count in wild-type mice after one-day barn air exposure was 8.76 times greater than their mutant counterpart ($p<0.05$).

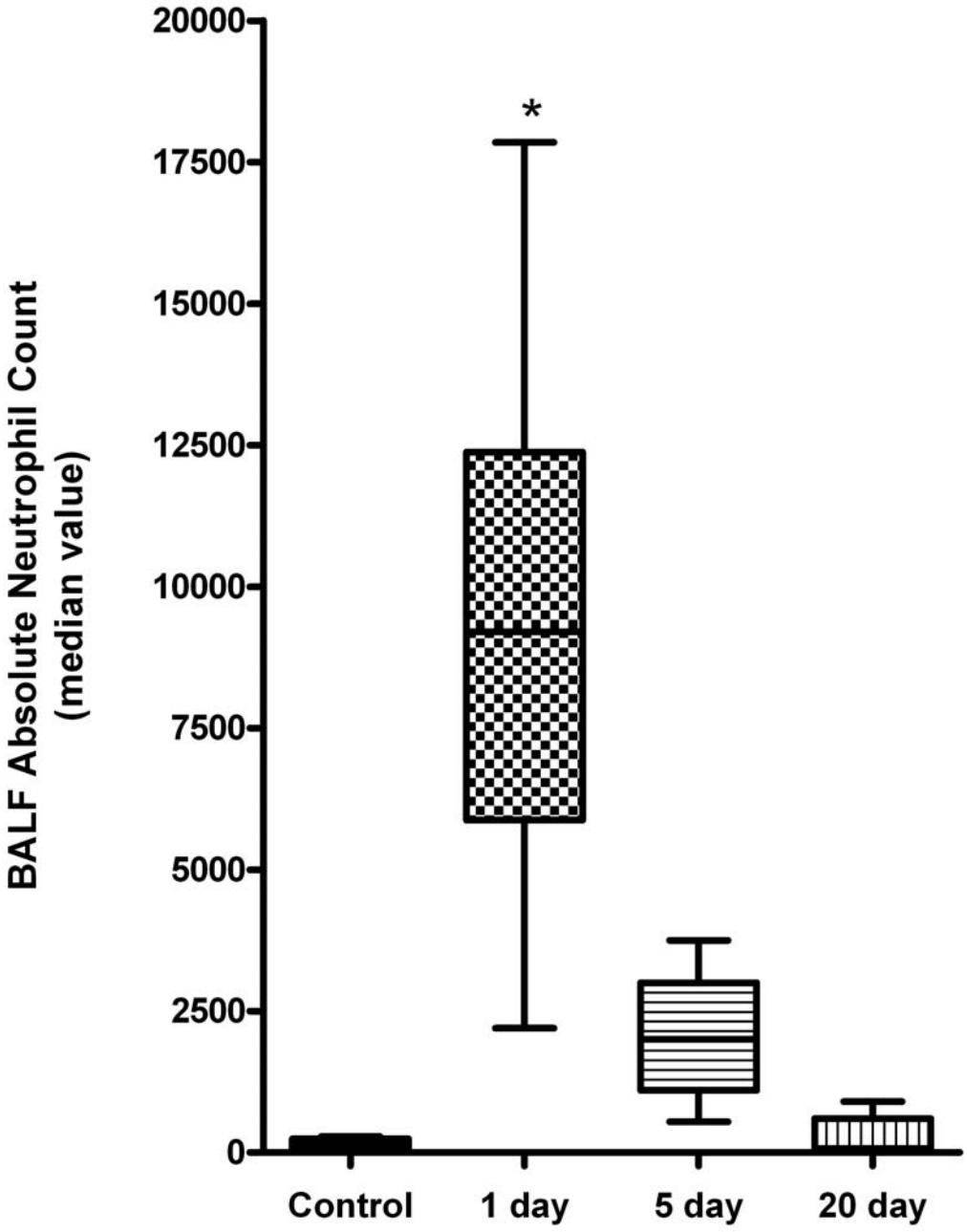

Figure 4-8: Broncho-alveolar lavage fluid (BALF) absolute neutrophils per millilitre BALF following 0-, 1-, 5-, or 20-day swine barn air exposures in wild-type (WT) animals showed a significant increase in neutrophil numbers after 1-day exposure (n=38). Expressed as mean ± standard deviation using one-way ANOVA and Bonferroni post-hoc analysis (* $p<0.05$ vs. control group).

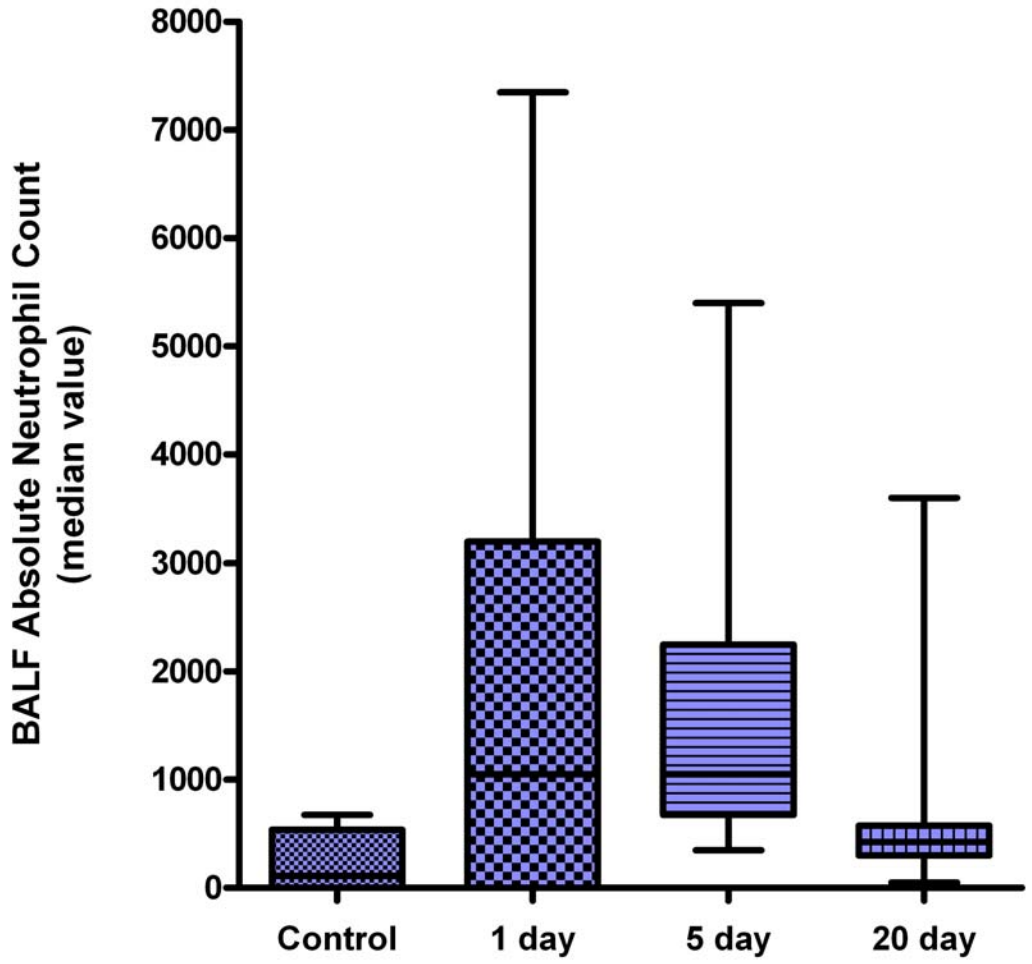

Figure 4-9: Broncho-alveolar lavage fluid (BALF) absolute neutrophils per millilitre BALF following 0-, 1-, 5-, or 20-day swine barn air exposures mutant (M) animals showed no significant differences between groups (n=38). Expressed as mean ± standard deviation using one-way ANOVA and Bonferroni post-hoc analysis ($p<0.05$ vs. control group).

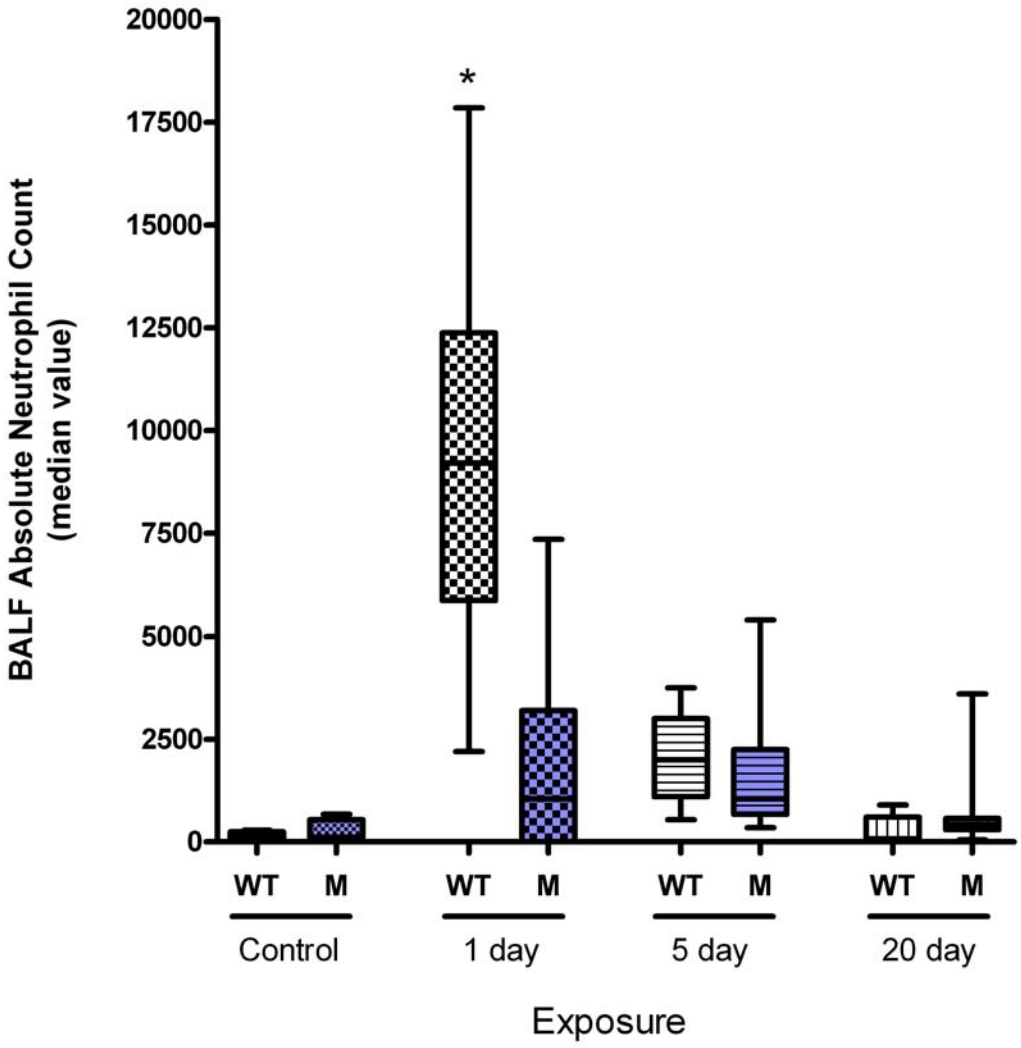

Figure 4-10: Broncho-alveolar lavage fluid (BALF) absolute neutrophil count in wild-type (WT) and mutant (M) animals per millilitre BALF following 0-, 1-, 5-, or 20-day swine barn air exposures (n=76). Observed a Toll-like receptor-4 (TLR4)-dependent increase in neutrophils after one-day barn air exposure. Neutrophil infiltration decreased over the 20-day exposure in wild-type animals. Mutant animals had no significant difference over time. Expressed as mean ± standard deviation using one-way ANOVA and Bonferroni post-hoc analysis (* $p<0.05$ vs. matched M animal).

4.4.3 Broncho-alveolar Lavage Fluid (BALF) Absolute Lymphocyte Count

Similar to the macrophage and neutrophil results, a TLR4 dependent increase in BALF absolute lymphocyte count was observed in wild-type mice after one-day barn air exposure (Figure 4-11). One-day exposure groups had 6.5 times greater lymphocyte count than the control group ($p<0.05$). A trend toward elevated lymphocyte counts was preserved after five-day barn air exposure. However, five-day and 20-day exposure groups were not significantly different from the control group, with median values of 2000 and 75, respectively. Toll-like Receptor-4 mutant mice showed a significant (1.6 times greater, $p<0.05$) elevation in absolute lymphocyte count after five-day barn air exposures when compared to control groups (Figure 4-12). There was a trend toward elevated lymphocyte levels after one-day barn air exposure, however, this trend was not significant, and was not maintained over the 20-day exposure period. Comparison of wild-type responses against TLR4-mutant strain responses clearly indicated a TLR4-dependent increase in lymphocyte counts after one-day swine barn air exposure (Figure 4-13). The mean absolute lymphocyte count in wild-type mice after one-day barn air exposure was approximately 2.4-fold greater than their mutant counterpart.

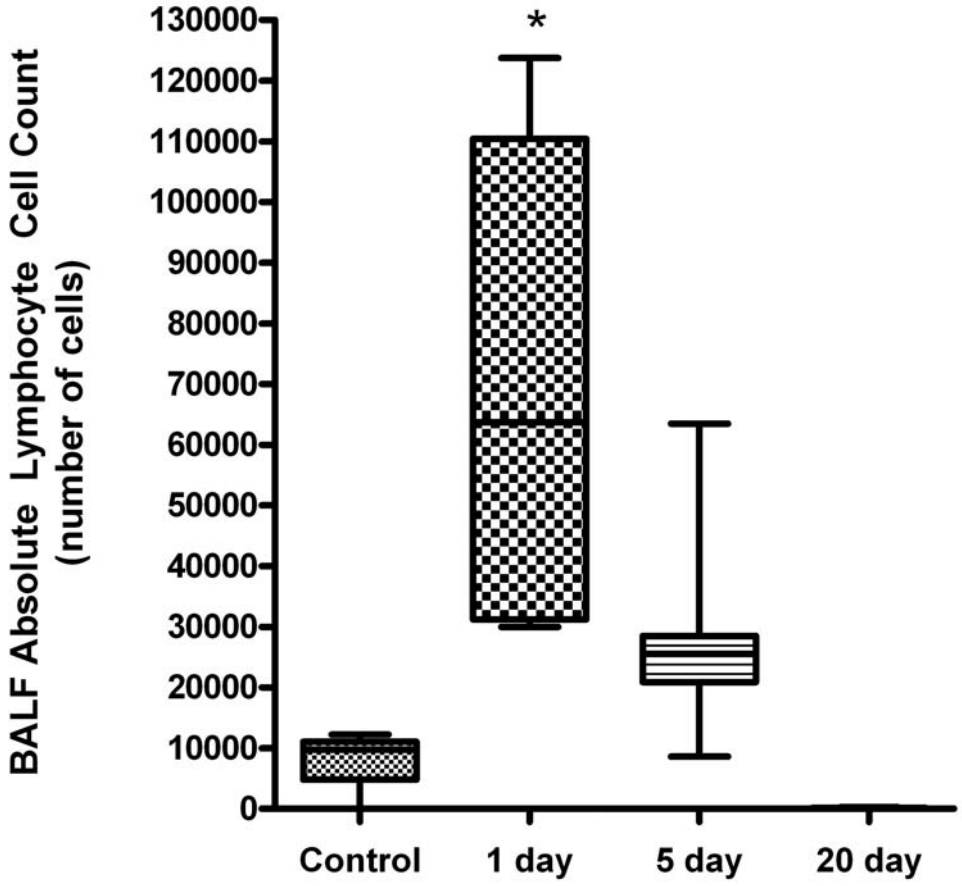

Figure 4-11: Broncho-alveolar lavage fluid (BALF) absolute lymphocytes per millilitre BALF following 0-, 1-, 5-, or 20-day swine barn air exposures in wild-type (WT) animals showed a significant increase in lymphocyte numbers after one-day exposure (n=38). Expressed as mean ± standard deviation using one-way ANOVA and Bonferroni post-hoc analysis (* $p<0.05$ vs. control group).

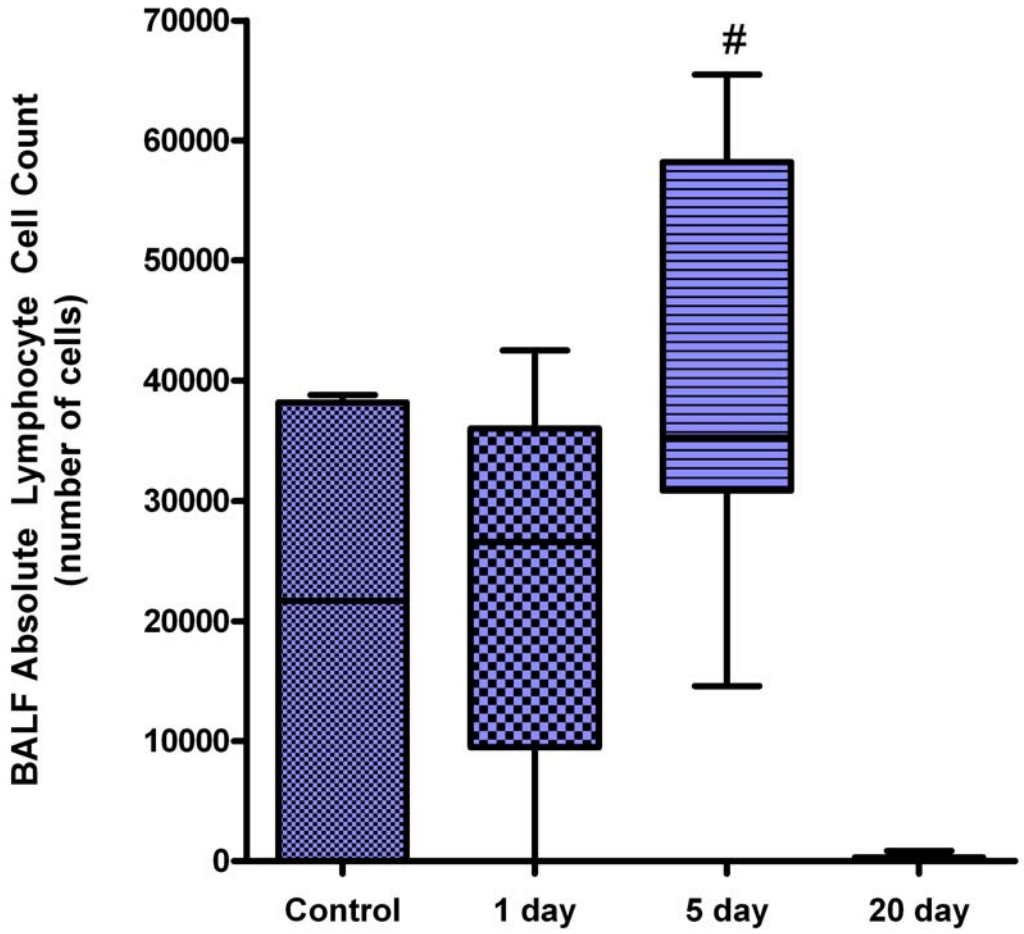

Figure 4-12: Broncho-alveolar lavage fluid (BALF) absolute lymphocytes per millilitre BALF following 0-, 1-, 5-, or 20-day swine barn air exposures mutant (M) animals showed no significant differences between groups (n=38). Expressed as mean ± standard deviation using one-way ANOVA and Bonferroni post-hoc analysis (# $p<0.05$ vs. control group and 20-day exposure group).

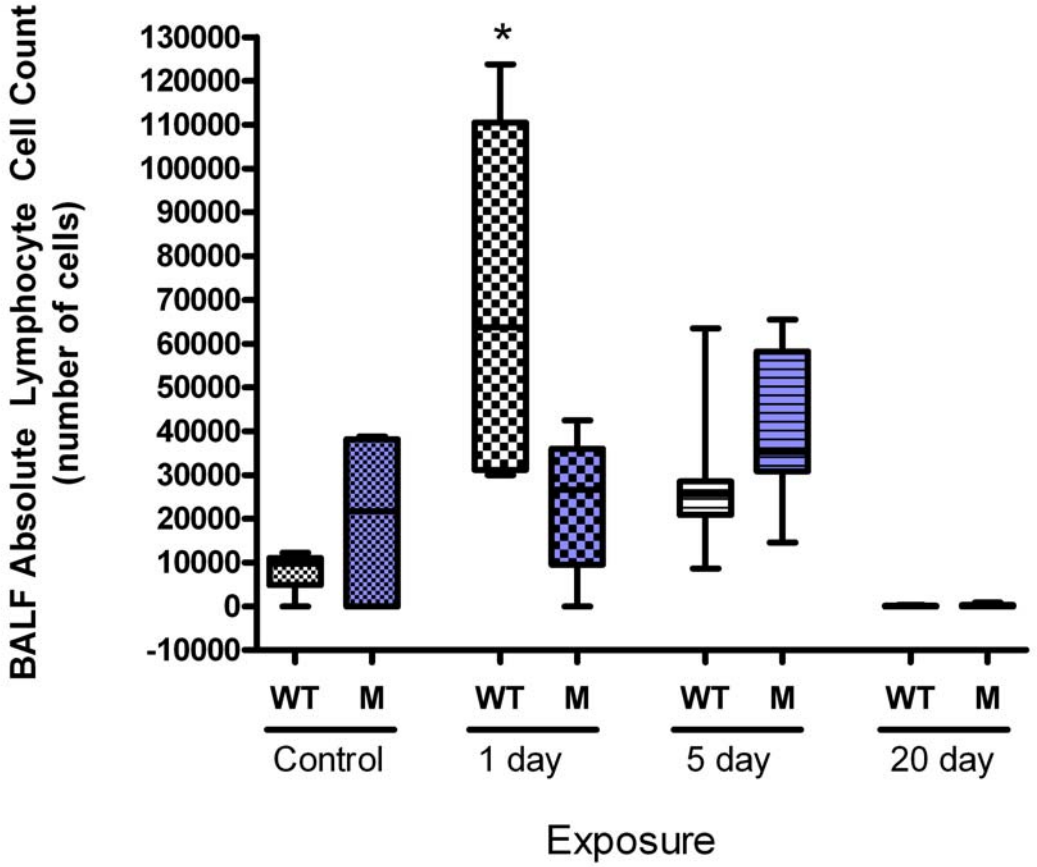

Figure 4-13: Broncho-alveolar lavage fluid (BALF) absolute lymphocytes count in wild-type (WT) and mutant (M) animals per millilitre BALF following 0-, 1-, 5-, or 20-day swine barn air exposures (n=76). Observed a Toll-like receptor-4 (TLR4)-dependent increase in lymphocytes after one-day barn air exposure. Lymphocyte infiltration decreased over the 20-day exposure in wild-type animals. Mutant animals had no significant difference over time. Expressed as mean ± standard deviation using one-way ANOVA and Bonferroni post-hoc analysis (* $p<0.05$ vs. matched M animal).

4.5 Blood Total Leukocyte Count

Blood total leukocyte counts (TLC) were obtained in a blinded fashion by hemocytometer analysis. Leukocytes were distinguished from the smaller red blood cells. Blood total leukocyte counts exhibited similar patterns to the BALF total leukocyte counts. A TLR4 dependent increase in blood total leukocytes was observed in wild-type mice after one-day barn air exposure (Figure 4-14), with one-day exposure groups having 2.6-times greater total leukocyte count than the control group. Five- and 20-day exposure groups were not significantly different from the control group, however, the trend toward higher leukocyte counts was preserved. Toll-like Receptor-4 mutant mice exhibited no difference in blood total leukocyte count after one-, five- or 20-day barn air exposures when compared to control groups (Figure 4-15). Comparison of wild-type blood total leukocytes against TLR4-mutant strain responses clearly indicated a TLR4-dependent increase in leukocyte counts after one-day swine barn air exposure (Figure 4-4). The mean leukocyte value in wild-type mice after one-day barn air exposure was twice that of their mutant counterpart ($p<0.05$).

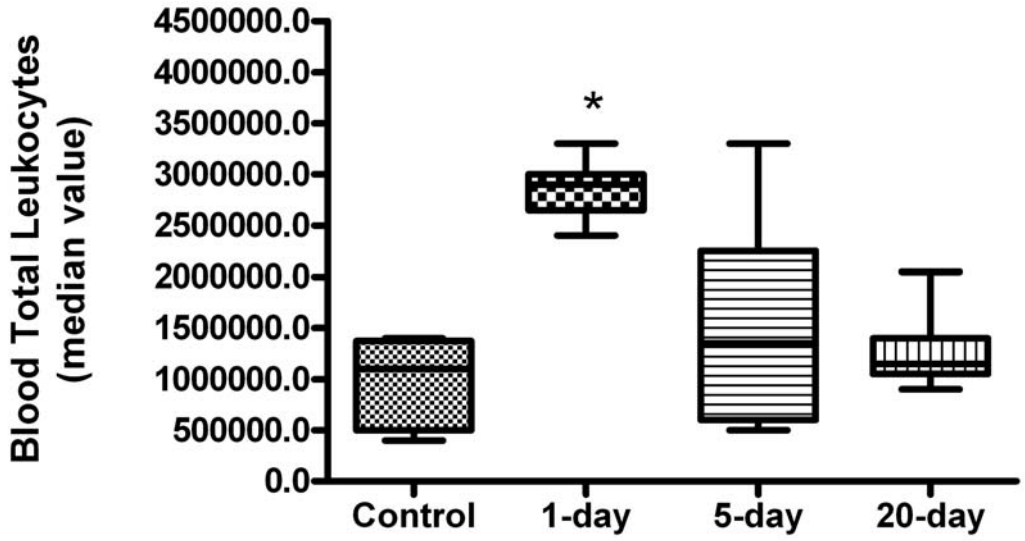

Figure 4-14: Blood total leukocytes per millilitre blood following 0-, 1-, 5-, or 20-day swine barn air exposures in wild-type (WT) animals showed a significant increase in leukocyte numbers after 1-day exposure (n=38). Expressed as mean ± standard deviation using one-way ANOVA and Bonferroni post-hoc analysis (* $p<0.05$ vs. control group).

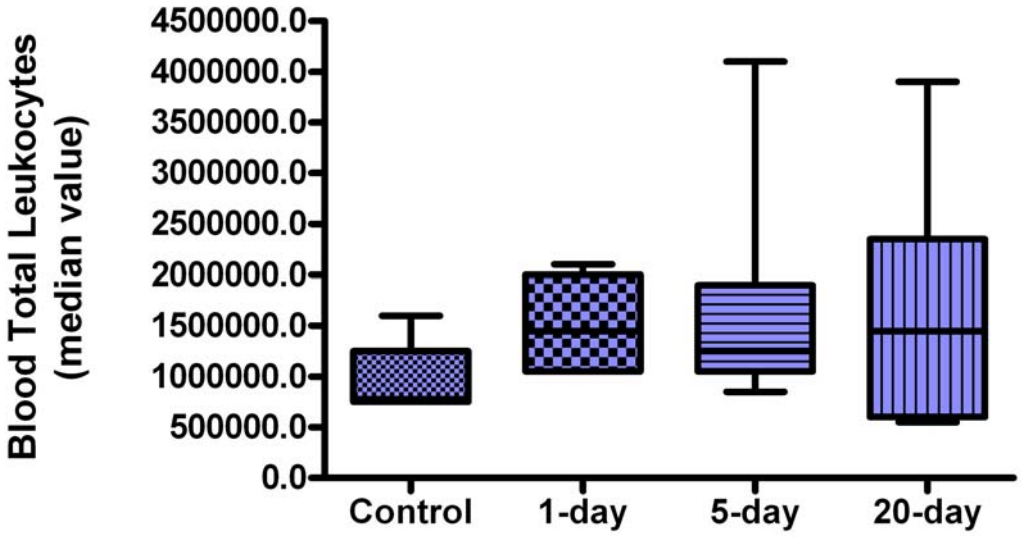

Figure 4-15: Blood total leukocytes per millilitre blood following 0-, 1-, 5-, or 20-day swine barn air exposures mutant (M) animals showed no significant differences between groups (n=38). Expressed as mean ± standard deviation using one-way ANOVA and Bonferroni post-hoc analysis ($p<0.05$ vs. control group).

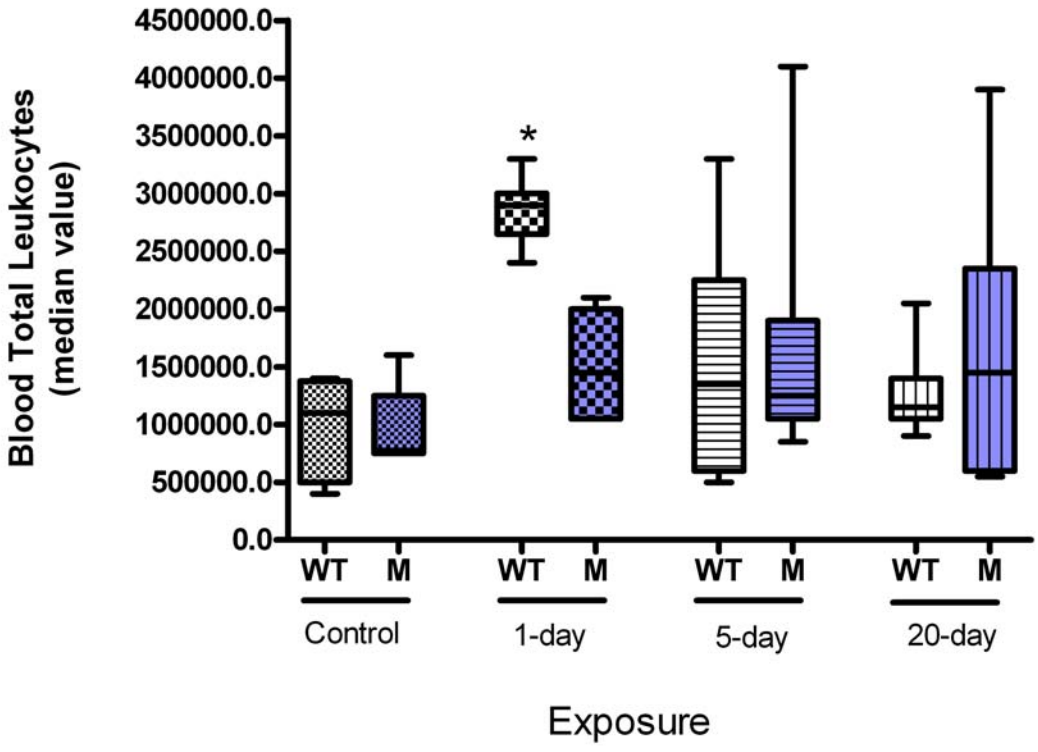

Figure 4-16: Comparative blood total leukocyte counts in wild-type (WT) and mutant (M) animals per millilitre blood following 0-, 1-, 5-, or 20-day swine barn air exposures (n=76). A Toll-like receptor-4 (TR4)-dependent increase in leukocyte count after one-day barn air exposure was observed in WT animals. Leukocyte infiltration decreased over the 20-day exposure in wild-type and mutant strains. Expressed as mean ± standard deviation using one-way ANOVA and Bonferroni post-hoc analysis (* $p<0.05$ vs. matched M animal).

4.6 Immunohistochemistry (IHC)

Immunohistochemistry (IHC) is a molecular technique that can allow for qualitative assessment of protein expression in histological specimens. Positive and negative controls sections are generated to ensure there are no problems with the methods or the antibodies and reagents being used.

Positive (purple stain present) and negative control sections (no purple staining) for the immunohistochemistry are given in Figure 4-17.

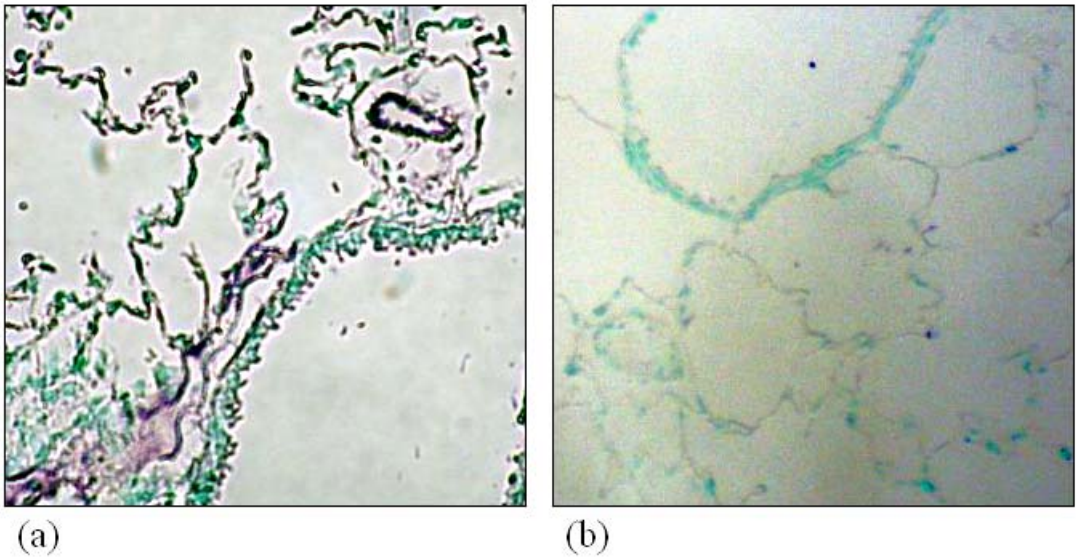

Figure 4-17: Control sections used for immunohistochemistry in the alveolar septum: (a) positive control section (using vonWillebrand Factor; vWf), and (b) negative control section (using bovine serum albumin; BSA) (10x optical magnification).

4.6.1 Toll-Like receptor-4 (TLR4)

Visualization of the lung tissue clearly showed expression of TLR4 in both the wild-type and mutant lungs (Figure 4-18). As expected, the TLR4-mutant animals do express TLR4 at levels lower than observed in the wild-type animal (Figure 4-17). Based upon the mutation described for the TLR4-mutant animal their TLR4 is hyporesponsive to LPS. As such, the TLR4 carried by the mutant strain should not result in a TLR4-mediated inflammatory response to endotoxin. There did not appear to be induction of this receptor in mutant strains following multiple barn air exposures. To confirm the differences in TLR4 expression between wild-type and TLR4-mutant strains, immunohistochemistry was performed using a goat anti-mouse TLR4 antibody. Positive staining for TLR4 is observed as the dark purple areas of the lung.

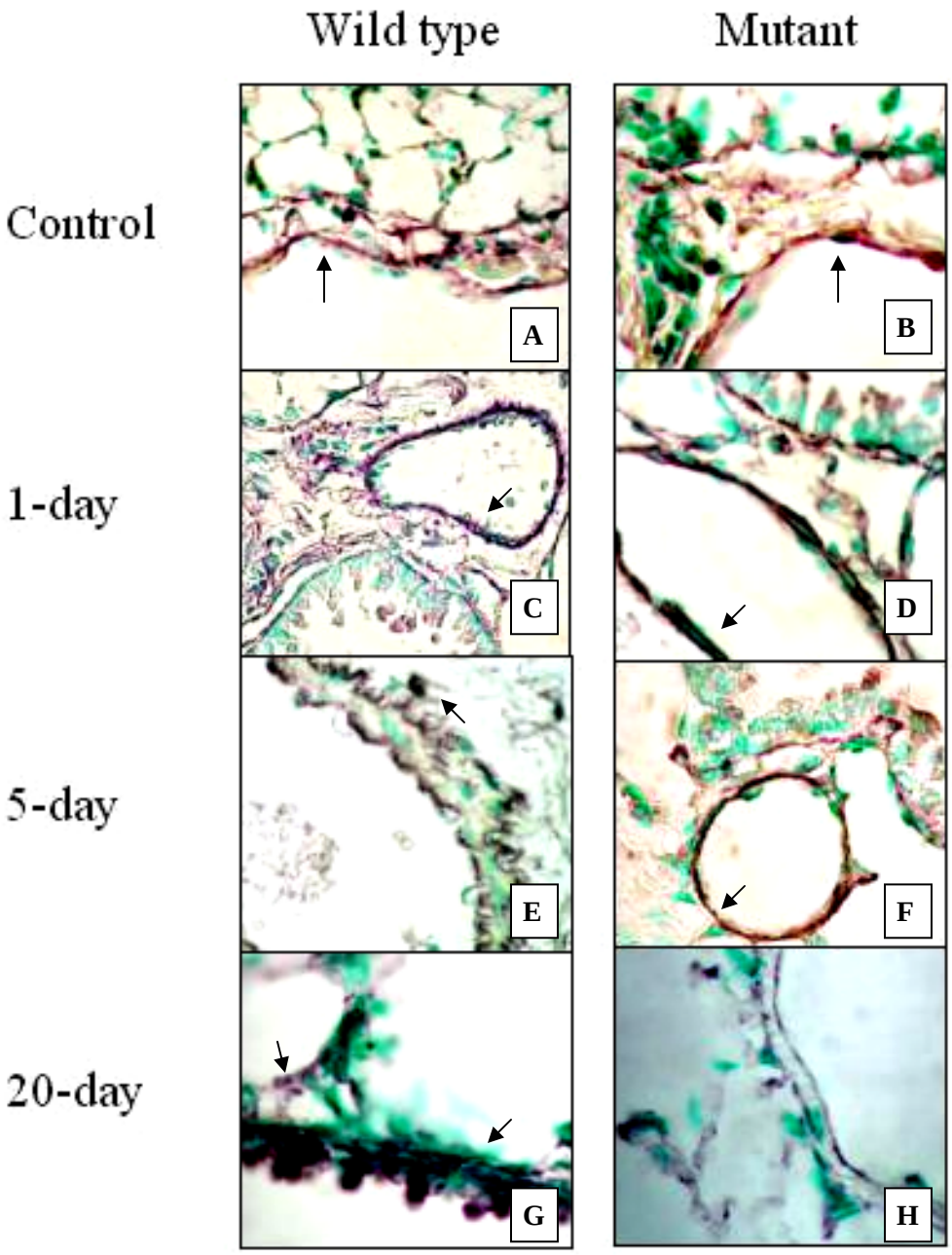

Figure 4-18: Comparative Toll-like Receptor-4 immuohistochemistry in the alveolar septum of wild-type and mutant mouse lungs following 1-, 5- or 20-day swine barn air exposures (40x optical magnification). Arrows show: A & B – TLR4 stained pulmonary epithelial cells; C, D & F – TLR4 staining on endothelial cells; E – TLR4 staining on alveolar macrophage; G – high TLR4 expression on bronchiolar epithelial cells and endothelial cells.

4.6.1.1 Toll-like Receptor-4 and bronchiolar epithelial cells

For both wild-type and mutant mouse strains, TLR4 was observed in the bronchiolar areas. Wild-type mice expressed TLR4 to higher degree in the peri-bronchiolar areas, though staining for TLR4 was observed in both strains (Figure 4-19, arrows). Wild-type mice expressed TLR4 on the apical side of the bronchiolar epithelium. This pattern of expression was not observed in the mutant strain of mouse, even after 20-days barn air exposure (Figure 4-19, section b).

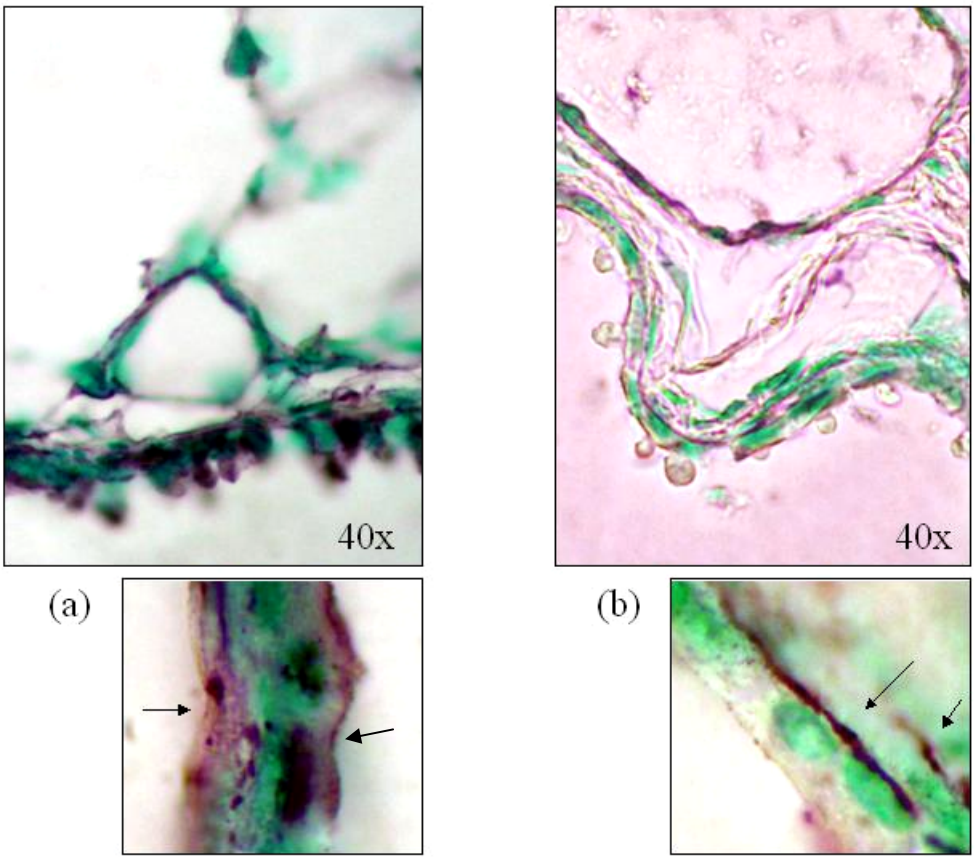

Figure 4-19: Comparative Toll-like Receptor-4 immuohistochemistry of bronchiolar epithelial cells in the alveolar septum of wild-type (a) and mutant (b) mouse lungs following 20-day swine barn air exposures (40x and 100x optical magnification). Expression of TLR4 in the peri-bronchiolar areas of the alveolar septum was observed for both wild-type and mutant mouse strains, with wild-type tissues exhibiting both apical and basolateral staining (see arrows).

4.6.1.2 Toll-like Receptor-4 and vascular endothelial cells

Toll-like Receptor-4 was expressed on vascular endothelial cells of both wild-type and mutant strains. As observed with the bronchiolar epithelial cells, wild-type mice expressed TLR4 to higher degree than the mutant strains, as evidenced by darker and more condensed staining (Figure 4-20).

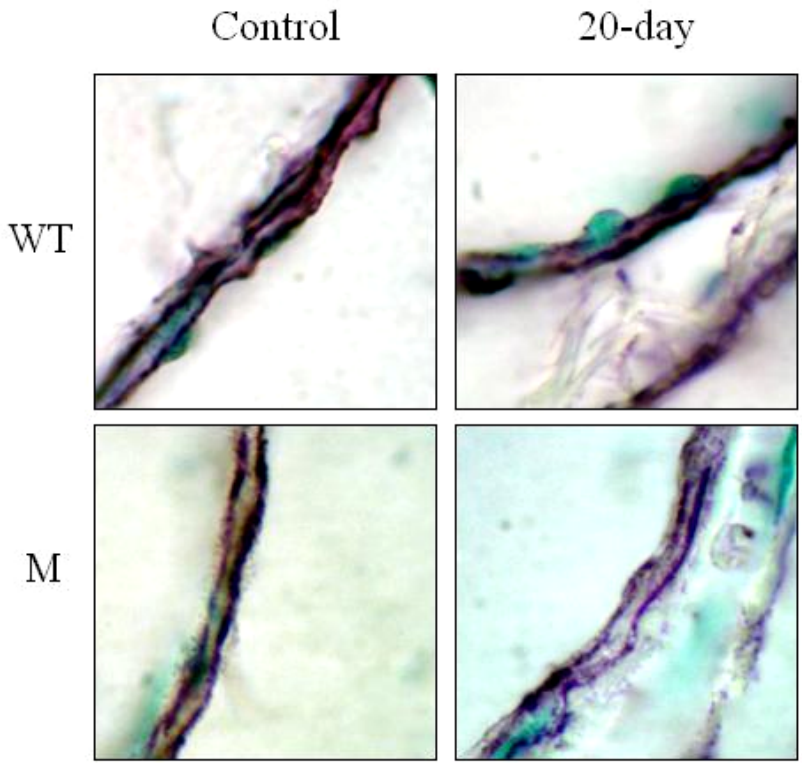

Figure 4-20: Comparative Toll-like Receptor-4 immuohistochemistry of vascular endothelial cells and epithelial cells in the blood vessels of the septum of wild-type (WT) and mutant (M) mouse lungs in control animal lungs and following 20-day swine barn air exposures (100x optical magnification). Toll-like Receptor-4 is clearly expressed on the vascular endothelial cells of both mutant and wild-type animals, but to much higher degree in wild-type tissues.

4.2.1.3 Toll-like Receptor-4 and macrophages/monocytes

Toll-like Receptor-4 was expressed macrophages/monocytes of wild-type animals, and showed marked induction of expression with multiple swine barn air exposures (Figure 4-21). Mutant mice macrophages/monocytes did not express TLR4 to large degree on macrophage/monocyte cells, and showed no change in TLR4 expression over time (Figure 4-21).

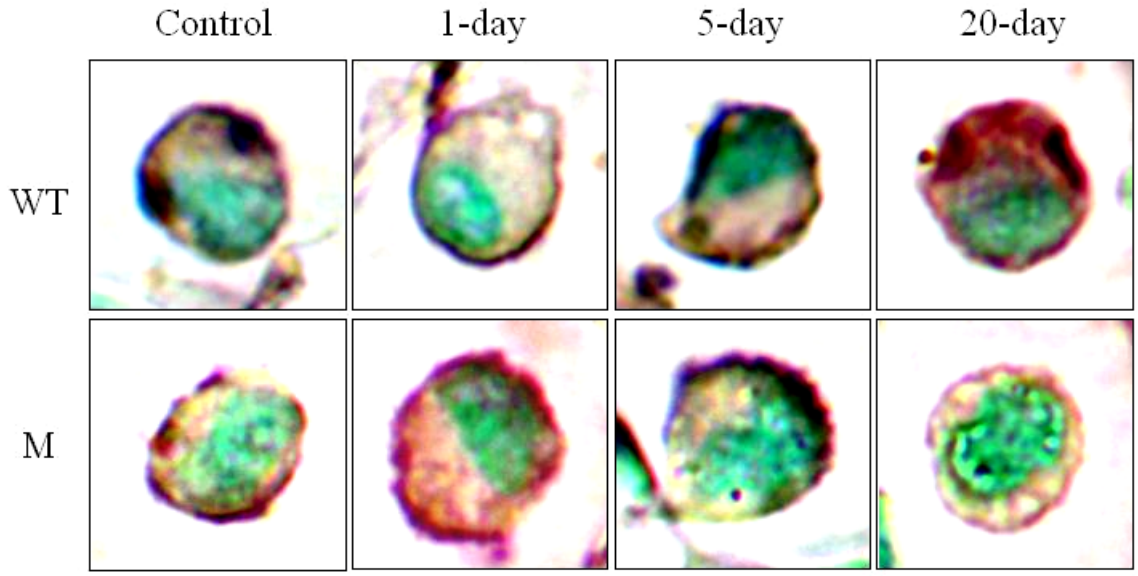

Figure 4-21: Comparative Toll-like Receptor-4 immuohistochemistry of macrophages/monocytes in the alveolar septum of wild-type (WT) and mutant (M) mouse lungs following 20-day swine barn air exposures compared against respective controls (100x optical magnification). Toll-like Receptor-4 is up-regulated in wild-type but not mutant mice over time, as shown.

4.6.2 Vascular Endothelial Growth Factor-A (VEGF-A)

Immunohistochemical characterization of the expression of VEGF-A protein in the mouse lungs was done using goat anti-human VEGF-A antibody. Positive staining for VEGF-A is observed as the dark purple areas of the lung tissue. Visualization of the lung tissue shows high expression of VEGF-A in both wild-type and TLR4-mutant mouse strains in the alveolar septum, to the point of saturation (Figure 4-22). No barn air exposure-related increases in VEGF-A protein expression were visually identified.

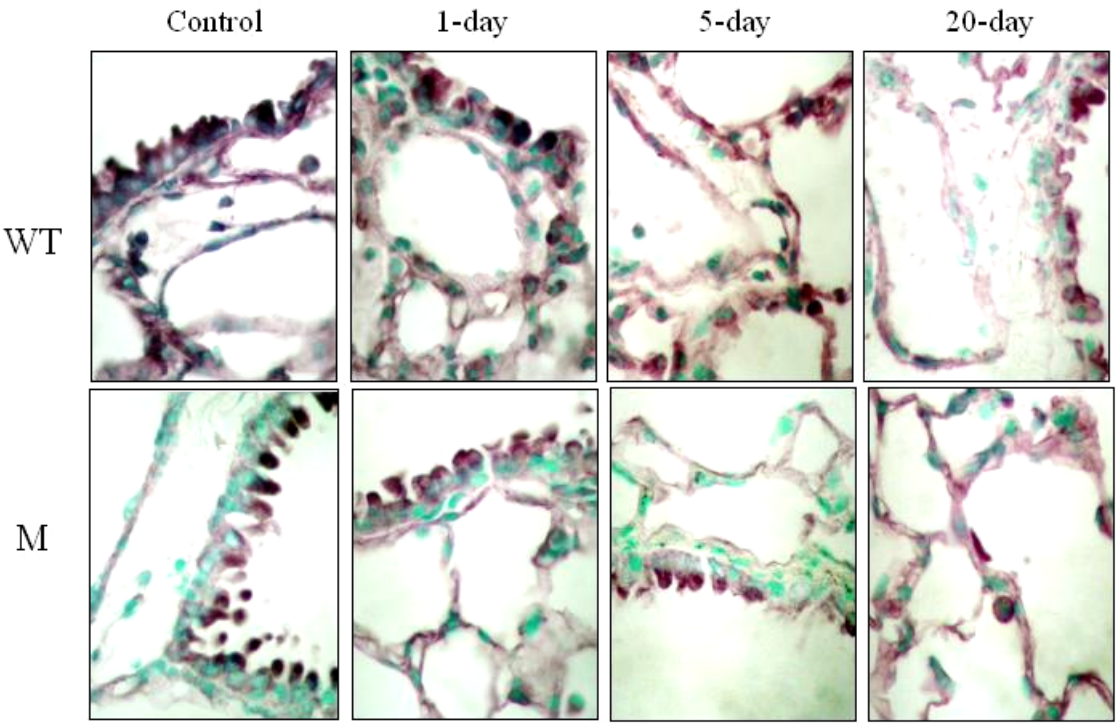

Figure 4-22: Comparative Vascular Endothelial Growth Factor-A immunohistochemistry in the alveolar septum of wild-type (WT) and mutant (M) mouse lungs following 1-, 5- or 20-day swine barn air exposures (40x optical magnification).

4.6.3 Vascular Endothelial Growth Factor Receptor-1 (VEGFR-1)

The possibility of changes to receptor expression following multiple barn air exposures was explored by IHC characterization of VEGFR-1 expression in mouse lungs. Characterization of the expression of VEGFR-1 was done using a goat anti-human VEGFR-1 antibody. Positive staining for VEGFR-1 is observed as the dark purple areas of the lung tissue. Visualization of the lung tissue shows medium- to high-expression of VEGFR-1 in both wild-type and mutant strains in the bronchiolar epithelium and the capillary endothelium (Figure 4-23). No barn air exposure-related increases in VEGFR-1 protein expression were visually identified.

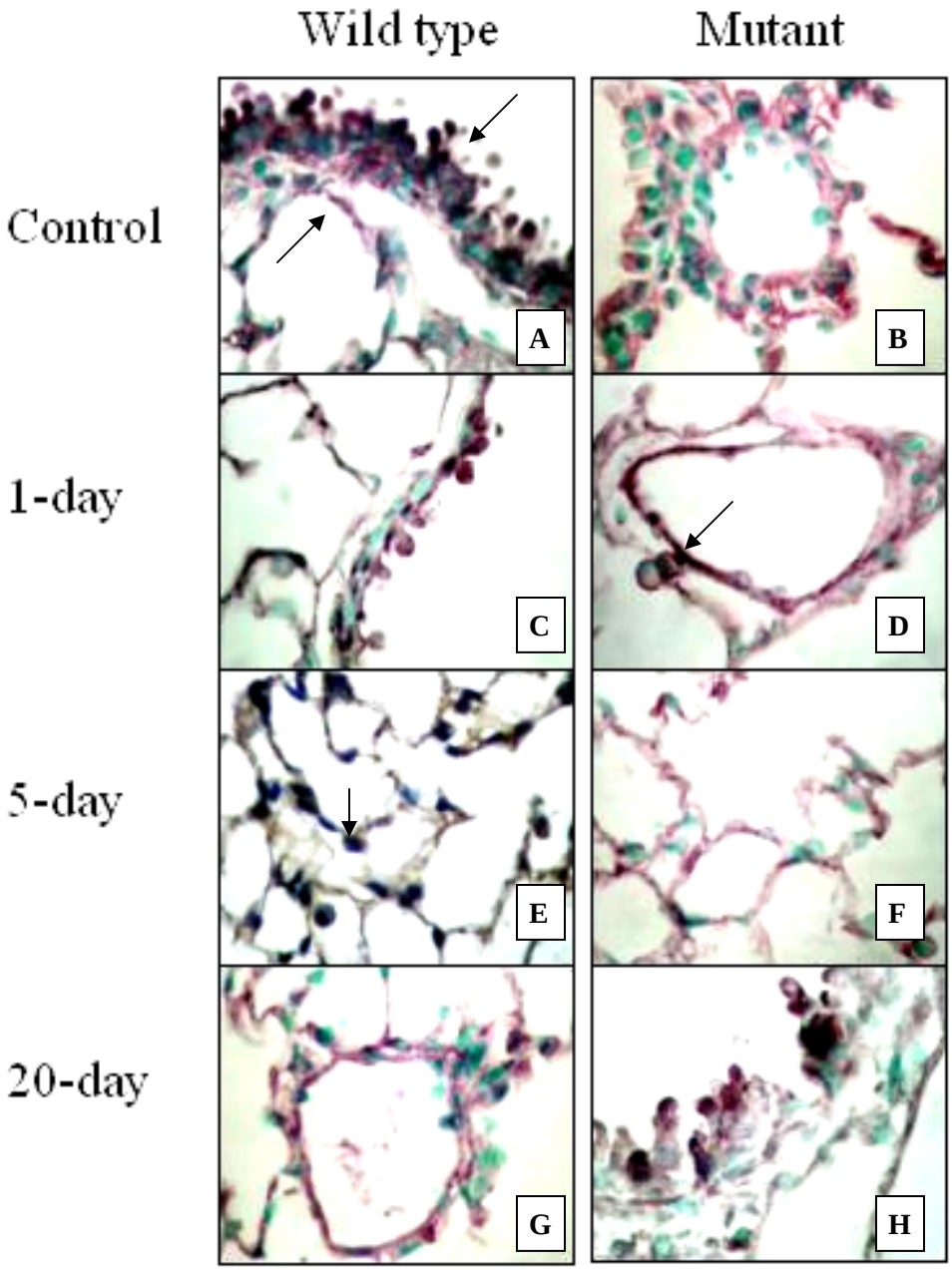

Figure 4-23: Comparative Vascular Endothelial Growth Factor Receptor-1 (VEGFR-1) immunohistochemistry in the alveolar septum of wild-type and mutant mouse lungs following 1-, 5- or 20-day swine barn air exposures (40x optical magnification). Arrows show: A – VEGFR-1 staining in the bronchiolar epithelium and the capillary endothelium; D – VEGFR-1 staining in the capillary endothelium and on macrophages; E – macrophages expressing VEGFR-1.

4.6.4 Vascular Endothelial Growth Factor Receptor-2 (VEGFR-2)

The possibility of changes to receptor expression following multiple barn air exposures was explored by IHC characterization of VEGFR-2 expression in mouse lungs. Characterization of the expression of VEGFR-2 was done using rabbit anti-mouse VEGFR-2 antibody (Appendix D). Positive staining for VEGFR-2 would have been evident as dark purple areas of the lung tissue. Lung tissues showed no expression of VEGFR-2 in both wild-type and TLR4-mutant strains (as demonstrated by the lack of purple staining; Figure 4-24). Lack of staining may be due to the lack of protein expression, or to the amount of protein being below the limit of detection for the VEGFR-2 antibody used. Nonetheless, further characterization of VEGFR-2 protein expression was deemed unnecessary, and no ELISA was done for this receptor, though genetic expression was evaluated using qPCR techniques.

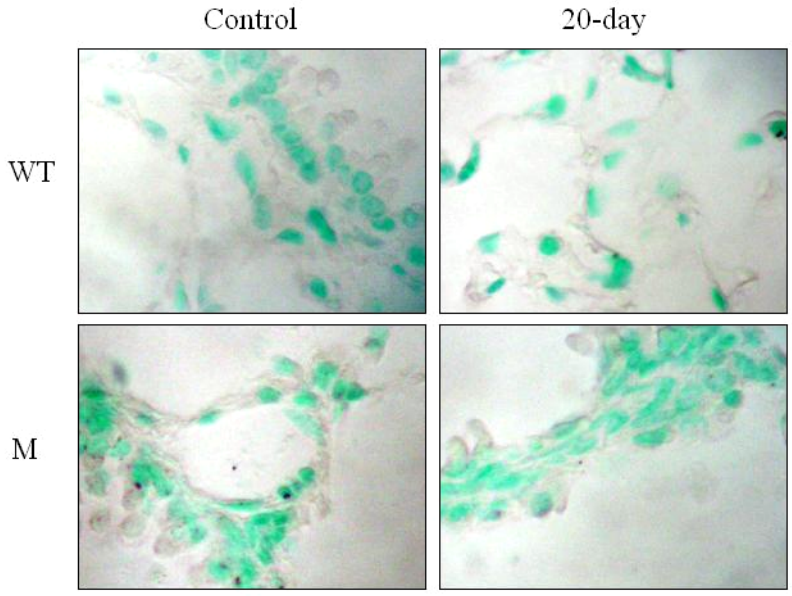

Figure 4-24: Comparative Vascular Endothelial Growth Factor Receptor-2 (VEGFR-2) immunohistochemistry in the alveolar septum of wild-type (WT) and mutant (M) mouse lungs of control animals and animals following 20-day swine barn air exposures (40x optical magnification).

4.7 Vascular Density Analysis

Mouse lungs were stained with the anti-CD34 Antibody to visualize the capillaries of the alveolar septum. Images were randomly taken of the alveolar septum proximal to bronchioles or large blood vessels to allow for sterological evaluation of capillary density, identified by the number of capillary intersections. The replicates were averaged and statistical analyses were performed.

When evaluating the histology of control animals from both wild-type and mutant groups, it is apparent that there are morphological differences in septal capillary density between the strains (Figure 4-25). Mutant animals appear to have larger alveoli, and less septum when compared to their wild-type counterparts.

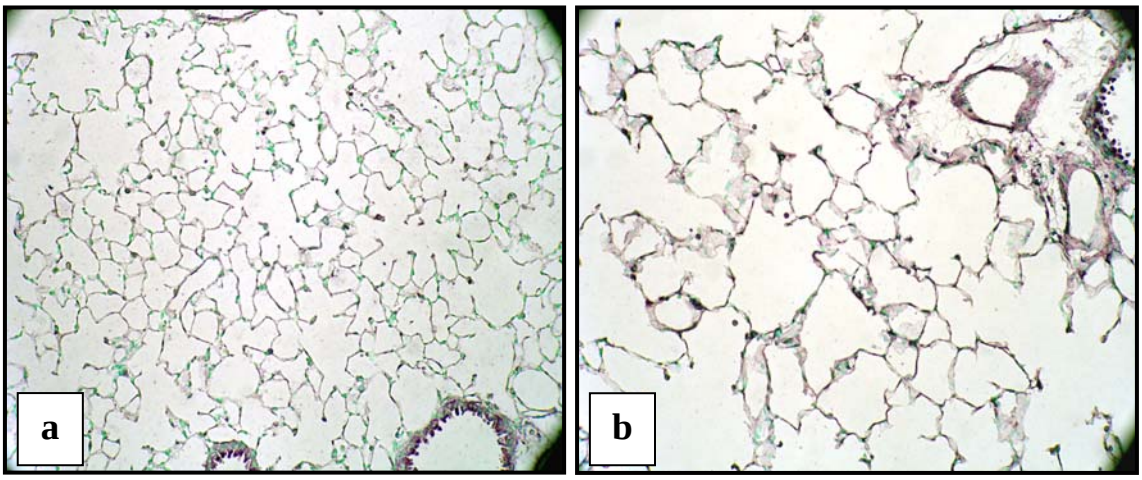

Figure 4-25: Comparative pulmonary vascular density of: a) wild-type and b) mutant animals stained for anti-CD34 antibody (10X optical magnification).

Capillary density was increased by 127% ($p<0.05$) in wild-type animals after 20-days swine barn air exposure when compared to control group (Figure 4-26). There was no change in capillary density observed in mutant animals exposed to the barn air (Figure 4-27). The differences in capillary density between wild-type and mutant mice were apparent even in the control groups. At all time periods (control group, one-day, five-day and 20-day barn air exposures), the wild-type mice showed approximately 1.55-times higher capillary density than their mutant counterparts ($p<0.05$, Figure 4-28).

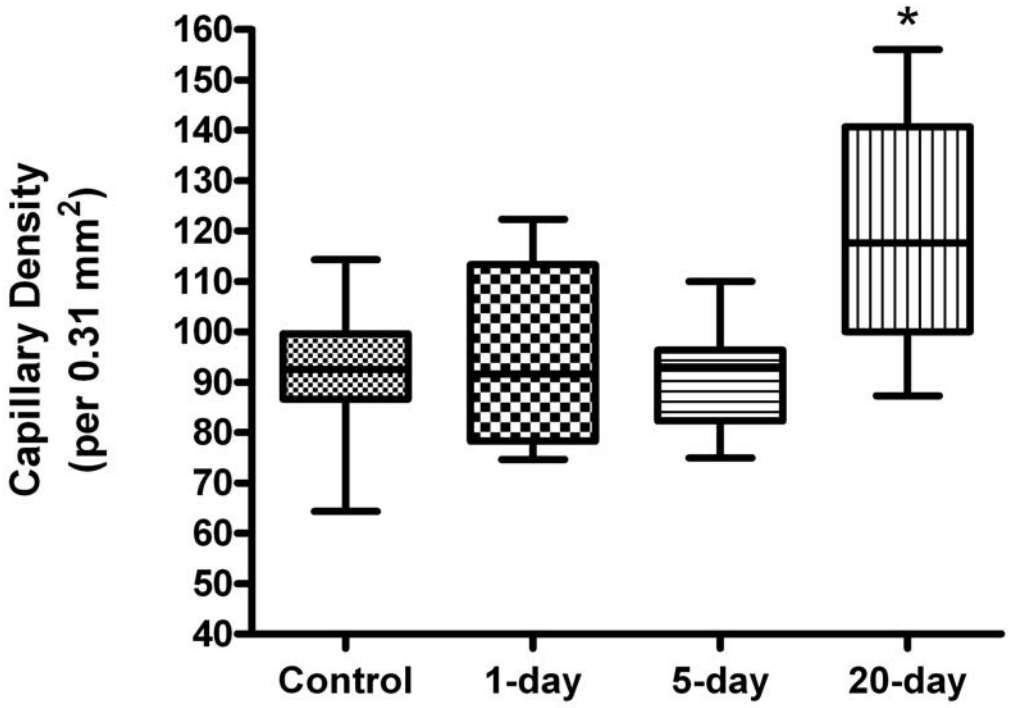

Figure 4-26: Capillary density as capillary intersections (per 0.31 mm^2) in the alveolar septum of wild-type (WT) animals following 0-, 1-, 5-, or 20-day barn exposures (n=38). Expressed as mean ± standard deviation using one-way ANOVA and Bonferroni post-hoc analysis (* $p<0.05$ vs. control group).

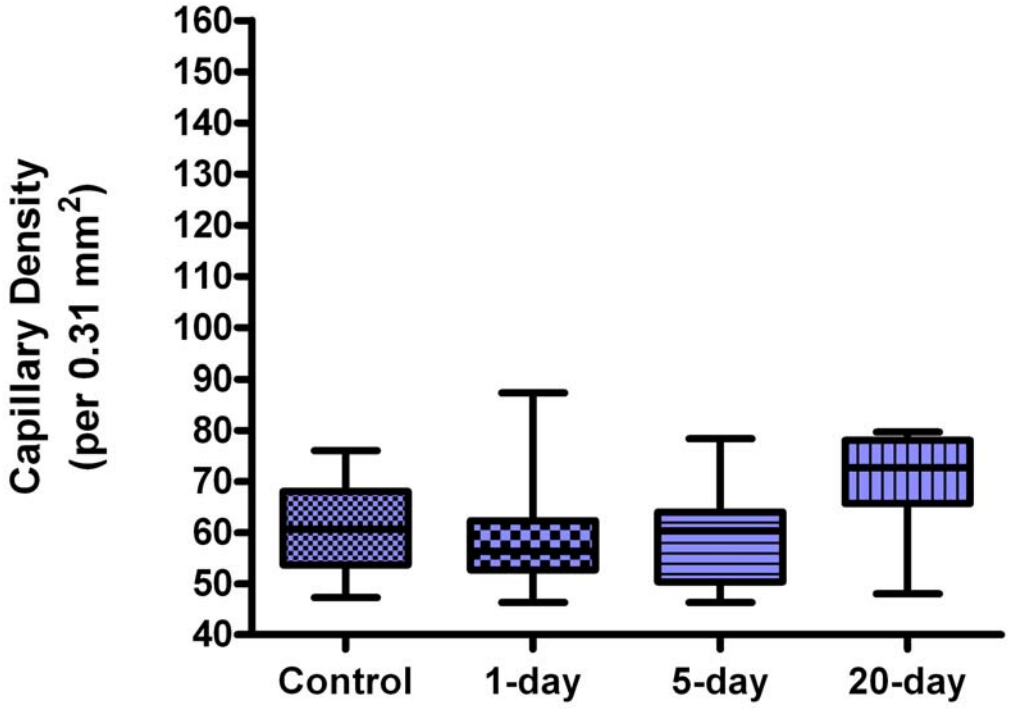

Figure 4-27: Capillary density as capillary intersections (per 0.31 mm^2) in the alveolar septum of mutant (M) animals following 0-, 1-, 5-, or 20-day barn exposures (n=38). Expressed as mean ± standard deviation using one-way ANOVA and Bonferroni post-hoc analysis (* $p<0.05$ vs. control group).

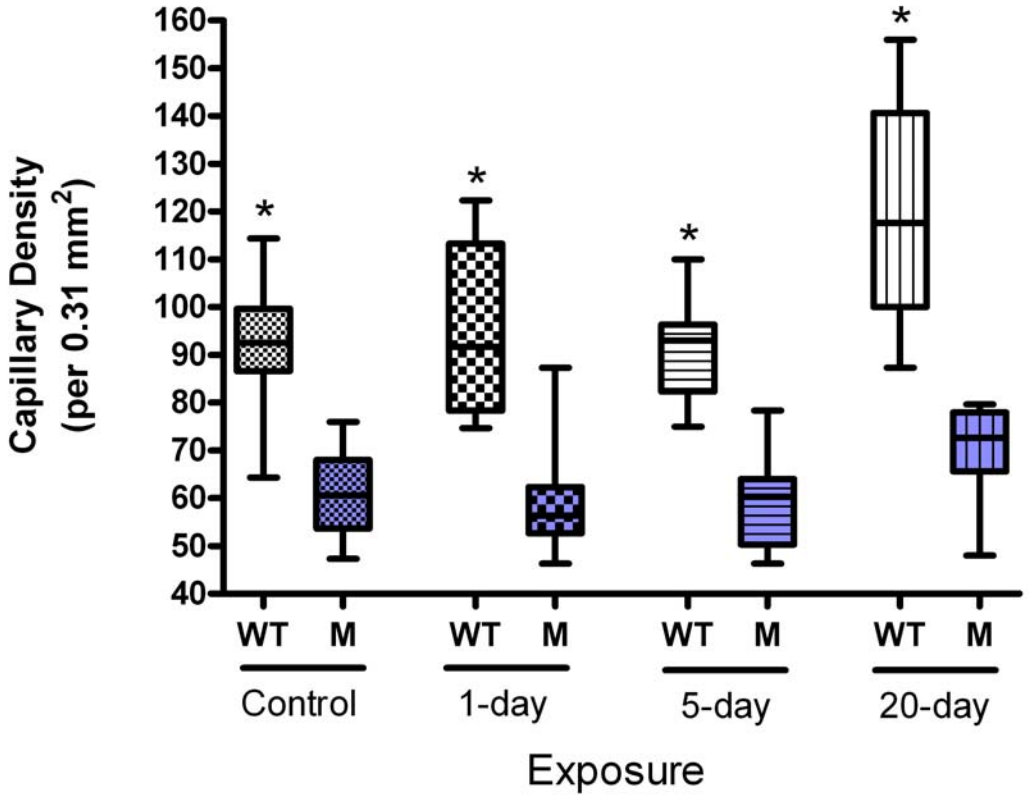

Figure 4-28: Comparative capillary density as capillary intersections (per 0.31 mm^2) in wild-type (WT) and mutant (M) animals following 0-, 1-, 5-, or 20-day swine barn air exposures (n=76). WT animals showed significantly higher capillary density than M animals over all time periods. Expressed as mean ± standard deviation using one-way ANOVA and Bonferroni post-hoc analysis (* $p<0.05$ vs. matched M animal).

4.8 ELISA Results

To determine whether the vascular endothelial growth factor family or its receptors were responsible for the observed increase in capillary density, ELISAs were performed for both Vascular Endothelial Growth Factor-A (VEGF-A) and VEGF Receptor-1 (VEGFR-1). Assays were run using either the broncho-alveolar lavage fluid (BALF) or mouse lung tissue. There were no differences in VEGF-A or VEGFR-1 expression in BALF, and these results have not been shown.

4.8.1 Vascular Endothelial Growth Factor-A (VEGF-A)

Vascular Endothelial Growth Factor-A protein was decreased by 0.62 times ($p<0.05$) in wild-type animals following one-day barn air exposures when compared to the control group (Figure 4-29). This reduction was not maintained over time, and may be the result of VEGF-A depletion following a pro-angiogenic event. No changes in VEGF-A expression in lung tissue were observed for TLR4-mutant animals exposed to barn air for one-, five- or 20-day exposures when compared to the control group (Figure 4-30). When comparing VEGF-A expression in wild-type and TLR4-mutant mice, it is apparent that there are no difference in VEGF-A expression in the lung at all time periods when compared to their matched group (Figure 4-31).

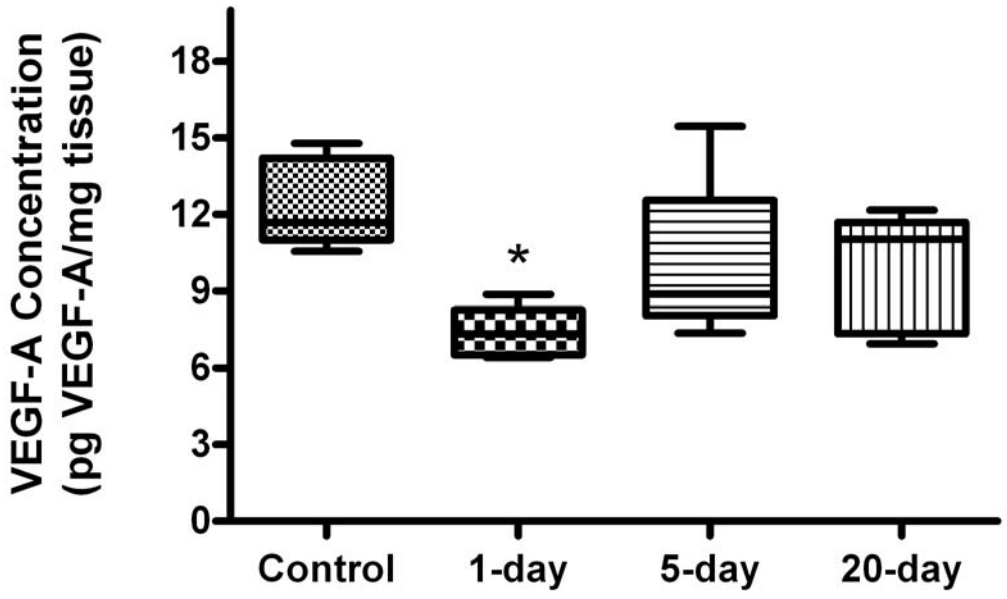

Figure 4-29: Vascular Endothelial Growth Factor-A (VEGF-A) Concentrations (pg VEGF-A/mg tissue) in wild-type (WT) animals following 0-, 1-, 5-, or 20-day barn exposures (n=38). Expressed as mean ± standard deviation using one-way ANOVA and Bonferroni post-hoc analysis (* $p<0.05$ vs. control group).

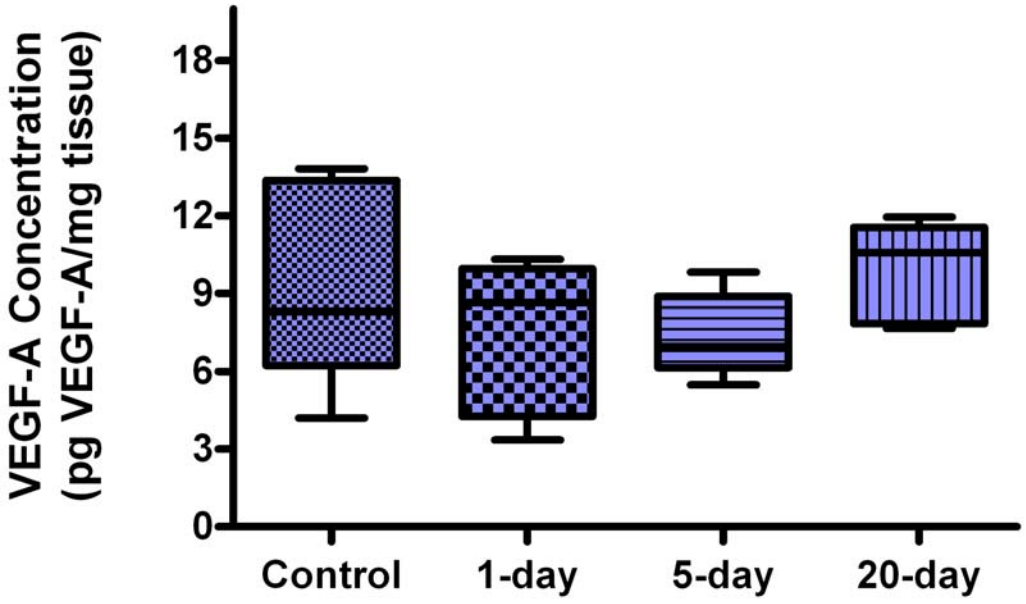

Figure 4-30: Vascular Endothelial Growth Factor-A (VEGF-A) concentrations (pg VEGF-A/mg tissue) in mutant (M) animals following 0-, 1-, 5-, or 20-day barn exposures (n=38). Expressed as mean ± standard deviation using one-way ANOVA and Bonferroni post-hoc analysis (* $p<0.05$ vs. control group).

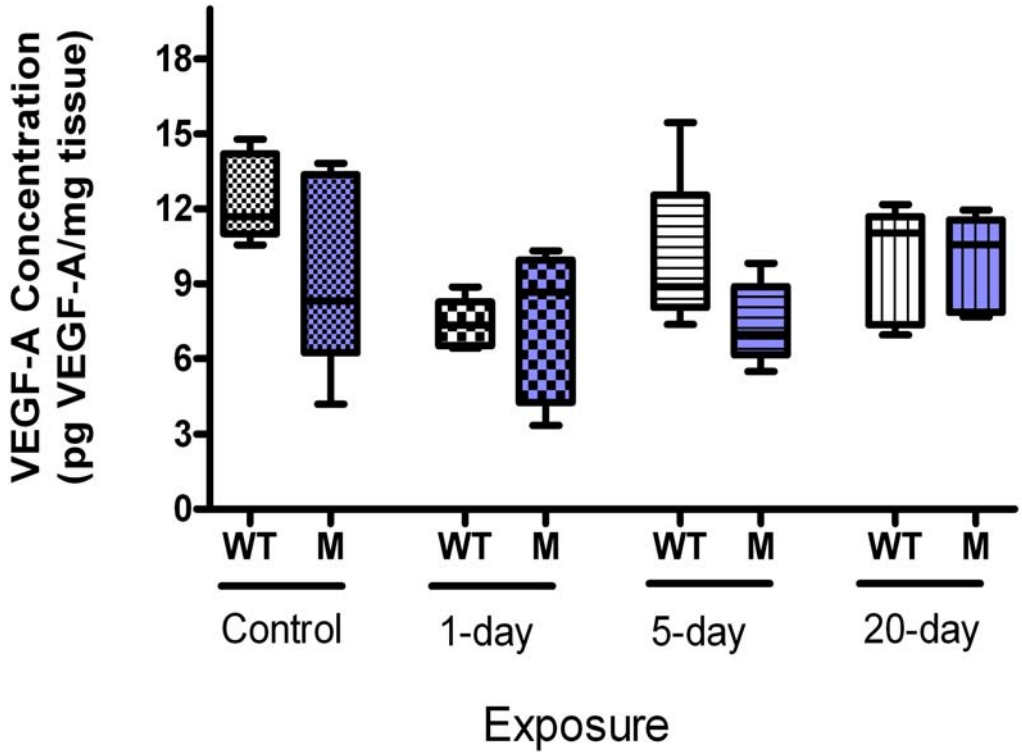

Figure 4-31: Comparative Vascular Endothelial Growth Factor-A (VEGF-A) concentration (pg VEGF-A/mg tissue) in wild-type (WT) and mutant (M) animals following 0-, 1-, 5-, or 20-day swine barn air exposures (n=76). Expressed as mean ± standard deviation using one-way ANOVA and Bonferroni post-hoc analysis (* $p<0.05$ vs. control group).

4.8.2 Vascular Endothelial Growth Factor Receptor-1 (VEGFR-1)

There were no changes to the expression of VEGFR-1 to lung tissues in wild-type animals exposed to barn air for one-, five-, or 20-days when compared to the control group (Figure 4-32). No changes in VEGFR-1 expression in lung tissue were observed for mutant animals exposed to barn air for one-, five- or 20-day exposures when compared to the control group (Figure 4-33). When comparing VEGFR-1 expression in wild-type and mutant mice, there were no differences in VEGFR-1 expression in the lung at all time periods when compared to their matched group (Figure 4-34).

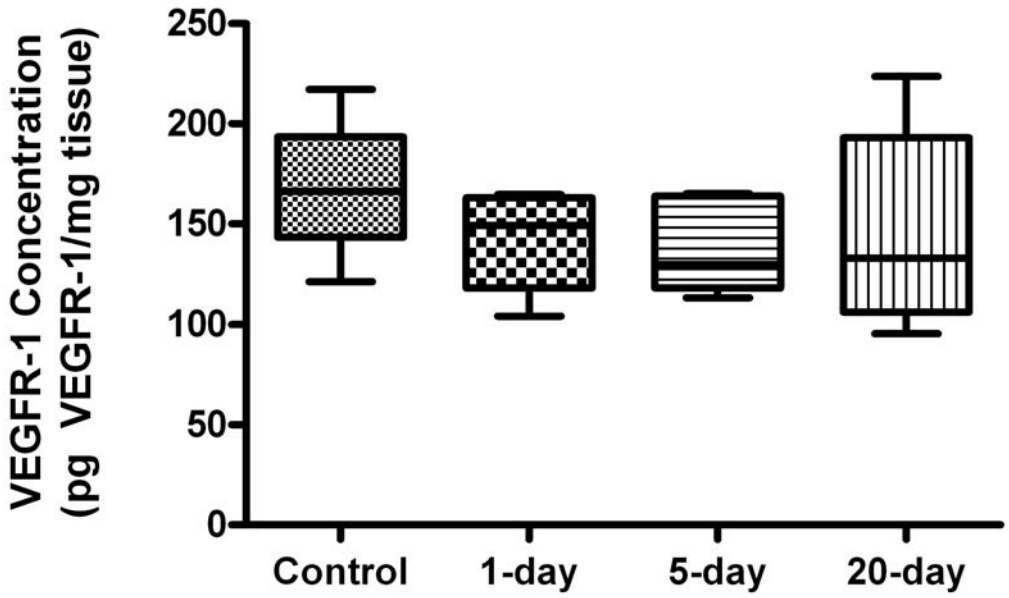

Figure 4-32: Vascular Endothelial Growth Factor Receptor-1 (VEGFR-1) concentrations (pg VEGFR-1/mg tissue) in wild-type (WT) animals following 0-, 1-, 5-, or 20-day barn exposures (n=38). Expressed as mean ± standard deviation using one-way ANOVA and Bonferroni post-hoc analysis (* $p<0.05$ vs. control group).

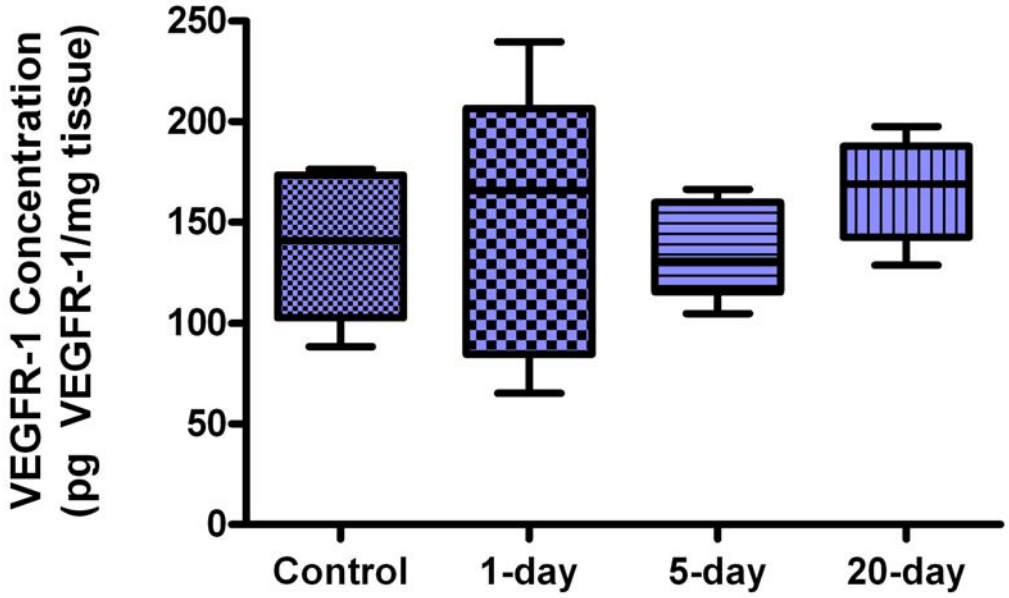

Figure 4-33: Vascular Endothelial Growth Factor Receptor-1 (VEGFR-1) concentrations (pg VEGFR-1/mg tissue) in mutant (M) animals following 0-, 1-, 5-, or 20-day barn exposures (n=38). Expressed as mean ± standard deviation using one-way ANOVA and Bonferroni post-hoc analysis (* $p<0.05$ vs. control group).

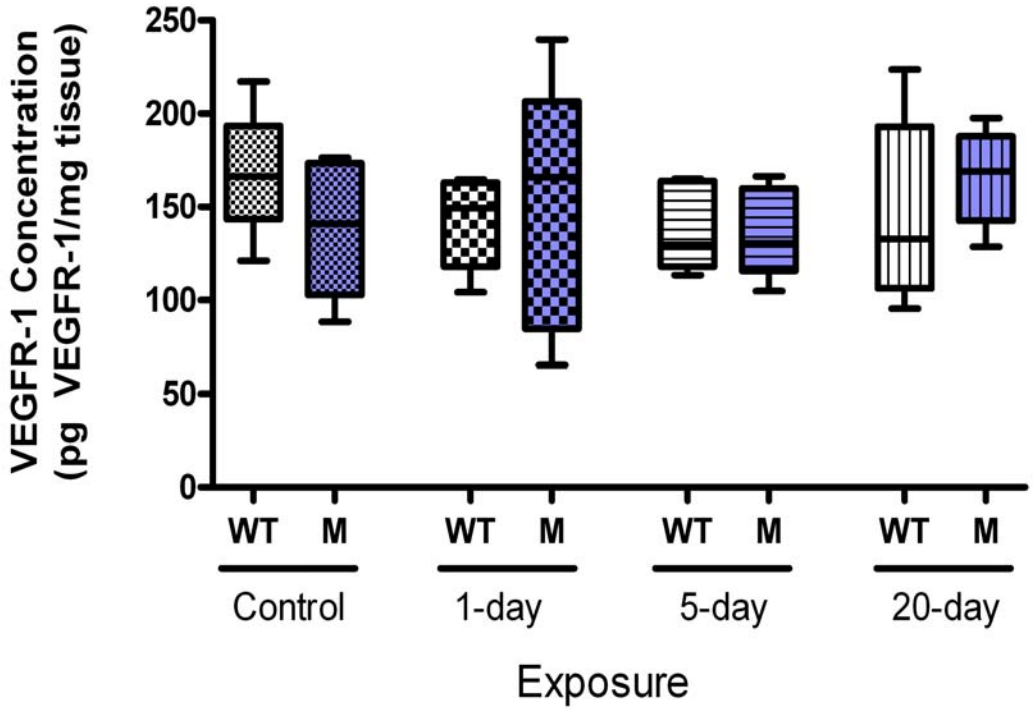

Figure 4-34: Comparative Vascular Endothelial Growth Factor Receptor-1 (VEGFR-1) concentration (pg VEGFR-1/mg tissue) in wild-type (WT) and mutant (M) animals following 0-, 1-, 5-, or 20-day swine barn air exposures (n=76). Expressed as mean ± standard deviation using one-way ANOVA and Bonferroni post-hoc analysis (* $p<0.05$ vs. control group).

4.9 Real-time Reverse Transcriptase-Polymerase Chain Reaction (qPCR)

Changes to the capillary density were observed in wild-type animals after 20-day barn air exposures. However, these changes could not be attributed to protein expression of VEGF-A or its receptors, as evidenced by ELISA results. Thus, quantitative real-time reverse transcriptase-polymerase chain reaction (qPCR) assays were run for VEGF-A, and two of its receptors, VEGFR-1 and VEGFR-2. The purpose of these assays was to determine whether changes to messenger RNA (mRNA; poly(A)+ RNA) expression in mouse lungs could account for morphological changes seen following barn air exposures.

Results are given as a Relative Quantity because the Stratagene MX3005P QPCR apparatus is restricted to determining fluorescence relative to a reference fluorescence (set at dRn = 1.0). In all cases, the reference for relative fluorescence is the wild-type control group (designated WT Control).

4.9.1 qPCR Results for Vascular Endothelial Growth Factor-A

Analysis of VEGF-A mRNA expression wild-type and TLR4-mutant mice lung (n=3 per group) showed that the relative fluorescence for VEGF-A mRNA was higher in wild-type animals over all time periods. Though the relative fluorescence did not appear to increase greatly, the biological significance of this increase could not be determined. Toll-like Receptor-4 mutant mice showed fluorescence for VEGF-A mRNA, however, this fluorescence was approximately one-third lower that of the wild-type animals (Figure 4-35). This result appears to reflect the morphological differences observed in septal density between wild-type and TLR4-mutant mice.

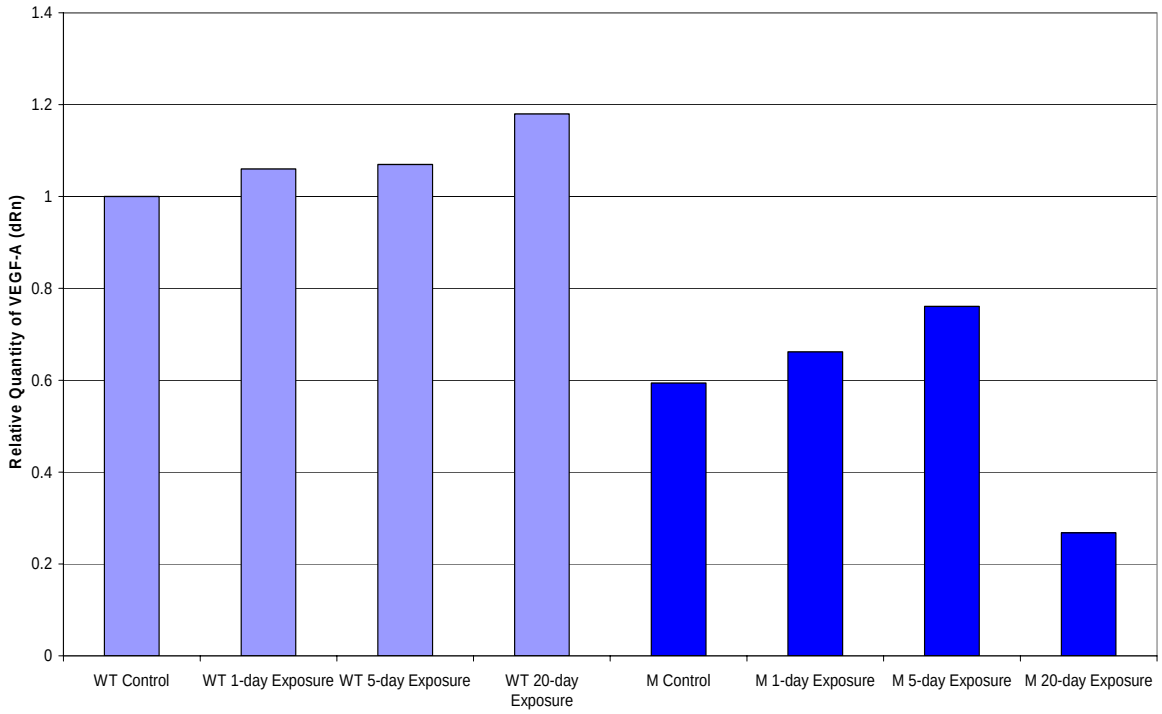

Figure 4-35: Comparative relative fluorescence (dRn) for Vascular Endothelial Growth Factor-A (VEGF-A) mRNA in wild-type (WT) and mutant (M) animals following 0-, 1-, 5-, or 20-day swine barn air exposures (n=24).

4.9.2 qPCR Results for Vascular Endothelial Growth Factor Receptor-1

Analysis of VEGFR-1 mRNA expression wild-type and TLR4-mutant mice lung (n=2 per group) showed wild-type control and TLR4-mutant control groups showed no difference in their VEGFR-1 mRNA expression (baseline expression). The relative fluorescence for VEGFR-1 was increased in wild-type animals over all exposure periods (Figure 4-36). One-, five- and 20-day exposures increased VEGFR-1 mRNA expression by 3.1, 2.75 and 2.20 folds compared to the wild-type control animals. Toll-like Receptor-4 mutant mice showed fluorescence for VEGFR-1 mRNA. As opposed to observations in wild-type animals, the relative quantity of VEGFR-1 mRNA in TLR4-mutant animals decreased by half after 1-day swine barn air exposure. The relative

quantity of VEGFR-1 mRNA rebounded to approximately baseline levels after 20-days barn air exposure.

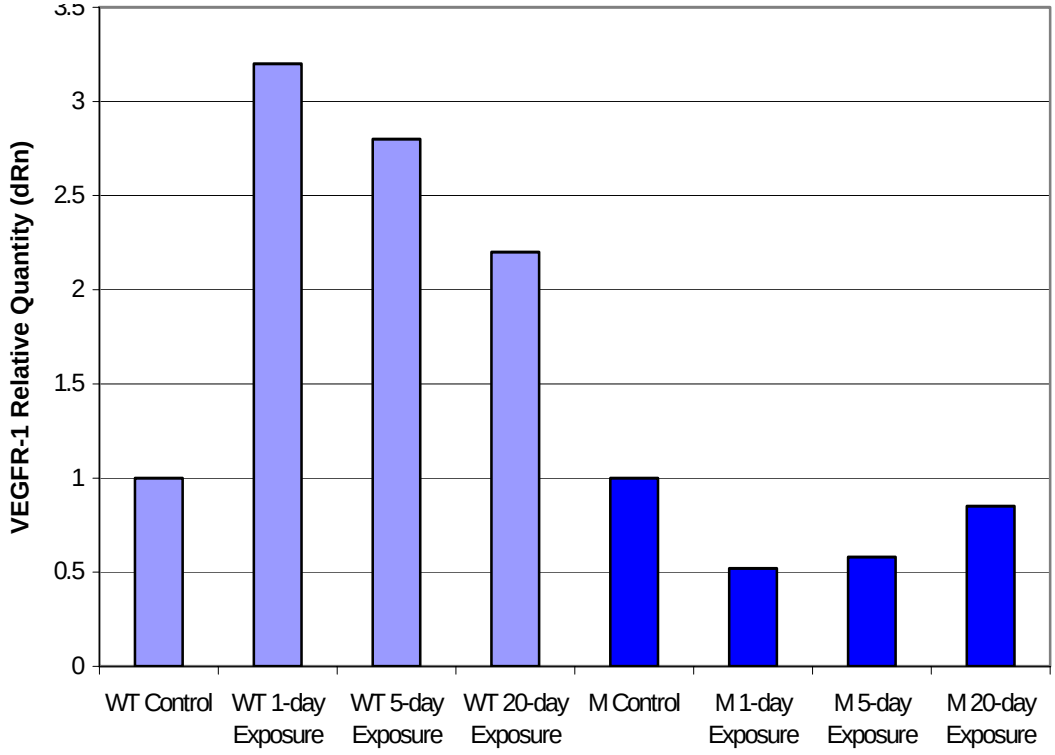

Figure 4-36: Comparative relative fluorescence (dRn) for Vascular Endothelial Growth Factor Receptor 1 (VEGFR-1) mRNA in wild-type (WT) and mutant (M) animals following 0-, 1-, 5-, or 20-day swine barn air exposures (n=16).

4.9.3 qPCR Results for Vascular Endothelial Growth Factor Receptor-2

Analysis of VEGFR-2 mRNA expression wild-type and TLR4-mutant mice lung (n=2 per group) showed wild-type control and TLR4-mutant control groups showed no difference in their VEGFR-2 mRNA expression (baseline expression). The relative fluorescence for VEGFR-2 was increased in wild-type animals over all exposure periods, with the highest levels, 1.85 times that of control groups, observed after 20-day barn air

exposures (Figure 4-37). TLR4-mutant mice showed fluorescence for VEGFR-2 mRNA. A similar pattern of VEGFR-2 mRNA expression was observed, when compared to the wild-type animals, though levels never reached those observed for the wild-type animals (maximum increase of 1.43 times that of M control group). However, 20-day exposures to the barn air appeared to induce higher levels of VEGFR-2 mRNA in the wild-type mice compared to the mutant animals

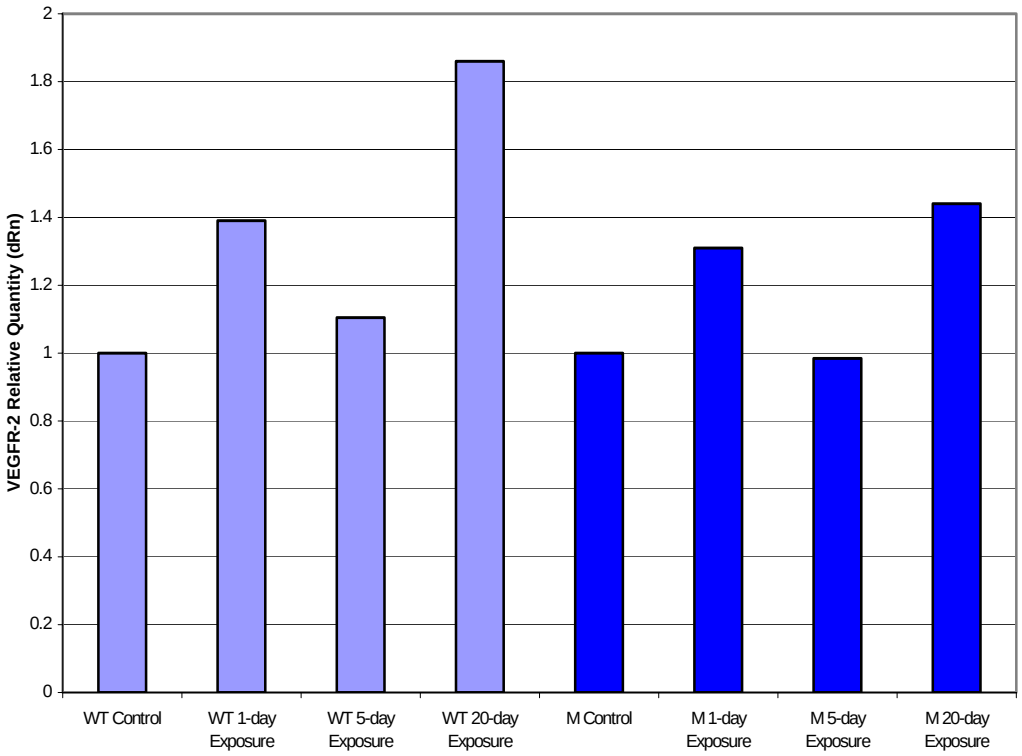

Figure 4-37: Comparative relative fluorescence (dRn) for Vascular Endothelial Growth Factor Receptor 2 (VEGFR-2) mRNA in wild-type (WT) and mutant (M) animals following 0-, 1-, 5-, or 20-day swine barn air exposures (n=16).

5.0 DISCUSSION AND CONCLUSIONS

5.1 Air Quality

The swine barn air contained bacteria and endotoxin. Though the actual composition of Gram-negative vs. Gram-positive bacteria was not quantified, bacterial enumeration showed that there was a median of 105 500 CFU/m^3 in the barn atmosphere. Dust sampled from the barn air using the SKC air sampler contained high levels of endotoxin, confirming the presence of Gram-negative bacteria. After eight-hour sample collection the median endotoxin level in the barn was 1.66 x 10^3 EU per mg dust, which is approximately 500 times the endotoxin level in ambient indoor air (Long *et al.*, 2001; Schulze *et al.*, 2006).

Of the bacteria, 85% had a diameter of less than 7 μm and were respirable. Due to sub-optimal sampler performance, the percentage of respirable bacteria may be under-represented in the data. Optimal flow rate for the Flow Sensor Microbial Sampler is 60 ft^3/hour, but all samples were run at 40 ft^3/hour. Due to decreased flow rate the bacterial particles had a greater likelihood for impacting the higher stages of the six-stage impinger, resulting in higher colony counts in the larger particle-size stages (Stage 1 $\geq$7 μm, Stages 2-6 < 7 μm (Figure 3-4)). As such, the percentage of particles in each size range will be skewed toward higher percentage of large particles, with particles <7 μm being considered respirable. Bacteria were quantified on all 6 of the stages, clearly demonstrate that bacteria and endotoxin are entering the deep lung. Therefore, for the purposes of this research the skewed results have no bearing because the intention of the measurements was to show that bacterial particles were able to penetrate the deep lung.

5.2 Evaluation of the Model

Inhalation and injection models are frequently used to determine the effects of purified LPS on the lung (George *et al.*, 2001; Lorenz *et al.*, 2001; Moreland *et al.*, 2002; Savov *et al.*, 2002; Brass *et al.*, 2003; Savov *et al.*, 2003; Brass *et al.*, 2004; Hollingsworth *et al.*, 2004; Savov *et al.*, 2005; Brass *et al.*, 2007). The approach used in this study is novel in that it uses a whole-barn air model to determine the effects of LPS on pulmonary inflammation following multiple barn air exposures. By using an inhalation model rather than an injection model we were able to account for epithelial-endothelial-leukocyte interactions, with the epithelium being the first line of defence following exposure to barn air. In contrast to the majority of published endotoxin studies whereby the subjects inhale pure LPS to mimic the effects of endotoxin-rich barn air, we exposed the mice directly to swine barn air. This allowed us to account for the effects of other barn air components such as dust, bacteria and irritant chemicals including ammonia and hydrogen sulphide (Zhang, 1998), which are also risk factors for the development of chronic respiratory symptoms and lung dysfunction (Zejda *et al.*, 1993; Zejda *et al.*, 1994).

To confirm whether the model selected for this experiment was appropriate to determining the differences in angiogenesis for wild-type and TLR4-mutant mice to barn air stimuli, several immunological and histological variables were evaluated. The following sections outline observations made between the strains used for this model with respect to airway responsiveness, TLR4 expression, the cellular inflammatory response, and finally the vascular density parameters following multiple swine barn air exposures.

5.2.1 Airway Responsiveness

Changes to airway responsiveness were independent of TLR4, as demonstrated by the fact that wild-type and mutant strains showed the same patterns of airway responsiveness after comparative barn exposures. Control animals showed a dose-dependent decrease in airway responsiveness, with air-flow decreasing to 50% of T_{ev1} after exposure to 1.5 mg methacholine. Changes to airway responsiveness in one-day exposure groups were not significantly different from the control groups. After five days of barn air exposure both wild-type and mutant groups showed increased methacholine sensitivity ($p<0.05$) with airflow being 40% lower than control groups at 1.5 mg methacholine exposure. Conversely, 20-days barn air exposures had wild-type and mutant groups exhibiting a maximum decrease in air-flow to 20% of T_{ev1} after exposure to 1.5 mg methacholine. Thus, after 20-days exposure, animals were less sensitive to methacholine than control groups ($p<0.05$).

The observed airway responsiveness patterns are independent of TLR4. The changes to methacholine sensitivity may have been the result of chemical or physical irritation by barn air components other than endotoxin. Examples of these types of chemicals are ammonia and hydrogen sulphide (Zhang, 1998), both of which form acids upon contact with water found in the airways. The resulting acids may damage the airway epithelium, resulting in irritation, and causing increased airway sensitivity after barn air exposure. The decreased airway sensitivity observed after 20-day swine barn air exposure may be due to alteration to the airway epithelium, to the sensitivity of the autonomic nervous system, or to the acid-base balance of the tissues.

These data differ from the results obtained from mice exposed to sub-acute concentrations of pure LPS where airway responsiveness was shown to be dependent on intact TLR4 and showed no dampening even after multiple exposures (Schwartz, 2002). The precise reasons for these differences are not clear but it may largely be due to biochemical complexity of the barn air compared to pure LPS.

5.3 Expression of Toll-like Receptor-4

Immunohistochemical analysis of the tissues clearly showed that TLR4 was expressed in the wild-type mouse tissues (bronchiolar epithelial cells, peribronchiolar areas, monocytes/macrophages, vascular endothelial cells). Mutant mice also expressed TLR4 in the airway and vascular cells, albeit at lower levels compared to the wild-type animals. Mutant (C3H/HeJ) mice contain a defective lipopolysaccharide (LPS) response allele $Tlr4^{Lps\text{-}d}$, making them endotoxin-resistant. The TLR4 defect is derived from a spontaneous mutation at the lipopolysaccharide response locus, which renders the mice unresponsive to the toxic effects of the lipid A component of LPS. Thus, there was no up-regulation of TLR4 expression in the mutant mice following barn air exposures. These results were expected in the mutant strain and were consistent with previously published studies (Nill *et al.*, 1995; Ryan and Vermeulen, 1995), and can be attributed to the non-responsive nature of the TLR4 being expressed.

5.4 Evaluation of the Cellular Inflammatory Response

Activation of the TLR4 signalling pathway results in pro-inflammatory stimuli, as previously discussed (see Introduction). To confirm the activation of these pathways in

the wild-type animal, and more specifically to determine the level of TLR4-mediated inflammatory response in the endotoxin hyporesponsive TLR4-mutant animals, we evaluated of the number of leukocytes in the broncho-alveolar lavage fluid (BALF) and the blood. Further to general leukocyte counts, absolute macrophage/monocyte, neutrophil and lymphocyte counts were performed and showed induction of the inflammatory response in the tissue following endotoxin exposure. Since TLR4 is involved with the innate immune response we expected to see increased macrophage/monocyte recruitment to the tissues exposed to endotoxin when compared to other cell-types.

Total leukocyte counts in BALF and the blood of exposed wild-type animals showed a spike in the number of cells after one-day barn air exposures. After one-day barn air exposures, wild-type mice showed a 750% increase ($p<0.05$) in BALF total leukocytes and a 2.6-fold increase in blood total leukocytes when compared to control groups. Five-day exposure groups were not significantly different from the control groups, however the trend toward higher leukocyte counts was preserved. After 20-days, the exposed mice showed no significant difference in leukocyte count when compared to controls. The decrease in leukocyte counts in both blood and BALF may be attributed to endotoxin tolerance and was not unexpected. The spike in leukocyte counts after one-day barn air exposure was not observed in the TLR4-mutant animals, indicating a TLR4-dependent response.

Further evaluation of the leukocyte profile was done through BALF cytospin analysis, which allowed for characterization of monocytes/macrophages, neutrophils and lymphocytes following Wright's staining. Neutrophil, macrophage and leukocyte numbers were expressed as a percentage and extrapolated to total BALF values. In all cases, the cellular trends were similar to the total BALF and blood counts, with dramatic increases in cell counts after one-day barn air exposures in wild-type animals. Monocytes and macrophages were by far the major component of the cellular immune response, with median values increasing by 6.5-fold after one-day wild-type barn air exposure.

Neutrophils experienced a 56.6-fold increase after one-day barn air exposures when compared to their control groups. The remainder of the cells counted were classified generally as lymphocytes, and the numbers increased by 6.5-times when compared to their control group. These increases were attenuated over time, likely due to endotoxin tolerance. Toll-like Receptor-4 mutant mice did not exhibit these types of innate immune response, which confirms that the TLR4 expressed in their tissues is non-functional or hyporesponsive.

These results show that TLR4 plays a critical role in lung inflammation following exposures to swine barn air. This result is in accordance with our hypothesis and with the high concentrations of endotoxin detected in the barn air. An interesting finding was that some inflammation was observed in the lungs of mutant animals. This may be the result

of other barn air constituents such as ammonia and dust, or it may be the result of lesser Toll-like Receptor pathways and bears further investigation.

5.5 Confirmation of the Model

Evaluation of immunological and histological differences between wild-type and TLR4-mutant mice strains confirmed that this model exhibits appropriate TLR4 expression and inflammatory responses suitable to this experiment. Wild-type animals demonstrated an immune response consistent with TLR4 mediated innate immunity following endotoxin exposure. Toll-like Receptor-4 mutant strains did not show an immune response following identical swine barn air exposures, thereby confirming that the TLR4-mutant strain does not exhibit TLR4-mediated responses following swine barn air exposures. Thus, any differences in angiogenesis observed between the wild-type and TLR4-mutant mouse strains following multiple swine barn air exposures may be attributed to endotoxin-induced TLR4-mediated effects.

5.6 Vascular Density Analysis

Mouse lungs were stained with anti-CD34 antibody to visualize the capillaries of the alveolar septum. Images were randomly taken of the alveolar septum proximal to bronchioles or large blood vessels and evaluated by a modified sterological technique that allowed for consistent enumeration of microvessels per unit surface area. Unfortunately, this method did not allow for quantification of the relative percentage of epithelial cells to endothelial cells in the alveolar septum. As such, it is impossible to determine whether there are proportionally more endothelial cells (i.e., as the result of angiogenesis) in the

septum, or simply more septum. These types of results could best be obtained through flow cytometry but it was not possible to run flow cytometry in our experiment due to a conflict with tissue processing techniques. Nonetheless, the results obtained do give an idea of inherent differences in the morphology between lungs from wild-type and TLR4-mutant mice, and the changes that occur in the lung following multiple exposures to endotoxin in swine barn air.

5.6.1 Morphological differences between strains

Morphological differences in the alveolar septum were observed between wild-type and TLR4-mutant mice. Wild-type mice had approximately 1.55-times the septal density of their TLR4-mutant counterparts ($p<0.05$). The differences in septal density were unexpected, and were observed for all groups including the control groups. To the best of our knowledge, a difference in septal density or air space volume between the C3HeB/FeJ and C3H/HeJ mouse strains has never been reported in the literature. Dissimilarity in pulmonary architecture is important for the design of toxicologically-based respiratory studies. Differences in pulmonary surface area and tidal volume may affect the dose of toxicant an animal receives over a given period of exposure, thus rendering this model inappropriate for toxicological, or physiological comparison.

5.6.2 Changes to vascular density after multiple barn air exposures

With respect to TLR4-mediated changes to vascular density, results indicated that capillary density was increased by 127% ($p<0.05$) in wild-type animals after 20-days swine barn air exposure when compared to control groups. This is consistent with

previous studies of angiogenesis in rats following exposure to the bacteria *Mycoplasma pulmonis* (Dahlqvist *et al.*, 1999), and may be related to the presence of activated macrophages or other cell types, including endothelial cells. As previously stated, TLRs, including TLR4, have been demonstrated to play a significant role in the pro-angiogenic switch in macrophages (Pinhal-Enfield *et al.*, 2003). The observed increase in capillary density was not seen in mutant animals subjected to the same experimental conditions. Given that LPS is the ligand for TLR4, and that only the wild-type mice showed an increase in lymphocyte count and exhibited any change to vascular density in the alveolar septum, we can conclude 1) that endotoxin is contributing to the observed change in vascular density, and 2) that TLR4 plays a role in septal angiogenesis following swine barn air exposures. Damage to the lung via endotoxin has been demonstrated to induce the transcription of VEGF mRNA, and the release of VEGF (Hahn, 2003), thus elucidation of the role of VEGF and its two receptors in endotoxin-induced angiogenesis was the next logical step for this experiment.

5.7 Expression of pro-angiogenic factors

To determine whether Vascular Endothelial Growth Factor-A (VEGF-A), or two of its receptors, VEGFR-1 and VEGFR-2, played a role in the changes to vascular density observed in wild-type animals after 20-day swine barn air exposures, several molecular techniques were employed. Immunohistochemistry (IHC) allowed for qualitative evaluation of VEGF-A, VEGFR-1 and VEGFR-2 protein expression. Enzyme-linked Immunosorbant Assays (ELISAs) were performed to quantify the proteins of interest

identified with the IHC techniques. Evaluation of gene regulation was done using quantitative real-time reverse-transcriptase PCR (qPCR) for all three proteins of interest.

5.7.1 Vascular Endothelial Growth Factor-A (VEGF-A)

Immunohistochemistry was not sensitive enough to show differences in protein expression of VEGF-A in the lung. All groups for both wild-type and TLR4-mutant strains showed high levels of VEGF-A expression. This was not unexpected (Shifren *et al.*, 1994; Corne *et al.*, 2000; Voelkel *et al.*, 2006), however, to quantify the expression of VEGF-A protein in the lungs ELISAs were performed. Vascular Endothelial Growth Factor-A was found in wild-type lung tissues at a median level of approximately 10 pg VEGF-A/mg lung tissue. The ELISAs demonstrated that VEGF-A protein was decreased by 0.62 times ($p<0.05$) in wild-type animals following one-day barn air exposures when compared to controls. This reduction was not maintained over time, and may be the result of VEGF-A depletion following a pro-angiogenic event. No changes in VEGF-A expression in lung tissue (average median: 9 pg VEGF-A/mg lung tissue) were observed for TLR4-mutant animals exposed to barn air for one-, five- or 20-day exposures when compared to the control group.

A possible reason for the decrease in VEGF-A expression after one-day swine barn air exposure is the initiation of angiogenesis. If VEGF-A was acting in a pro-angiogenic fashion, the level of the mitogenic protein may have been depleted in the tissue where it was being used. Thus, if translation of the protein was not immediately up-regulated within the tissue, it is possible that VEGF-A protein levels in the lung may have been

decreased for a short period of time. To determine whether VEGF-A translation was up-regulated, evaluation of VEGF-A mRNA expression was done using qPCR techniques. Analysis showed that the relative fluorescence for VEGF-A mRNA was higher in wild-type animals over all time periods, and increased with barn air exposures. Though the relative fluorescence in wild-type animals did not increase greatly, the biological significance of this increase could not be determined. It is possible that the increase in mRNA translation was due to an inflammatory cell-mediated increased VEGF-A activity (and hence, angiogenesis) in the lung (Mor *et al.*, 2004). Toll-like Receptor-4 mutant mice showed fluorescence for VEGF-A mRNA, however, this fluorescence was approximately one-third lower that of the wild-type animals. The lower VEGF-A mRNA expression may account for morphological differences observed in septal density observed between wild-type and TLR4-mutant mice (Nill *et al.*, 1995). These results could be evidence of a role for VEGF-A in endotoxin-induced angiogenesis in mice expressing a functional TLR4.

5.7.2 Vascular Endothelial Growth Factor Receptors (VEGFRs)

Both VEGFR-1 and VEGFR-2 were evaluated in this experiment. The possibility of changes to receptor expression following multiple barn air exposures was explored by IHC characterization of VEGFR-1 expression in mouse lungs. Vascular Endothelial Growth Factor Receptor-1 was expressed throughout the lungs of both wild-type and TLR4-mutant mice on the endothelial cells and the surface of macrophages. Expression of VEGFR-1 on these cell types was expected because VEGFR-1 is involved in vascular organization and the migration of macrophages toward VEGF-A (Fong *et al.*, 1999;

Olsson *et al.*, 2006; Shibuya, 2006; Shibuya and Claesson-Welsh, 2006). ELISA techniques indicated that VEGFR-1 protein expression did not change over time in either wild-type or TLR4-mutant mice strains. The approximate median level of VEGFR-1 in the lung tissue was 150 pg VEGFR-1/mg lung tissue. There was no apparent up- or down-regulation of VEGFR-1 protein expression following exposure to swine barn air. Analysis of VEGFR-1 mRNA expression wild-type and TLR4-mutant mice lung by qPCR showed that the relative fluorescence for VEGFR-1 was increased in wild-type animals over all exposure periods. One-day exposure groups had VEGFR-1 mRNA increased by 3.1-fold, with mRNA expression being slightly decreased after five- and 20-day exposures. Though there is increased mRNA transcription, it does not necessarily follow that there would be increased VEGFR-1 translation, however, this could partly explain the increase in vascular density observed in wild-type animals after 20-day swine barn air exposures. Though the specific roles of VEGFR-1 are still being elucidated, it has been suggested that this receptor is involved in vascular organization and the migration of macrophages toward VEGF-A (Fong *et al.*, 1999; Olsson *et al.*, 2006; Shibuya, 2006; Shibuya and Claesson-Welsh, 2006). Toll-like Receptor-4 mutant mice showed fluorescence for VEGFR-1 mRNA. However, as opposed to observations in wild-type animals, the relative quantity of VEGFR-1 mRNA in TLR4-mutant animals decreased by one-half after 1-day swine barn air exposure. Thus, there appears to be a role for VEGFR-1 in the changes to vascular density observed in the lungs of wild-type mice under conditions of multiple swine barn air exposures.

The possibility of changes to VEGFR-2 receptor expression following multiple barn air exposures was explored by IHC characterization. VEGFR-2 was not observed through histological analyses. Lack of staining may be due to the lack of protein expression, or to the amount of protein being below the limit of detection for the VEGFR-2 antibody used. Given that VEGFR-2 plays no role in vascular organization (Fong *et al.*, 1995; Mura *et al.*, 2004; Olsson *et al.*, 2006; Shibuya, 2006; Shibuya and Claesson-Welsh, 2006), it is more likely that this protein is not being expressed in the adult mouse lung and further characterization of VEGFR-2 protein expression was deemed unnecessary. No ELISA was done for this receptor for the reasons stated above, though genetic expression was evaluated using qPCR techniques. Analysis of VEGFR-2 mRNA expression wild-type and TLR4-mutant mice lung showed wild-type control and TLR4-mutant control groups showed no difference in their VEGFR-2 mRNA expression (baseline expression). The relative fluorescence for VEGFR-2 mRNA was increased in wild-type animals over all exposure periods, with the highest levels, 1.85 times that of control groups, observed after 20-day barn air exposures. Toll-like Receptor-4 mutant mice showed fluorescence for VEGFR-2 mRNA. A similar pattern of VEGFR-2 mRNA expression was observed in TLR4-mutant strains when compared to the wild-type animals, though levels never reached those observed for the wild-type animals (maximum increase of 1.43 times that of mutant control group). Based upon these results, but primarily upon the fact that protein expression was not observed in either strain of mouse lungs after any time point, it was concluded that VEGFR-2 is not expressed at levels that would result in pro-angiogenic events in the mouse lung following multiple swine barn air exposures.

Though there appears to be a role for VEGF-A and VEGFR-1 in the manifestation of TLR4-induced angiogenesis in the lung, it is important to caution that these pro-angiogenic factors may not be the not the major contributors to the vascular changes, nor should they explain them in their totality.

5.8 Conclusions

In conclusion, we have determined that the murine inhalation model for endotoxin-induced angiogenesis was appropriate for this type of study. The wild-type mouse (C3HeB/FeJ) expressed a functional TLR4, and exhibited appropriate innate immune responses following multiple swine barn air exposures. The TLR4-mutant mouse (C3H/HeJ) expressed TLR4 to low level, but this TLR4 was non-functional or hypo-responsive, as evidenced by a lack of immunological response following endotoxin exposure in the swine barn.

Using this model, we determined that TLR4 does play a role in changes to vascular density following multiple swine barn air exposures. This conclusion was reached because the increase in vascular density was only observed in the wild-type mouse strain after multiple swine barn air exposures, and after an appropriate biological timeframe had passed. As previously stated, TLR4 has been demonstrated to play a significant role in the pro-angiogenic switch in macrophages (Pinhal-Enfield *et al.*, 2003). Given that LPS is the ligand for TLR4, and that only the wild-type mice exhibited any change to vascular density in the alveolar septum, we can conclude that TLR4 plays a role in septal angiogenesis following swine barn air exposures.

Damage to the lung via endotoxin has been demonstrated to induce the release of VEGF (Hojo *et al.*, 2000; Pakala *et al.*, 2002), perhaps due to increased inflammatory or epithelial cell activity (Mura *et al.*, 2004; Voelkel *et al.*, 2006; Zittermann and Issekutz, 2006). A direct correlation between endotoxin damage and VEGF-A activity was not observed using our mouse model, however, this type of relationship can be supported by the fact that VEGF-A protein levels were decreased after one-day swine barn air exposure in wild-type animals. This indicates that the VEGF-A protein is temporarily being depleted in response to a pro-angiogenic event (Shifren *et al.*, 1994). To compensate for the depletion of VEGF-A protein in the lung, transcription of VEGF-A mRNA was up-regulated in wild-type animals after all swine barn air exposure periods. Thus, VEGF-A is translated at a higher frequency and is involved in the vascular changes observed in LPS-sensitive mice after multiple swine barn air exposures.

To further support the role for VEGF-A in septal angiogenesis following barn air exposures, VEGFR-1 showed increased mRNA transcription over all time points. One-day exposure groups had VEGFR-1 mRNA increased by 3.1-fold, with mRNA expression being slightly decreased after five- and 20-day exposures. Thus, there appears to be an endotoxin-induced TLR4-mediated role for VEGFR-1 in the changes to vascular density observed in the lungs of wild-type mice under conditions of multiple swine barn air exposures. Vascular Endothelial Growth Factor Receptor-2 is not affected by endotoxin-induced TLR4-mediated initiation of angiogenesis.

6.0 REFERENCES

Achen, M. G., Jeltsch, M., Kukk, E., Makinen, T., Vitali, A., Wilks, A. F., Alitalo, K., and Stacker, S. A. (1998). Vascular endothelial growth factor D (VEGF-D) is a ligand for the tyrosine kinases VEGF receptor 2 (Flk1) and VEGF receptor 3 (Flt4). *Proc Natl Acad Sci U S A* **95**, 548-553.

Alon, T., Hemo, I., Itin, A., Pe'er, J., Stone, J., and Keshet, E. (1995). Vascular endothelial growth factor acts as a survival factor for newly formed retinal vessels and has implications for retinopathy of prematurity. *Nat Med* **1**, 1024-1028.

Andersen, A. A. (1958). New sampler for the collection, sizing, and enumeration of viable airborne particles. *J Bacteriol* **76**, 471-484.

Anderton, S. M., and Wraith, D. C. (2002). Selection and fine-tuning of the autoimmune T-cell repertoire. *Nat Rev Immunol* **2**, 487-498.

Backhed, F., Meijer, L., Normark, S., and Richter-Dahlfors, A. (2002). TLR4-dependent recognition of lipopolysaccharide by epithelial cells requires sCD14. *Cell Microbiol* **4**, 493-501.

Barleon, B., Totzke, F., Herzog, C., Blanke, S., Kremmer, E., Siemeister, G., Marme, D., and Martiny-Baron, G. (1997). Mapping of the sites for ligand binding and receptor dimerization at the extracellular domain of the vascular endothelial growth factor receptor FLT-1. *J Biol Chem* **272**, 10382-10388.

Benjamin, L. E., and Keshet, E. (1997). Conditional switching of vascular endothelial growth factor (VEGF) expression in tumors: induction of endothelial cell shedding and regression of hemangioblastoma-like vessels by VEGF withdrawal. *Proc Natl Acad Sci U S A* **94**, 8761-8766.

Brass, D. M., Hollingsworth, J. W., McElvania-Tekippe, E., Garantziotis, S., Hossain, I., and Schwartz, D. A. (2007). CD14 is an essential mediator of LPS induced airway disease. *Am J Physiol Lung Cell Mol Physiol*.

Brass, D. M., Savov, J. D., Gavett, S. H., Haykal-Coates, N., and Schwartz, D. A. (2003). Subchronic endotoxin inhalation causes persistent airway disease. *Am J Physiol Lung Cell Mol Physiol* **285**, L755-761.

Brass, D. M., Savov, J. D., Whitehead, G. S., Maxwell, A. B., and Schwartz, D. A. (2004). LPS binding protein is important in the airway response to inhaled endotoxin. *J Allergy Clin Immunol* **114**, 586-592.

Cebe-Suarez, S., Zehnder-Fjallman, A., and Ballmer-Hofer, K. (2006). The role of VEGF receptors in angiogenesis; complex partnerships. *Cell Mol Life Sci* **63**, 601-615.

Charavaryamath, C., Janardhan, K. S., Townsend, H. G., Willson, P., and Singh, B. (2005). Multiple exposures to swine barn air induce lung inflammation and airway hyper-responsiveness. *Respir Res* **6**, 50.

Cochran, J. R., Khan, A. M., Elidemir, O., Xue, H., Cua, B., Fullmer, J., Larsen, G. L., and Colasurdo, G. N. (2002). Influence of lipopolysaccharide exposure on airway function and allergic responses in developing mice. *Pediatr Pulmonol* **34**, 267-277.

Conejo-Garcia, J. R., Buckanovich, R. J., Benencia, F., Courreges, M. C., Rubin, S. C., Carroll, R. G., and Coukos, G. (2005). Vascular leukocytes contribute to tumor vascularization. *Blood* **105**, 679-681.

Corne, J., Chupp, G., Lee, C. G., Homer, R. J., Zhu, Z., Chen, Q., Ma, B., Du, Y., Roux, F., McArdle, J., Waxman, A. B., and Elias, J. A. (2000). IL-13 stimulates vascular endothelial cell growth factor and protects against hyperoxic acute lung injury. *J Clin Invest* **106**, 783-791.

Corthay, A. (2006). A three-cell model for activation of naive T helper cells. *Scand J Immunol* **64**, 93-96.

Dahlqvist, K., Umemoto, E. Y., Brokaw, J. J., Dupuis, M., and McDonald, D. M. (1999). Tissue macrophages associated with angiogenesis in chronic airway inflammation in rats. *Am J Respir Cell Mol Biol* **20**, 237-247.

Davis-Smyth, T., Chen, H., Park, J., Presta, L. G., and Ferrara, N. (1996). The second immunoglobulin-like domain of the VEGF tyrosine kinase receptor Flt-1 determines ligand binding and may initiate a signal transduction cascade. *Embo J* **15**, 4919-4927.

Dosman, J. A., Senthilselvan, A., Kirychuk, S. P., Lemay, S., Barber, E. M., Willson, P., Cormier, Y., and Hurst, T. S. (2000). Positive human health effects of wearing a respirator in a swine barn. *Chest* **118**, 852-860.

Dvorak, H. F., Brown, L. F., Detmar, M., and Dvorak, A. M. (1995). Vascular permeability factor/vascular endothelial growth factor, microvascular hyperpermeability, and angiogenesis. *Am J Pathol* **146**, 1029-1039.

Dziarski, R., Wang, Q., Miyake, K., Kirschning, C. J., and Gupta, D. (2001). MD-2 enables Toll-like receptor 2 (TLR2)-mediated responses to lipopolysaccharide and enhances TLR2-mediated responses to Gram-positive and Gram-negative bacteria and their cell wall components. *J Immunol* **166**, 1938-1944.

Fan, H., and Cook, J. A. (2004). Molecular mechanisms of endotoxin tolerance. *J Endotoxin Res* **10**, 71-84.

Fan, J., Frey, R. S., and Malik, A. B. (2003). TLR4 signaling induces TLR2 expression in endothelial cells via neutrophil NADPH oxidase. *J Clin Invest* **112**, 1234-1243.

Faure, E., Equils, O., Sieling, P. A., Thomas, L., Zhang, F. X., Kirschning, C. J., Polentarutti, N., Muzio, M., and Arditi, M. (2000). Bacterial lipopolysaccharide activates NF-kappaB through toll-like receptor 4 (TLR-4) in cultured human dermal endothelial cells. Differential expression of TLR-4 and TLR-2 in endothelial cells. *J Biol Chem* **275**, 11058-11063.

Finberg, R. W., Re, F., Popova, L., Golenbock, D. T., and Kurt-Jones, E. A. (2004). Cell activation by Toll-like receptors: role of LBP and CD14. *J Endotoxin Res* **10**, 413-418.

Fitzgerald, K. A., Rowe, D. C., and Golenbock, D. T. (2004). Endotoxin recognition and signal transduction by the TLR4/MD2-complex. *Microbes Infect* **6**, 1361-1367.

Fong, G. H., Rossant, J., Gertsenstein, M., and Breitman, M. L. (1995). Role of the Flt-1 receptor tyrosine kinase in regulating the assembly of vascular endothelium. *Nature* **376**, 66-70.

Fong, G. H., Zhang, L., Bryce, D. M., and Peng, J. (1999). Increased hemangioblast commitment, not vascular disorganization, is the primary defect in flt-1 knock-out mice. *Development* **126**, 3015-3025.

Gangloff, M., and Gay, N. J. (2004). MD-2: the Toll 'gatekeeper' in endotoxin signalling. *Trends Biochem Sci* **29**, 294-300.

George, C. L., Jin, H., Wohlford-Lenane, C. L., O'Neill, M. E., Phipps, J. C., O'Shaughnessy, P., Kline, J. N., Thorne, P. S., and Schwartz, D. A. (2001). Endotoxin responsiveness and subchronic grain dust-induced airway disease. *Am J Physiol Lung Cell Mol Physiol* **280**, L203-213.

Gerber, H. P., Dixit, V., and Ferrara, N. (1998). Vascular endothelial growth factor induces expression of the antiapoptotic proteins Bcl-2 and A1 in vascular endothelial cells. *J Biol Chem* **273**, 13313-13316.

Gon, Y., Asai, Y., Hashimoto, S., Mizumura, K., Jibiki, I., Machino, T., Ra, C., and Horie, T. (2004). A20 inhibits toll-like receptor 2- and 4-mediated interleukin-8 synthesis in airway epithelial cells. *Am J Respir Cell Mol Biol* **31**, 330-336.

Gunsilius, E., Petzer, A., Stockhammer, G., Nussbaumer, W., Schumacher, P., Clausen, J., and Gastl, G. (2000). Thrombocytes are the major source for soluble vascular endothelial growth factor in peripheral blood. *Oncology* **58**, 169-174.

Hahn, R. G. (2003). Endotoxin boosts the vascular endothelial growth factor (VEGF) in rabbits. *J Endotoxin Res* **9**, 97-100.

Harter, L., Mica, L., Stocker, R., Trentz, O., and Keel, M. (2004). Increased expression of toll-like receptor-2 and -4 on leukocytes from patients with sepsis. *Shock* **22**, 403-409.

Heumann, D., Lauener, R., and Ryffel, B. (2003). The dual role of LBP and CD14 in response to Gram-negative bacteria or Gram-negative compounds. *J Endotoxin Res* **9**, 381-384.

Hojo, Y., Ikeda, U., Maeda, Y., Takahashi, M., Takizawa, T., Okada, M., Funayama, H., and Shimada, K. (2000). Interaction between human monocytes and vascular smooth muscle cells induces vascular endothelial growth factor expression. *Atherosclerosis* **150**, 63-70.

Hollingsworth, J. W., 2nd, Cook, D. N., Brass, D. M., Walker, J. K., Morgan, D. L., Foster, W. M., and Schwartz, D. A. (2004). The role of Toll-like receptor 4 in environmental airway injury in mice. *Am J Respir Crit Care Med* **170**, 126-132.

Joukov, V., Sorsa, T., Kumar, V., Jeltsch, M., Claesson-Welsh, L., Cao, Y., Saksela, O., Kalkkinen, N., and Alitalo, K. (1997). Proteolytic processing regulates receptor specificity and activity of VEGF-C. *Embo J* **16**, 3898-3911.

Kamachi, A., Nasuhara, Y., Nishimura, M., Takahashi, T., Homma, Y., Ohtsuka, Y., and Munakata, M. (2002). Dissociation between airway responsiveness to methacholine and responsiveness to antigen. *Eur Respir J* **19**, 76-83.

Kaner, R. J., and Crystal, R. G. (2001). Compartmentalization of vascular endothelial growth factor to the epithelial surface of the human lung. *Mol Med* **7**, 240-246.

Koay, M. A., Gao, X., Washington, M. K., Parman, K. S., Sadikot, R. T., Blackwell, T. S., and Christman, J. W. (2002). Macrophages are necessary for maximal nuclear factor-kappa B activation in response to endotoxin. *Am J Respir Cell Mol Biol* **26**, 572-578.

Kobayashi, K. S., and Flavell, R. A. (2004). Shielding the double-edged sword: negative regulation of the innate immune system. *J Leukoc Biol* **75**, 428-433.

Lamagna, C., Aurrand-Lions, M., and Imhof, B. A. (2006). Dual role of macrophages in tumor growth and angiogenesis. *J Leukoc Biol* **80**, 705-713.

Larsson, K. A., Eklund, A. G., Hansson, L. O., Isaksson, B. M., and Malmberg, P. O. (1994). Swine dust causes intense airways inflammation in healthy subjects. *Am J Respir Crit Care Med* **150**, 973-977.

Lee, C. G., Link, H., Baluk, P., Homer, R. J., Chapoval, S., Bhandari, V., Kang, M. J., Cohn, L., Kim, Y. K., McDonald, D. M., and Elias, J. A. (2004). Vascular endothelial growth factor (VEGF) induces remodeling and enhances TH2-mediated sensitization and inflammation in the lung. *Nat Med* **10**, 1095-1103.

Lee, C. G., Yoon, H. J., Zhu, Z., Link, H., Wang, Z., Gwaltney, J. M., Landry, M., and Elias, J. A. (2000). Respiratory syncytial virus stimulation of vascular endothelial cell growth Factor/Vascular permeability factor. *Am J Respir Cell Mol Biol* **23**, 662-669.

Lin, S. M., Frevert, C. W., Kajikawa, O., Wurfel, M. M., Ballman, K., Mongovin, S., Wong, V. A., Selk, A., and Martin, T. R. (2004). Differential regulation of membrane CD14 expression and endotoxin-tolerance in alveolar macrophages. *Am J Respir Cell Mol Biol* **31**, 162-170.

Long, C. M., Suh, H. H., Kobzik, L., Catalano, P. J., Ning, Y. Y., and Koutrakis, P. (2001). A pilot investigation of the relative toxicity of indoor and outdoor fine particles: in vitro effects of endotoxin and other particulate properties. *Environ Health Perspect* **109**, 1019-1026.

Lorenz, E., Jones, M., Wohlford-Lenane, C., Meyer, N., Frees, K. L., Arbour, N. C., and Schwartz, D. A. (2001). Genes other than TLR4 are involved in the response to inhaled LPS. *Am J Physiol Lung Cell Mol Physiol* **281**, L1106-1114.

Ludwig, I. S., Geijtenbeek, T. B., and van Kooyk, Y. (2006). Two way communication between neutrophils and dendritic cells. *Curr Opin Pharmacol* **6**, 408-413.

Manual (1980). Operating Manual for Microbial Samplers. *Flow Sensor, A Divison of Flow General Inc.*

Martin, T. R. (2000). Recognition of bacterial endotoxin in the lungs. *Am J Respir Cell Mol Biol* **23**, 128-132.

Miggin, S. M., and O'Neill, L. A. (2006). New insights into the regulation of TLR signaling. *J Leukoc Biol* **80**, 220-226.

Mor, F., Quintana, F. J., and Cohen, I. R. (2004). Angiogenesis-inflammation cross-talk: vascular endothelial growth factor is secreted by activated T cells and induces Th1 polarization. *J Immunol* **172**, 4618-4623.

Moreland, J. G., Fuhrman, R. M., Pruessner, J. A., and Schwartz, D. A. (2002). CD11b and intercellular adhesion molecule-1 are involved in pulmonary neutrophil recruitment in lipopolysaccharide-induced airway disease. *Am J Respir Cell Mol Biol* **27**, 474-480.

Moreno, C., Merino, J., Ramirez, N., Echeverria, A., Pastor, F., and Sanchez-Ibarrola, A. (2004). Lipopolysaccharide needs soluble CD14 to interact with TLR4 in human monocytes depleted of membrane CD14. *Microbes Infect* **6**, 990-995.

Muir, A., Soong, G., Sokol, S., Reddy, B., Gomez, M. I., Van Heeckeren, A., and Prince, A. (2004). Toll-like receptors in normal and cystic fibrosis airway epithelial cells. *Am J Respir Cell Mol Biol* **30**, 777-783.

Mura, M., dos Santos, C. C., Stewart, D., and Liu, M. (2004). Vascular endothelial growth factor and related molecules in acute lung injury. *J Appl Physiol* **97**, 1605-1617.

Nill, M. R., Oberyszyn, T. M., Ross, M. S., Oberyszyn, A. S., and Robertson, F. M. (1995). Temporal sequence of pulmonary cytokine gene expression in response to endotoxin in C3H/HeN endotoxin-sensitive and C3H/HeJ endotoxin-resistant mice. *J Leukoc Biol* **58**, 563-574.

Nomura, F., Akashi, S., Sakao, Y., Sato, S., Kawai, T., Matsumoto, M., Nakanishi, K., Kimoto, M., Miyake, K., Takeda, K., and Akira, S. (2000). Cutting edge: endotoxin tolerance in mouse peritoneal macrophages correlates with down-regulation of surface toll-like receptor 4 expression. *J Immunol* **164**, 3476-3479.

Olsson, A. K., Dimberg, A., Kreuger, J., and Claesson-Welsh, L. (2006). VEGF receptor signalling - in control of vascular function. *Nat Rev Mol Cell Biol* **7**, 359-371.

Pakala, R., Watanabe, T., and Benedict, C. R. (2002). Induction of endothelial cell proliferation by angiogenic factors released by activated monocytes. *Cardiovasc Radiat Med* **3**, 95-101.

Papetti, M., and Herman, I. M. (2002). Mechanisms of normal and tumor-derived angiogenesis. *Am J Physiol Cell Physiol* **282**, C947-970.

Peck, O. M., Williams, D. L., Breuel, K. F., Kalbfleisch, J. H., Fan, H., Tempel, G. E., Teti, G., and Cook, J. A. (2004). Differential regulation of cytokine and chemokine production in lipopolysaccharide-induced tolerance and priming. *Cytokine* **26**, 202-208.

Pinhal-Enfield, G., Ramanathan, M., Hasko, G., Vogel, S. N., Salzman, A. L., Boons, G. J., and Leibovich, S. J. (2003). An angiogenic switch in macrophages involving synergy between Toll-like receptors 2, 4, 7, and 9 and adenosine A(2A) receptors. *Am J Pathol* **163**, 711-721.

Pugin, J., Schurer-Maly, C. C., Leturcq, D., Moriarty, A., Ulevitch, R. J., and Tobias, P. S. (1993). Lipopolysaccharide activation of human endothelial and epithelial cells is mediated by lipopolysaccharide-binding protein and soluble CD14. *Proc Natl Acad Sci U S A* **90**, 2744-2748.

Qu, J., Zhang, J., Pan, J., He, L., Ou, Z., Zhang, X., and Chen, X. (2003). Endotoxin tolerance inhibits lipopolysaccharide-initiated acute pulmonary inflammation and lung injury in rats by the mechanism of nuclear factor-kappaB. *Scand J Immunol* **58**, 613-619.

Ryan, L. K., and Vermeulen, M. W. (1995). Alveolar macrophages from C3H/HeJ mice show sensitivity to endotoxin. *Am J Respir Cell Mol Biol* **12**, 540-546.

Savov, J. D., Brass, D. M., Berman, K. G., McElvania, E., and Schwartz, D. A. (2003). Fibrinolysis in LPS-induced chronic airway disease. *Am J Physiol Lung Cell Mol Physiol* **285**, L940-948.

Savov, J. D., Brass, D. M., Lawson, B. L., McElvania-Tekippe, E., Walker, J. K., and Schwartz, D. A. (2005). Toll-like receptor 4 antagonist (E5564) prevents the chronic airway response to inhaled lipopolysaccharide (LPS). *Am J Physiol Lung Cell Mol Physiol*.

Savov, J. D., Gavett, S. H., Brass, D. M., Costa, D. L., and Schwartz, D. A. (2002). Neutrophils play a critical role in development of LPS-induced airway disease. *Am J Physiol Lung Cell Mol Physiol* **283**, L952-962.

Schulze, A., van Strien, R., Ehrenstein, V., Schierl, R., Kuchenhoff, H., and Radon, K. (2006). Ambient endotoxin level in an area with intensive livestock production. *Ann Agric Environ Med* **13**, 87-91.

Schwartz, D. A. (2002). TLR4 and LPS hyporesponsiveness in humans. *Int J Hyg Environ Health* **205**, 221-227.

Shibuya, M. (2006). Differential roles of vascular endothelial growth factor receptor-1 and receptor-2 in angiogenesis. *J Biochem Mol Biol* **39**, 469-478.

Shibuya, M., and Claesson-Welsh, L. (2006). Signal transduction by VEGF receptors in regulation of angiogenesis and lymphangiogenesis. *Exp Cell Res* **312**, 549-560.

Shifren, J. L., Doldi, N., Ferrara, N., Mesiano, S., and Jaffe, R. B. (1994). In the human fetus, vascular endothelial growth factor is expressed in epithelial cells and myocytes, but not vascular endothelium: implications for mode of action. *J Clin Endocrinol Metab* **79**, 316-322.

Sica, A., Schioppa, T., Mantovani, A., and Allavena, P. (2006). Tumour-associated macrophages are a distinct M2 polarised population promoting tumour progression: potential targets of anti-cancer therapy. *Eur J Cancer* **42**, 717-727.

Singh, J., and Schwartz, D. A. (2005). Endotoxin and the lung: Insight into the host-environment interaction. *J Allergy Clin Immunol* **115**, 330-333.

Sly, L. M., Rauh, M. J., Kalesnikoff, J., Song, C. H., and Krystal, G. (2004). LPS-induced upregulation of SHIP is essential for endotoxin tolerance. *Immunity* **21**, 227-239.

Suzuki, T. (1999). Role of NF-kB in Macrophage Activation; Chapter 32 in: Endotoxin in Health and Disease. Ed: Brade H, Opal SM, Vogel SN, and Morrison DC.

Tsan, M. F., and Gao, B. (2004). Endogenous ligands of Toll-like receptors. *J Leukoc Biol* **76**, 514-519.

Ushio, H., Nakao, A., Supajatura, V., Miyake, K., Okumura, K., and Ogawa, H. (2004). MD-2 is required for the full responsiveness of mast cells to LPS but not to PGN. *Biochem Biophys Res Commun* **323**, 491-498.

Veikkola, T., and Alitalo, K. (1999). VEGFs, receptors and angiogenesis. *Semin Cancer Biol* **9**, 211-220.

Voelkel, N. F., Vandivier, R. W., and Tuder, R. M. (2006). Vascular endothelial growth factor in the lung. *Am J Physiol Lung Cell Mol Physiol* **290**, L209-221.

Wellmann, S., Taube, T., Paal, K., Graf, V. E. H., Geilen, W., Seifert, G., Eckert, C., Henze, G., and Seeger, K. (2001). Specific reverse transcription-PCR quantification of vascular endothelial growth factor (VEGF) splice variants by LightCycler technology. *Clin Chem* **47**, 654-660.

Yoshimura, A., Ohishi, H. M., Aki, D., and Hanada, T. (2004). Regulation of TLR signaling and inflammation by SOCS family proteins. *J Leukoc Biol* **75**, 422-427.

Zejda, J. E., Barber, E., Dosman, J. A., Olenchock, S. A., McDuffie, H. H., Rhodes, C., and Hurst, T. (1994). Respiratory health status in swine producers relates to endotoxin exposure in the presence of low dust levels. *J Occup Med* **36**, 49-56.

Zejda, J. E., Hurst, T. S., Rhodes, C. S., Barber, E. M., McDuffie, H. H., and Dosman, J. A. (1993). Respiratory health of swine producers. Focus on young workers. *Chest* **103**, 702-709.

Zhang, Y., Tanaka, A., Dosman, J.A., Senthilselvan A., Barber, E.M., Kirychuk, S.P., Holfeld, L.E., Hurst T.S. (1998). Acute Respiratory Responses of Human Subjects to Air Quality in a Swine Building. *J. agric. Engng Res.* **70**, 367 - 373.

Zittermann, S. I., and Issekutz, A. C. (2006). Endothelial growth factors VEGF and bFGF differentially enhance monocyte and neutrophil recruitment to inflammation. *J Leukoc Biol* **80**, 247-257.

Appendices

A – Information on the wild-type mouse strain (C3HeB/FeJ)
B – Information on the mutant mouse strain (C3H/HeJ)
C – Endotoxin Analysis Protocol (VIDO)
D – Antibodies used for Immunohistochemistry
E – ELISA protocol
F – RNA extraction with TRIZOL reagent
G – Primers used for quantitative RT-PCR

Appendix A: Information on the wild-type mouse strain (C3HeB/FeJ)

From: http://jaxmice.jax.org/strain/000658.html

JAX Mice Datasheet
Strain Name: C3HeB/FeJ
Stock Number: 000658

Product Information

Strain Details

Type Inbred Strain
Additional information on Inbred Strains.

TJL Mating System Sibling x Sibling (Female x Male)

Species laboratory mouse
H2 Haplotype *k*
Generation F201 (14-DEC-06)

Appearance
agouti
Related Genotype: *A*/*A*

Important Note
This strain does not carry mouse mammary tumor virus (MMTV). See JAX Notes, May 2000, #480. This strain is also homozygous for the retinal degeneration allele *Pde6b*^{rd1}. See article "Genetic Background Effects: Can Your Mice See?", JAX Notes Spring 2002, No. 485.

Gene & Allele Details

Allele Symbol *Pde6b*^{rd1}
Allele Name retinal degeneration 1
Common Name(s) rd; rd-1; rodless retina;
Gene Symbol and Name *Pde6b*, phosphodiesterase 6B, cGMP, rod receptor, beta polypeptide
Chromosome 5
Gene Common Name(s) CSNB3; PDEB; Pdeb; nmf137; phosphodiesterase, cGMP, rod receptor, beta polypeptide; r; rd; rd-1; rd1; rd10; retinal degeneration; retinal degeneration 1; retinal degeneration 10;
General Note Pde6b^{rd1}, retinal degeneration 1, recessive. Formerly r, rd, rd1. A mutation causing retinal degeneration described by Bruckner (J:25576) and by Tansley (J:15333) in various

stocks was later found to be present in many inbred strains (J:114). Keeler (J:5007) thought it to be identical with the rodless retina mutation he had described in 1924 (J:24999); the identity has recently been proven by analyses of DNA from Keeler's original slides (J:15231).

Homozygotes are fully viable and fertile.Eyes develop normally up to 7 to 10 days after birth. At this stage the outer segment of the rod cell has begun to form, and in wild type mice it elongates rapidly during the 10th to 15th days. In Pde6b^{rd1}/Pde6b^{rd1} mice the nascent outer segments and the rod cells degenerate rapidly so that by 15 days there is only a thin layer of rod cells left, and they have disappeared completely by 35 days (J:5250, J:5708). The inner nuclear layer and the retinal ganglion cells appear normal butmay show slight quantitative reduction (J:5812, J:5292).

Although the eyes of Pde6b^{rd1} homozygotes are devoid of normal rods, the mice have some visual capacity (J:5980). About 3% of cones among the visual cells degenerate at a much slower rate than do rods, so that a few cones are still present at 18 months (J:5988). The surviving cones are postulated (J:25157) as the light receptors required for the persistence of circadian responses to dawn and dusk in Pde6b^{rd1} homozygotes past the sstage when rods have disappeared (J:29236).

In fusion chimeras between wild type and Pde6b^{rd1} homozygous embryos, the Pde6b^{rd1} mutant acts in the photoreceptor cells rather than in the pigment epithelium of the retina (J:5708). Action within photoreceptor cells is also implied by the long term survival of wild type rod cells transplanted into Pde6b^{rd1} homozygote retinas (J:20769). At a stage before degeneration can be seen, a deficiency of cGMP-PDE, andan excess of cGMP, appears in rod photoreceptor cells (J:5332).

The rate of retinal degeneration in mutants doubly homozygous for two retinal degeneration mutations (Pde6b^{rd1} and Rds^{Rd2}) is intermediate between those of the two homozygotes (J:12044). The double homozygote shows an intermediate level of mRNAs for the ß subunit of cGMP-PDE and for several other phototransduction related proteins, suggesting an interaction between Pde6b^{rd1} and Rds^{Rd2} (J:2579).

Genbank ID for mutant sequence: M75166

Molecular Note Two mutations have been identified in rd1 mice. A murine leukimia virus (Xmv-28) insertion in reverse orientation in intron 1 is found in all mouse strains with the rd1 phenotype. Further, a nonsense mutation (C to A transversion) in codon 347 that results in a truncation eliminating more than half of the predicted encoded protein, including the catalytic domain has also been identified in all rd1 strains of mice. A specific degradation of mutant transcript during or after pre-mRNA splicing is suggested.

Colony Maintenance

Diet Information LabDiet® 5K52/5K67

Phenotypic Data

Mouse Phenome Database
Festing Inbred Strain Characteristics: C3HeB

Additional Web Information

C3H strains free of exogenous MMTV
Genetic Quality Control Annual Report
JAX Notes, April 1988; 433. H-2 Haplotypes of Mice from Jackson Laboratory Production Colonies.
JAX Notes, July 1987; 430. LPS Responsiveness of C3H Substrains.
JAX Notes, May 2000; 480. C3H Strains Free of Exogenous MMTV.
JAX Notes, Spring 2002; 485. Genetic Background Effects: Can Your Mice See?

Animal Health Reports

Room Number MP14

Research Applications

This mouse can be used to support research in many areas including:

Research Tools: General Purpose

Sensorineural Research
Retinal Degeneration (Homozygous for $Pde6b^{rd1}$)

$Pde6b^{rd1}$ related

Mouse/Human Gene Homologs
retinitis pigmentosa, autosomal recessive

Appendix B: Information on the mutant mouse strain (C3H/HeJ)

From: http://jaxmice.jax.org/strain/000659.html

JAX Mice Datasheet
Strain Name: C3H/HeJ
Stock Number: 000659

Product Information

Strain Details

Type Inbred Strain
Additional information on Inbred Strains.
Type JAX® GEMM® Strain - Spontaneous Mutation
Additional information on JAX® GEMM® Strains.
TJL Mating System Sibling x Sibling (Female x Male)

Species laboratory mouse
H2 Haplotype *k*
Generation F260 (14-DEC-06)

Appearance
agouti
Related Genotype: *A*/*A*

Important Note
This strain does not carry mouse mammary tumor virus (MMTV). See JAX Notes, May 2000, #480. This strain is homozygous for retinal degeneration allele *Pde6b*^{rd1}, the defective lipopolysaccharide response allele *Tlr4*$^{Lps\text{-}d}$, and for a chromosomal inversion on Chromosome 6.

Strain Description
C3H/HeJ mice are used as a general purpose strain in a wide variety of research areas including cancer, immunology and inflammation, sensorineural, and cardiovascular biology research. C3H/HeJ mice and all other Jackson substrains are homozygous for the retinal degeneration 1 mutation (*Pde6b*^{rd1}), which causes blindness by weaning age. There is also a high incidence of hepatomas in C3H mice (reportedly 72-91% in males at 14 months, 59% in virgin females, 30-38% in breeding females). Despite the lack of exogenous mouse mammary tumor virus (*MMTV*), virgin and breeding females may still develop some mammary tumors later in life. C3H/HeJ mice, fed an atherogenic diet (1.25% cholesterol, 0.5% cholic acid and 15% fat), fail to develop atherosclerotic aortic lesions in contrast to several highly susceptible strains of mice (e.g. C57BL/6J, Stock No. 000664; C57L/J, Stock No. 000668, C57BR/cdJ, Stock No. 000667, and SM/J, Stock No. 000687).

C3H/HeJ mice spontaneously develop alopecia areata (AA) at a reported incidence of approximately 0.25% by 18 months of age. Alopecia areata has been demonstrated to be surgically-induced by grafting a small piece of skin from an older, donor animal with AA onto a younger, isogenic C3H/HeJ recipient. Visit the JAX® Surgical Model for Alopecia Areata Web page for more information on this surgically induced model.

A spontaneous mutation occurred in C3H/HeJ at lipopolysaccharide response locus (mutation in toll-like receptor 4 gene, *Tlr4*$^{Lps\text{-}d}$) making C3H/HeJ mice endotoxin resistant. C3H/HeJ (*Tlr4*$^{Lps\text{-}d}$) mice are highly susceptible to infection by Gram-negative bacteria such as *Salmonella enterica*. Mice infected with *Salmonella* exhibit delayed chemokine production, impaired nitric oxide generation and attenuated cellular immune responses. Mortality in infected mice appears to be the result of enhanced bacterial growth within the liver Kupffer cell network (Vazquez-Torres et al., 2004).

The C3H/HeJ substrain is homozygous for an inversion on Chromosome 6 named In(6)1J. The inversion covers 20% of Chromosome 6 between *D6Mit124* (~30.3 cM) and *D6Mit150* (~51.0 cM). The inversion has no apparent effect on phenotype. Results from screening other C3H substrains and cryopreserved stock from C3H/HeJ suggest that the mutation arose after 1952. See JAX Notes, Fall 2003, No. 491.

Strain Development
The C3H parent strain was developed by LC Strong in 1920 from a cross of a Bagg albino female with a DBA male followed by selection for high incidence of mammary tumors. This high incidence resulted from exogenous mouse mammary tumor virus (MMTV) transmitted through the mother's milk. The Jackson Laboratory maintains four C3H substrains, C3H/HeJ (Stock No. 000659), C3H/HeOuJ (Stock No. 000635), C3HeB/FeJ (Stock No. 000658) and C3H/HeSnJ (Stock No. 000661) that are now free of exogenous MMTV. C3H/HeJ and C3H/HeOuJ mice previously carried MMTV but were rederived in 1999 during planned efforts to increase the overall health status of the mice and the virus was not reintroduced. C3H/HeJ and C3H/HeOuJ substrains were separated in 1952 and are genetically very similar. However, a spontaneous mutation occurred in C3H/HeJ sometime between 1960 and 1968 at lipopolysaccharide response locus (mutation in toll-like receptor 4 gene, *Tlr4*^{lps}) making C3H/HeJ mice endotoxin resistant while the other three C3H strains are endotoxin sensitive.

Gene & Allele Details

Allele Symbol In(6)1J
Allele Name inversion, Chr 6, Jackson 1
Strain of Origin C3H/HeJ
General Note C3H/HeJ and C3H/HeJBir carry this inversion; C3H/HeSnJ and C3HeB/FeJ do not. Examination of recombination distances in Recombinant Inbred (RI) strain sets developed using C3H/HeJ as a progenitor suggest none of these harbor the inversion. Mouse strains carrying spontaneous mutations that arose on the C3H/HeJ background after 1965-1970 could

carry the inversion and are expected to if the mutation arose after the early 1970s.

Molecular Note The In(6)1J inversion covers approximately 20% of Chr 6 in C3H/HeJ mice. Therefore, linkage crosses using C3H/HeJ will show no recombination in this region of Chr 6. Genetic analyses of congenic construction crosses suggested that the suppressed region lies between D6Mit124 (cytological band 6C3) and D6Mit150 (cytological band 6F1). FISH analyses using flanking BACs detected a paracentric chromosomal region between ~73 Mb and ~116 Mb.

Allele Symbol *Pde6b*^{rd1}

Allele Name retinal degeneration 1

Common Name(s) rd; rd-1; rodless retina;

Gene Symbol and Name *Pde6b*, phosphodiesterase 6B, cGMP, rod receptor, beta polypeptide

Chromosome 5

Gene Common Name(s) CSNB3; PDEB; Pdeb; nmf137; phosphodiesterase, cGMP, rod receptor, beta polypeptide; r; rd; rd-1; rd1; rd10; retinal degeneration; retinal degeneration 1; retinal degeneration 10;

General Note Pde6b^{rd1}, retinal degeneration 1, recessive. Formerly r, rd, rd1. A mutation causing retinal degeneration described by Bruckner (J:25576) and by Tansley (J:15333) in various stocks was later found to be present in many inbred strains (J:114). Keeler (J:5007) thought it to be identical with the rodless retina mutation he had described in 1924 (J:24999); the identity has recently been proven by analyses of DNA from Keeler's original slides (J:15231).

Homozygotes are fully viable and fertile.Eyes develop normally up to 7 to 10 days after birth. At this stage the outer segment of the rod cell has begun to form, and in wild type mice it elongates rapidly during the 10th to 15th days. In Pde6b^{rd1}/Pde6b^{rd1} mice the nascent outer segments and the rod cells degenerate rapidly so that by 15 days there is only a thin layer of rod cells left, and they have disappeared completely by 35 days (J:5250, J:5708). The inner nuclear layer and the retinal ganglion cells appear normal butmay show slight quantitative reduction (J:5812, J:5292).

Although the eyes of Pde6b^{rd1} homozygotes are devoid of normal rods, the mice have some visual capacity (J:5980). About 3% of cones among the visual cells degenerate at a much slower rate than do rods, so that a few cones are still

present at 18 months (J:5988). The surviving cones are postulated (J:25157) as the light receptors required for the persistence of circadian responses to dawn and dusk in Pde6b^{rd1} homozygotes past the sstage when rods have disappeared (J:29236).

In fusion chimeras between wild type and Pde6b^{rd1} homozygous embryos, the Pde6b^{rd1} mutant acts in the photoreceptor cells rather than in the pigment epithelium of the retina (J:5708). Action within photoreceptor cells is also implied by the long term survival of wild type rod cells transplanted into Pde6b^{rd1} homozygote retinas (J:20769). At a stage before degeneration can be seen, a deficiency of cGMP-PDE, andan excess of cGMP, appears in rod photoreceptor cells (J:5332).

The rate of retinal degeneration in mutants doubly homozygous for two retinal degeneration mutations (Pde6b^{rd1} and Rds^{Rd2}) is intermediate between those of the two homozygotes (J:12044). The double homozygote shows an intermediate level of mRNAs for the ß subunit of cGMP-PDE and for several other phototransduction related proteins, suggesting an interaction between Pde6b^{rd1} and Rds^{Rd2} (J:2579).

Genbank ID for mutant sequence: M75166

Molecular Note Two mutations have been identified in rd1 mice. A murine leukimia virus (Xmv-28) insertion in reverse orientation in intron 1 is found in all mouse strains with the rd1 phenotype. Further, a nonsense mutation (C to A transversion) in codon 347 that results in a truncation eliminating more than half of the predicted encoded protein, including the catalytic domain has also been identified in all rd1 strains of mice. A specific degradation of mutant transcript during or after pre-mRNA splicing is suggested.

Allele Symbol *Tlr4^{Lps-d}*

Allele Name defective lipopolysaccharide response

Common Name(s) Tlr4^{-}; lps^{d};

Strain of Origin C3H/HeJ

Gene Symbol and Name *Tlr4*, toll-like receptor 4

Chromosome 4

Gene Common Name(s) CD284; Lps; RAS-like, family 2, locus 8; Rasl2-8; TOLL; hToll; lipopolysaccharide response;

General Note C3H/HeJ mice carry this allele. Various combinations of Lps-associated traits have been followed in crosses between C3H/HeJ and other C3H substrains, and the traits have in all cases segregated together (J:30692, J:5557, J:5593, J:5938). Some of the traits show dominance of the $Tlr4^{Lps\text{-}n}$ allele; others, including $Tlr4^{Lps\text{-}d}$, show codominance.

Molecular Note This allele corresponds to a mutation in the third exon of the gene. The substitution of an A to C at nucleotide position 2342, results in an amino acid substitution that replaces proline with histidine at position 712.

Colony Maintenance

Diet Information LabDiet® 5K52/5K67

Phenotypic Data

UPDATED Body Weight Information - JAX® Mice Strain C3H/HeJ (000659)
(This chart reflects the typical correlation between body weight and age for mice maintained in production colonies at The Jackson Laboratory.)

Mouse Phenome Database
Mouse Phenome Database - body weight
Mouse Phenome Database - cardiovascular
Mouse Phenome Database - disease susceptibility
Mouse Phenome Database - ethanol effects
Mouse Phenome Database - food and water intake
Mouse Phenome Database - hematology
Mouse Phenome Database - lungs
Mouse Phenome Database / SNP Facility
Festing Inbred Strain Characteristics: C3H

Additional Web Information

A Surgically Induced Model of Alopecia Areata.
C3H strains free of exogenous MMTV
Genetic Quality Control Annual Report
JAX Notes, April 1988; 433. H-2 Haplotypes of Mice from Jackson Laboratory Production Colonies.
JAX Notes, Fall 2003; 491. Chromosomal Inversion Discovered in C3H/HeJ Mice
JAX Notes, January 1988; 432. Arthritis Models in the Mouse.
JAX Notes, July 1987; 430. LPS Responsiveness of C3H Substrains.
JAX Notes, July 1987; 430. Mammary Tumor Incidence in C3H/HeJ and C3H/OuJ.
JAX Notes, Spring 1995; 461. Neoplastic and Hyperplastic Lesions in the C3H/HeJ Mouse Strain.
JAX Notes, Spring 2003; 489. Malocclusion in the Laboratory Mouse.
JAX Notes, Spring 2005; 497. Update of Chromosome 6 Inversion in JAX&#-82; Mice Strain C3H/HeJ.
JAX Notes, Summer 2003; 490. Hydrocephalus in Laboratory Mice.

JAX Notes, Summer 2005; 498. Toll-like Receptor JAX&#-82; Mice for Immunological Research.
JAX Notes, Winter 2006; 504. JAX® Mice: the Gold Standard Just Got Better.
JAX Notes, Winter 2006; 504. Reliable New Sperm Cryopreservation Service Developed at The Jackson Laboratory.

Animal Health Reports

Room Number AX10
Room Number MP13

Research Applications

This mouse can be used to support research in many areas including:

Cancer Research
Increased Tumor Incidence (Hepatomas)
Increased Tumor Incidence (Mammary Gland Tumors: late onset)

Cardiovascular Research
Diet-Induced Atherosclerosis (Relatively Resistant)

Immunology and Inflammation Research
Immunodeficiency (Tlr deficiency)

Research Tools
General Purpose

Sensorineural Research
Retinal Degeneration (Homozygous for $Pde6b^{rd1}$)

Appendix C: Endotoxin Analysis Protocol (VIDO)

Endotoxin Assay Protocol/LAL (Limulus Amebocyte Lysate) Test
Updated April 27/04 JG

Materials:
- QCL-1000 LAL Assay Kit (Cambrex, #50-648U)
- Sterile injectable water (DIN 00624721; Astra Pharm Inc.; Mississauga, ON, Canada) Store at room temperature (RT)
- Stop reagent (10% w/v SDS)
- 5-mL polypropylene tubes (Falcon #2063; VWR)
- Disposable, pyrogen-free microplates (Falcon #3072; VWR)
- Multi-block heater, Vortex mixer
- Timer/microplate reader/Test tube rack/Gloves
- 200µL and 1000µL pipettors

Procedure:

1. General:

1. wear gloves
2. change pipette tips for each sample
3. test standards and blank duplicate

2. Reconstitute Reagents:

Store at 4^{o}C & use within 1 week

E. Coli (0111:B4) Endotoxin

i. Add 1.0 mL sterile injectable water (room temperature) to the vial.
ii. Vortex 15 minutes and keep at RT until use.

Chromogenic Substrate: Add 6.5mL sterile injectable water with volumetric pipet.

Limulus Amebocyte Lysate (LAL)

i. Add 3.0mL sterile injectable water with polypropylene volumetric pipet.
ii. Gently swirl the solution to avoid foaming.
iii. Pool contents of vials if more than one vial is required.

3. Prepare Standards:

Four standards will be prepared: 1.0, 0.5, 0.25, 0.1EU/mL.
The initial dilution from the stock solution will be 1/X, where X = the concentration of the endotoxin vial. This will yield a 1.0 EU/mL solution. i.e. If the potency of the endotoxin vial is 25 EU/mL, the initial dilution will be 1/25 or 0.1mL of stock solution in 2.4mL sterile injectable water.

Table 1. A summary of how the four standards are to be prepared.

	Standard 1 1.0EU/mL	Standard 2 0.5EU/mL	Standard 3 0.25EU/mL	Standard 4 0.1EU/mL	Standard 5 0.0EU/mL
Sterile Water	**(x-1)/10***	**0.5mL**	**1.5mL**	**0.9mL**	**1.0mL**
Stock Solution	**0.1mL**	**0**	**0**	**0**	**0**
Standard 1 Solution	**0**	**0.5mL**	**0.5mL**	**0.1mL**	**0**

*x = concentration of stock solution as indicated in the certificate

Standard 1 solution must be vortexed for 2 minutes before standards 2-4 can be prepared. In addition, standards 1-4, blank and all samples are to be vortexed for 2 minutes prior to analysis

4. Sample Preparation:

All samples will be analyzed in a dilution series (10^{-0}, 10^{-1}, 10^{-2}, $10^{-}3$) to ensure accurate readings on those samples that have concentrations that do not fit the standard curve.

Each dilution series should be vortexed for 2 minutes before the preparation of the next solution in the series.

5. Test Procedure:

i. Set multi-block heater at 37^{o}C and pre-heat microplate for 5 minutes or longer.
ii. While microplate is on the block heater dispense 50µL of samples, blank (sterile injectable water) and standards into appropriate wells. Remember to change pipette tip after every well.
iii. At T=0 add 50µL of LAL to all the wells. Begin timer when the LAL is added to the first well. Maintain a constant rate of pipetting. Once LAL has been added to all the wells remove the microplate from the block heater and gently tap the side of the plate 20 times in order to mix contents. Return microplate to heater after mixing.
iv. At T=10 minutes add 100µL of the chromogenic substrate to all wells. Substrate must be warmed to 37^{o}C by putting in an incubator for 10 minutes or longer. Again, remove microplate and gently tap side of plate 20 times, returning it to the heat after mixing is complete.
v. At T=16 minutes add 50µL stop solution (10% SDS) to all wells. Remove microplate from heat and mix by gently tapping side of plate 20 times.
vi. Read the absorbance at 405nm. Use a reference wavelength of 490nm. Plate should be read twice and an average of the readings used to calculate the concentrations.

Calculation of Endotoxin Concentration:

Plot the mean change in absorbance (absorbance minus background absorbance) for the 5 standards on the y-axis versus the corresponding endotoxin concentration in EU/mL on the x-axis. Draw a best-fit line between these points and determine the concentrations of

the samples graphically. In order to calculate the mean change in absorbance the mean absorbance of the blank must be subtracted from the standards and the samples. All of these calculations can be done in Microsoft Excel. Once the concentrations of the samples are determined, they must be multiplied by their dilution factors in order to obtain the actual concentration and those concentrations averaged for the final value. The geometric mean of the dilution series for each sample is calculated. The final concentration is expressed in EU/mL, whereas most of the literature expresses endotoxin concentrations in EU/m^3. Therefore, the following conversion factor is used:

$$\frac{\text{EU x 10 min x L x } m^3}{\text{mL x min 1000-L}}$$

Reference:

BioWhittaker, Inc. Limulus Amebocyte Lysate QCL-1000 Test Kit Manual. Cat. No. 50-648-U.

Appendix D: Antibodies used for Immunohistochemistry

Primary Antibodies	Concentration	Dilution	Manufacturer	Product Code	Secondary Antibody	Concentration	Dilution	Manufacturer	Product Code
TLR4	200 ug/mL	1:50	Santa Cruz	12511	rabbit anti-goat IgG	800 ug/mL	1:200	Dako Cytomation	E0466
TLR4 Blocking Peptide	200 ug/mL	1:50	Santa Cruz	12511 P	rabbit anti-goat IgG	800 ug/mL	1:200	Dako Cytomation	E0466
vWF	3.1 g/L	1:300	Dako Cytomation	A0082	goat anti-rabbit IgG	300 ug/mL	1:75	Dako Cytomation	P0448
CD34	200 ug/mL	1:50	Santa Cruz	7045	rabbit anti-goat IgG	800 ug/mL	1:200	Dako Cytomation	E0466
VEGF-A	200 ug/mL	1:50	Santa Cruz	152	goat anti-rabbit IgG	300 ug/mL	1:75	Dako Cytomation	P0448
VEGFR-1 (Flt-1)	200 ug/mL	1:50	Santa Cruz	316	goat anti-rabbit IgG	300 ug/mL	1:75	Dako Cytomation	P0448
VEGFR-2 (Flk-1)	200 ug/mL	1:50	Santa Cruz	505	goat anti-rabbit IgG	300 ug/mL	1:75	Dako Cytomation	P0448
Rabbit IgG	200 ug/mL	1:50	Santa Cruz	2027	goat anti-rabbit IgG	300 ug/mL	1:75	Dako Cytomation	P0448
Goat IgG	500 ug/mL	1:125	Santa Cruz	2028	rabbit anti-goat IgG	800 ug/mL	1:200	Dako Cytomation	E0466
1% BSA	-	-	-	-	anti- goat/rabbit IgG	-	-	-	-

	Concentration	Dilution	Manufacturer	Product Code
Streptavidin	620 ug/mL	1:155	Dako Cytomation	P0397

Appendix E: ELISA Protocol

Sample Preparation – Tissue

1. Get sample (frozen or fresh), and put in liquid nitrogen
2. Prepare 1X HBSS mixture
    a. 1 mL 10X HBSS: 9 mL dH_2O
3. Weigh out tissue
4. Dilute tissue in HBSS mix
    a. 100 mg tissue per mL HBSS mix
5. Homogenize
6. Keep samples on ice
7. Centrifuge to remove particulates once samples are prepared
    a. 25 000 Rcf
    b. 4 degrees C
    c. 15 min
8. Aliquot ~100 uL sample per microcentrifuge tube
9. Store at –80 degrees C until used

Sample Preparation – BAL

None required, except possibly dilution

ELISA method for VEGF-A Assay:

Purchased Quantikine ELISA kit (Catalogue Number MMV00). Methods outlined in kit instructions.

Bring all reagents to room temperature before use.

Reagent preparation for VEGF-A assay:

1) Reconstitute VEGF Kit Control with 1.0 mL deionized water
    a. Assay the control undiluted.
2) Add 25 mL wash buffer concentrate to dH_2O to prepare 625 mL Wash Buffer
3) Colour reagents A &B should be mixed together in equal volumes within 15 min of use. Add 100 uL per well.
4) Reconstitute the VEGF standard with 5.0 mL of calibrator diluent RD5T. Produces stock solution of 500 pg/mL. Allow standard to sit for 5 min with gentle mixing prior to making dilutions.
5) Pipette 20 uL Calibrator diluent RD5T into each polyprolylene tube. Use the stock solution to produce a 2-fold dilution series.

Supplies required:

- **Microplate reader** capable of measuring 450 nm, with the correction wavelength set at 540 nm or 570 nm.

- **Multi-channel pipette**, squirt bottle, manifold dispenser, or automated microplate washer
- 1000 mL graduated cylinder
- POLYPROPYLENE test tubes

Assay procedure for VEGF kit:

1) Prepare all reagents, working standards, and samples as directed in the previous sections.
2) Remove excess microplate strips from the plate frame, return them to the foil pouch containing the dessicant pack and reseal.
3) Add 50 uL of Assay Diluent RD1N to each well
4) Add 50 uL of standard, control or sample to each well. Mix by gently tapping the plate frame for 1 minute. Cover with adhesive strip. Incubate for 2 hours at room temperature.
5) Aspirate each well and wash, repeating the process 4 times for a total of 5 washes. Wash by filling each well with wash buffer (400 uL). Complete removal of liquid at each step is essential. After the last wash, remove any remaining wash buffer by aspirating or decanting. Invert the plate and blot it against clean paper towels.
6) Add 100 uL of mouse VEGF conjugate to each well. Cover with a new adhesive strip. Incubate for 2 hours at room temperature.
7) Repeat as in step 5
8) Add 100 uL of substrate solution to each well. Incubate for 30 min at room temperature. **Protect from light!**
9) Add 100 uL of stop solution to each well. Gently tap the plate to ensure thorough mixing.
10) Determine the optical density of each well within 30 min using a microplate reader set to 450 nm. Set wavelength correction to 540 nm or 570 nm. If wavelength correction is not available, subtract readings at 540 nm or 570 nm from the 450 nm reading to correct for optical imperfections in the plate.

Notes:
For best results, pipette reagents and samples into the centre of each well.
Complete all pipetting within 15 minutes

ELISA method for sVEGR-1 Assay:

Purchased Quantikine ELISA kit (Catalogue Number MVR100). Methods outlined in kit instructions.

Bring all reagents to room temperature before use.

Reagent preparation for sVEGFR-1 assay:

1) Reconstitute sVEGFR-1 Kit Control with 1.0 mL deionized water
    a. Assay the control undiluted.
2) Add 25 mL wash buffer concentrate to dH_2O to prepare 625 mL Wash Buffer
3) Colour reagents A &B should be mixed together in equal volumes within 15 min of use. Add 100 uL per well.
4) Reconstitute the VEGFR-1 standard with 2.0 mL of calibrator diluent RD5-3. Produces stock solution of 8000 pg/mL. Allow standard to sit for 5 min with gentle mixing prior to making dilutions.
5) Pipette 20 uL Calibrator diluent RD5-3 into each polyprolylene tube. Use the stock solution to produce a 2-fold dilution series.

Supplies required:

- **Microplate reader** capable of measuring 450 nm, with the correction wavelength set at 540 nm or 570 nm.
- **Multi-channel pipette**, squirt bottle, manifold dispenser, or automated microplate washer
- 1000 mL graduated cylinder
- POLYPROPYLENE test tubes

Assay procedure for VEGFR-1 kit:

1) Prepare all reagents, working standards, and samples as directed in the previous sections.
2) Remove excess microplate strips from the plate frame, return them to the foil pouch containing the dessicant pack and reseal.
3) Add 50 uL of Assay Diluent RD1-21 to each well
4) Add 50 uL of standard, control or sample to each well. Mix by gently tapping the plate frame for 1 minute. Cover with adhesive strip. Incubate for 2 hours at room temperature.
5) Aspirate each well and wash, repeating the process 4 times for a total of 5 washes. Wash by filling each well with wash buffer (400 uL). Complete removal of liquid at each step is essential. After the last wash, remove any remaining wash buffer by aspirating or decanting. Invert the plate and blot it against clean paper towels.
6) Add 100 uL of mouse VEGFR-1 conjugate to each well. Cover with a new adhesive strip. Incubate for 2 hours at room temperature.
7) Repeat as in step 5.
8) Add 100 uL of substrate solution to each well. Incubate for 30 min at room temperature. **Protect from light!**

9) Add 100 uL of stop solution to each well. Gently tap the plate to ensure thorough mixing.
10) Determine the optical density of each well within 30 min using a microplate reader set to 450 nm. Set wavelength correction to 540 nm or 570 nm. If wavelength correction is not available, subtract readings at 540 nm or 570 nm from the 450 nm reading to correct for optical imperfections in the plate.

Notes:
For best results, pipette reagents and samples into the centre of each well.
Complete all pipetting within 15 minutes

Appendix F : RNA extraction with TRIZOL reagent

FIRST PURIFICATION:
RNA Extraction with TRIZOL Reagent

1) **Homogenize** 50-100 mg tissue in liquid nitrogen, and transfer homogenate into 1 mL TRIZOL reagent.
2) **Incubate** for 5 min at **room temperature.**
3) **Add 200 µL $CHCl_3$** (chloroform), shake tubes vigorously by hand for 15 seconds and incubate at room temperature for 2 minutes.
4) **Centrifuge** at 10 000 rpm for 10 minutes at 4 °C.
5) **Transfer aqueous (top) phase** to fresh tube and **add 500 µL ispropoanol** (pre-chilled), incubate at room temperature for 15 minutes.
6) **Centrifuge** at 14 000 rpm for 20 min at 4 °C.
    i. this will precipitate RNA – **TURN CAP FLIP TO INSIDE OF CENTRIFUGE SO PELLET WILL FORM ON BOTTOM OF OUTSIDE OF TUBE**
7) Wash RNA pellet once with 200 µL 100% ethanol. Close the caps, vortex for <2 seconds and centrifuge at 12 000 rpm for 10 min at 4 °C.
8) Allow RNA pellet to dry (**looks translucent**) after draining ethanol. Do not dislodge the pellet when draining the ethanol.
9) **Re-distribute the pellet in 50 µL RNAse-free water:**
    i. Dissolve by tapping.
    ii. Store at –20 °C, or follow the purification steps immediately.

SECOND PURIFICATION: RNA Clean-up

1. **Adjust sample volume to 100 µL** with RNAse-free water.
2. Add **350 µL RLT** buffer and mix (ensure beta-mercaptoethanol is added to RLT before mixing!)
3. Add **250 µL** 100% ethanol.
4. Mix thoroughly by pipetting.
5. Apply **700 µL sample to RNeasy mini-column** placed in 2 mL collecting tube.
6. **Centrifuge** for 30 seconds at 14 000 rpm and discard flow-through.
7. Add **350 µL RW1.**
8. **Centrifuge** at 14 000 rpm for 30 seconds and discard flow-through.
9. **Centrifuge empty column** at 14 000 rpm for 30 seconds to dry membrane.
10. Make solution:
    i. **10 µL DNAse I + 70 µL RDD** for EACH sample
    ii. Add 80 µL mix to each filter
    iii. Let sit for 15 min at room temperature
11. Add **350 µL RW1.**
12. **Centrifuge** for 30 seconds at 14 000 rpm.
13. Add **500 µL RPE**
14. **Centrifuge** for 30 seconds at 14 000 rpm.
15. Add **500 µL RPE**
16. **Centrifuge 2 min** at 8 000 rcf.
17. Add **60 µL RNAse-free water**, wait 2 minutes at room temperature.
18. Put filter into microcentrifuge tube.
19. Centrifuge for 2 minutes at 14000 rpm to collect RNA in collecting tube.
20. Store at –20 °C.

Appendix G: Primers used for quantitative RT-PCR

Desalted Primers used for Quantitative Real-time Reverse-transcriptase Polymerase Chain Reaction (qPCR)

Mouse VEGF-A

Forward primer	ATG	AAC	TTT	CTG	CTC	TCT	TGG
Reverse primer	TGC	ACA	GCG	CAT	CAG	CGG	CAC

Mouse VEGFR-1

Forward primer	GGC	AGA	CCA	ATA	CAA	TCC	TAG	ATG
Reverse primer	ACC	AGG	GTA	ATT	CCA	GCT	CAT	TT

Mouse VEGFR-2

Forward primer	ATG	TGC	TGT	CTT	TAG	AAG
Reverse primer	AGA	CAT	CTC	TCT	ACA	GCT